WADD TECHNICAL REPORT 61-178

XF

THE USE OF ACOUSTIC SCALE MODELS FOR INVESTIGATING NEAR FIELD NOISE OF JET AND ROCKET ENGINES

WALTER V. MORGAN
L. C. SUTHERLAND
KENNETH J. YOUNG

AND

THE ACOUSTICS GROUP, AERO-SPACE DIVISION,
BOEING AIRPLANE COMPANY

APRIL 1961

FLIGHT DYNAMICS LABORATORY

CONTRACT NO. AF 33(616)-6834
PROJECT NO. 1370
TASK NO. 13786

AERONAUTICAL SYSTEMS DIVISION
AIR FORCE SYSTEMS COMMAND
UNITED STATES AIR FORCE
WRIGHT-PATTERSON AIR FORCE BASE, OHIO

FOREWORD

This report presents the results of a research study conducted by the Acoustics Group, Aero-Space Division, Boeing Airplane Company under Air Force Contract AF 33(616)-6834, Project No. 1370, "Dynamic Problems in Flight Vehicles", Task No. 13786, "Methods of Noise Prediction, Control, and Measurement". Mr. D. L. Smith of the Dynamics Branch, Flight Dynamics Laboratory, Aero-Mechanics Division, Directorate of Advanced Systems Technology, was Test Engineer. Research covered in this report started in January 1960 and is part of a continuing effort.

The research work was conducted under the supervision of Kenneth J. Young, Senior Group Engineer of the Acoustics Group, Aero-Space Division, Boeing Airplane Company. The Project Leader was Walter V. Morgan. The analytical basis for scaling acoustic models, as presented in Section II, was for the most part formulated by L. C. Sutherland, Dyna-Soar Acoustics and Vibration Group. Other members of the Acoustics Group who participated in the research include: Jerry Sugamele in planning and performing the calculation of the gas flow conditions for heated air and substitute gas testing, Mario P. Peila and Marion D. Lockleer in providing acoustic instrumentation and calibration, Robert H. Jeffries in performing the majority of the experimental work, James L. Walker in conducting the model rocket testing and in assisting with data presentations, and David A. Bateman in supervising design and fabrication of all mechanical test apparatus.

ABSTRACT

Analytical and experimental studies have been made to examine the feasibility of using acoustic scale models for near field noise investigations. Analyses show that the important characteristics of noise generation, propagation, and measurement can be scaled. A relatively few deviations from this involve small errors which are generally negligible in the near field. The most straightforward model is seen to be one which duplicates the gas flow parameters of the full scale engine. The validity of such models has been demonstrated by a series of tests for a wide variety of nozzle exit conditions, from turbojet through rocket exhausts, and whether in a free field or in the presence of objects which interfere with the flow, such as shaped nozzles and flame deflectors. It is further determined both analytically and experimentally that models, in certain cases, may be simplified without impairing the results of a scaled test. Considerations in simplifying a model include: reduction of the nozzle size; absence or presence of reflecting surfaces; use of fewer than the full scale number of engines; and use of a substitute gas which is different from and at a lower temperature than that in the full scale engine.

PUBLICATION REVIEW

This report has been reviewed and is approved.

FOR THE COMMANDER:

William C. Nielsen

WILLIAM C. NIELSEN
Colonel, USAF
Chief, Flight Dynamics Laboratory

TABLE OF CONTENTS

LIST OF ILLUSTRATIONS

LIST OF ILLUSTRATIONS

LIST OF ILLUSTRATIONS

LIST OF TABLES

I. INTRODUCTION

The noise fields associated with present day flight vehicles, and with foreseeable future flight vehicles, are primarily generated by large, expensive propulsion devices. Investigating these noise fields is usually costly due to the complex facilities required to operate the engines and to make measurements of the noise field. Another problem results from the fact that at the early stage of vehicle design an engine prototype usually is not available for several years for noise tests. For noise to be adequately considered at the early stage of vehicle design, an alternate means of studying the noise fields must be devised in order that such studies can be performed prior to prototype operation. The development of techniques of scaling models for acoustic purposes appears to be the logical solution to the above problems.

Among the advantages of using scaled models in place of full scale items are lower cost of experimental facilities and test operation, lower manpower requirements in conducting a noise survey and, in many cases, the possibility of using simplified and therefore less expensive instrumentation. The use of models can improve timing by making it possible to obtain experimental data early enough to influence vehicle design. This is of particular value in the near field, where other means of adequately defining the noise field are usually lacking.

Scale models of jet-type engines have been used for acoustic studies for several years, with varying degrees of success and acceptance. The acceptance of models for studying near field noise has not been comparable to that accorded models for studying far field noise, partly because of the added complications encountered in the near field. A considerable amount of near field model data are reported here for the purpose of demonstrating that near field acoustic models are valid. It is also hoped that the comprehensive study of model techniques which is reported here will result in improved, more useful acoustic models of near field noise. It is the specific intent of this study to establish the validity of using different types of models for near field noise investigations and to determine the limitations of near field acoustic models.

The technical content of this report is divided into several sections. Section II presents the analytical basis for major aspects of jet noise modeling. A description is made of the fundamentals involved in the generation, propagation, and measurement of noise. The techniques involved in properly scaling each of these elements is examined. Sections III and IV present the instrumentation, facilities and procedures which have been used in a variety of model tests involving near field noise. Results of the experimental program are presented in Section V. Comparisons are made between the measured jet and rocket noise fields of scale models with their full scale counterparts. The apparent suitability of several possible techniques which would simplify the use of models are considered. Conclutions regarding the overall usefulness of acoustic scale models for studying near field noise are summarized in Section VI.

Manuscript released by the authors 24 April 1961 for publication as a WADD Technical Report.

II. AN ANALYTICAL BASIS FOR MODELING

Any noise problem is necessarily concerned with the source, propagation, and measurement of the noise. In this section each of these three fundamental items will be considered in turn. It is intended that this will cover the major points which must be considered in the design of a scale model jet which can be satisfactorily used for studying near field noise.

The analytical approach presented here will be based on the physical model of jet noise as proposed by Lighthill.[8] This considers the noise field to be due to a distribution of quadrupole sources representing the noise generation by turbulent flow within the jet. Proceeding from this point, an attempt will be made to define valid scaling laws from the equations which describe the physical processes of generation and propagation of jet noise. The first part of this section considers the scaling concepts of noise generation by a simple source, application of these concepts to aerodynamic noise generation, and finally, brief consideration of sources of noise other than the basic turbulence noise. Succeeding portions of this section cover the scaling laws and sources of scale error applicable to propagation and measurement of noise from acoustic models.

A. Noise Generation

No one theory has been generally accepted which explains all of the experimentally observed characteristics of jet noise. Lighthill himself has pointed out the paradox of trying to explain the precision with which the acoustic power of subsonic jets varies with the eighth power of velocity. However, there seems to be little doubt that his theory will form the basis upon which a more general solution will be founded.[8,9,10,11,12,13,16] The similarity of aerodynamically generated noise fields will be analyzed by considering the problem as separable into three elements: (1) similarity of noise generation, (2) similarity of flow, (3) similarity of noise propagation. This over-simplification of the problem of aerodynamic noise generation is used solely as a basis for studying the similarity concepts from the point of view of the acoustician concerned with measurement of the noise field. For this reason, the first step will be to consider basic similarity rules for acoustic sources.

1. Acoustic Sources

Noise Generation by Spherical Sources

The simplest type of noise source can be considered as a stationary pulsating sphere whose surface fluctuates radially with a velocity, uniform over the surface,

$$U_i = \sqrt{2}\, U \cos \omega t \qquad (1)$$

where U is the rms value of the surface velocity.

When this boundary condition is imposed on the general solution to the spherical wave equation, the sound pressure radiated by this simple harmonic source[19] may be shown to be as follows:

$$p_i = \frac{\sqrt{2}\,\rho\omega\,[4\pi a^2 U]}{4\pi r}\left[\frac{Ka + j}{1+(Ka)^2}\right] \exp\left[j\omega t - K(r-a)\right]$$

where p_i = instantaneous sound pressure at the radius r

ρ = density of the medium surrounding the sphere

ω = angular frequency of oscillation = $2\pi f$

a = radius of sphere

r = distance from source to observation point

K = wave number = $2\pi/\lambda = \omega/c$

$j = \sqrt{-1}$

The strength of such a source is usually identified by its volume rate of flow at the surface, $Q_0 = (4\pi a^2 U)$. However, this is not an appropriate parameter to use for consideration of <u>similarity</u> of aerodynamic noise sources. A more convenient form of the above equation is given by the rms value of the real part as

$$p = U \cdot \frac{a}{r} \rho c \frac{Ka}{\sqrt{1 + (Ka)^2}} \qquad (2)$$

where c is the velocity of sound in the medium surrounding the sphere.

The specific radiation impedance imposed on this pulsating sphere is defined by the ratio of the pressure to velocity at the surface (r = a). This can be shown to be[22]

$$Z = \rho c \left[\frac{(Ka)^2 + j(Ka)}{1 + (Ka)^2}\right] \qquad (3)$$

The power radiated into the far field can be assumed to be the same as generated at the source, which is, assuming a "constant velocity" source,

$$W_o = U^2 \left[\rho c \cdot \frac{(Ka)^2}{1 + (Ka)^2}\right] 4\pi a^2 \qquad (4)$$

However, the rms pressure observed in the far field may be given by

$$p_r \approx \sqrt{\frac{\rho_o c_o}{\rho c}} \left[U \cdot \frac{a}{r} \cdot \rho c \frac{Ka}{\sqrt{1 + (Ka)^2}}\right]$$

which accounts for a difference that may exist between the value of ρc at the source

and the value $\rho_o c_o$ in the far field. This general form for expressing the power output and radiated pressure will be retained when considering other more complicated sources. Before proceeding, however, the significance of the term Ka needs to be considered. When expressed in the form

$$Ka = \frac{2\pi}{\lambda} \cdot a = \pi \cdot \frac{d}{\lambda} = \pi \cdot \frac{fd}{c_o} \tag{5}$$

it is more recognizable as a non-dimensional frequency, where d is taken to be the diameter of the source. Based on normalization of a large quantity of jet and rocket noise data, it has been shown recently[16] that the peak of the acoustic power spectral density occurs at a non-dimensional frequency

$$\frac{fd_c}{V_c} \cdot \frac{a^*}{c_o} \approx 0.25$$

where f = frequency

d_c = characteristic diameter of flow

V_c = characteristic velocity of flow

a^* = critical velocity of sound in flow

c_o = ambient speed of sound.

It is further suggested that for supersonic jets the characteristic velocity of flow in the region where the majority of the noise is generated is the same as the critical velocity of sound at this point (i.e.-the jet is just sonic at this point). In this case, then, the characteristic frequency becomes simply,

$$\frac{fd_c}{c_o} \approx 0.25$$

If the velocity of sound, c, used in equation (5) is, in fact, identified as the ambient velocity of sound in the air surrounding a jet, then a typical value of the parameter Ka should be, according to the above,

$$Ka \approx \pi \cdot \frac{fd_c}{c_o} \approx 0.8$$

The point of this exercise is to examine the validity of the assumption that is ordinarily made in considering the noise field of a dipole or quadrupole to be definable in terms of a combination of monopoles. The latter type of noise source is, of course, a special case of the spherical source where the size is assumed to be much smaller than a wave length so that the wavelength parameter, Ka is very much less than one for a monopole or point source. Since it appears that in practice Ka may not be small compared with one, the assumption of a point source may not be entirely accurate. In any event, it is clear that duplicating this parameter is fundamental to the scaling of acoustic sources. Equation (5) then yields the important result that the source diameter and characteristic frequency have an inverse first power relationship.

Monopole Source

As indicated above, when the size of the source is small enough the source is called a monopole and has an rms pressure field and power output described by the equations

$$P \approx \sqrt{\frac{\rho_o c_o}{\rho c}}\, U \rho c\, (Ka)\, \frac{a}{r} \qquad (6)$$

$$W_o = U^2 \cdot \left[\rho c\, (Ka)^2\right]\left[4\pi a^2\right]$$

An example of this type of source is the pulse jet, which creates noise by literally pumping gas into the air.

Dipole Source

The dipole source, formed when two monopole sources of opposing phase are placed a differentially small distance apart, generates a noise field which represents the noise radiated by flow of air over an obstacle or over the surface of a non-rigid plate.[20] The noise radiated by turbulent eddies in a jet passing through a shock wave also exhibits the directional characteristics of a dipole noise field. The physical model of such a source is the rigid sphere oscillating back and forth along a line through its center. The rms pressure radiated by this source and its power output are defined[20,21] by the equations

$$P = \sqrt{\frac{\rho_o c_o}{\rho c}}\, \frac{1}{2}\, U \left[\rho c\, (Ka)^2\right]\left[\frac{a}{r}\right]\left[1 + \left(\frac{1}{Kr}\right)^2\right]^{\frac{1}{2}} \cos\theta \qquad (7)$$

$$W_o = \frac{1}{12}\, U^2 \left[\rho c\, (Ka)^4\right]\left[4\pi a^2\right]$$

where U = rms velocity of the oscillating sphere.

θ = angle relative to axis of dipole.

Lateral Quadrupole

The combination of two opposing dipoles (or forces) which are acting along lines separated by a small amount is called a lateral quadrupole and has a physical model represented by a stationary sphere whose surface is deformed into a spheroid, first along one axis, and then along a second orthogonal axis. This is the simplest type of source which can be used to represent the generation of aerodynamic noise where no mass is introduced and no solid boundaries are present. The pressure radiated by this particular combination of point sources is proportional to[20]

$$P \propto \sqrt{\frac{\rho_o c_o}{\rho c}}\, U \left[\rho c\, (Ka)^3\right]\left[\frac{a}{r}\right]\left[\left(2 + \frac{3}{(Kr)^2}\right)^2 + \left(\frac{2}{Kr}\right)^2\right]^{\frac{1}{2}} \sin\theta \cos\theta \qquad (8)$$

where θ is the angle relative to the quadrupole axis.

In this case the source velocity, U, cannot conveniently be identified in the same way as for the dipole or monopole. Thus the source strength must be determined by dimensional analysis or by experiment. Another type of quadrupole, the longitudinal quadrupole, is also significant in defining the structure of aerodynamic noise, but as it differs primarily in directivity, it will not be considered here. The power output of either quadrupole source is proportional to

$$W_o \propto U^2 \left[\rho c (Ka)^6\right]\left[4\pi a^2\right] \tag{9}$$

This expression will become more recognizable after making certain simplifications. First the speed of sound associated with the region near the source is taken to be the ambient speed of sound.[8] The second simplification will be to employ the dimensional equivalence that

$$Ka = \pi \cdot \frac{2a}{\lambda} = \pi \cdot \frac{fd}{c_o} \propto \frac{U_c}{c_o}$$

That is, the diameter of the source, as measured in wavelengths, is dimensionally and qualitatively equivalent to the ratio of the typical flow velocity to the ambient speed of sound outside the flow. This procedure may seem more acceptable when stated in the form

$$\text{characteristic time} = \frac{d}{U_c} \approx \frac{\lambda}{c_o}$$

Employing the above considerations, equation (9) can now be written

$$W_o \propto \left[\rho U_c^3 \left(\frac{U_c}{c_o}\right)^5\right]\left[4\pi a^2\right]$$

and this is recognized as a form similar to the Lighthill equation. The source velocity, U, of a quadrupole has now been identified as being equivalent to a local stream velocity U_c. For the general types of sound sources described above, the mean square sound pressure in the near or far field can be expressed as

$$P^2_{(r,\theta)} \propto \rho_o c_o \cdot \frac{W_o}{\beta r^2} \cdot G_1(\theta) G_2(Kr)$$

which is

$$P^2_{(r,\theta)} \propto \left[\frac{\rho_o}{\rho}\right]\left[\rho U_c^2\right]^2\left[\frac{U_c}{c_o}\right]^n \cdot \frac{4\pi}{\beta}\left[\frac{a}{r}\right]^2 G_1(\theta) G_2(Kr) \tag{10}$$

where n = 0, 2, or 4 for a monopole, dipole or quadrupole

β = Solid angle of radiation (4π for free space)

$G_1(\theta)$ = Directivity factor

$G_2(Kr)$ = Near field factor.

Summary of Acoustic Similarity

A simple expression is now available which suggests the basis for scaling aerodynamic noise. The following tentative rules can then be chosen for obtaining comparable sound levels for jets, at scaled frequencies.

(1) Fluctuating pressures within the flow, signified qualitatively for now by the term ρU_c^2, must be maintained the same.
(2) A velocity characteristic of the source must be maintained the same, relative to the velocity of sound in the ambient atmosphere.
(3) The position of the observation point must be maintained at the same angle and radius (in source diameters) from the source.
(4) The overall geometry of the noise source and nearby reflecting surfaces must be maintained.

In general, scaling the geometry is readily accomplished in any model experiment to any reasonable degree of accuracy desired. Less certain, however, is the amount of error that may be introduced by subtle changes in the position of reflecting planes or obstacles in the noise field. This aspect of scaling is considered in more detail later in this section along with other problems involved with the propagation of the noise field. A far more difficult problem in scaling jet noise fields is associated with the first two rules indicated above, duplicating flow parameters on a scale model. It may even be desirable to scale (rather than duplicate) flow parameters such as temperature and pressure, further complicating the problem.

2. Noise Generation by Jet Turbulence

The theory of jet noise generation, as developed by Lighthill, considers the turbulent flow of a jet as acoustically equivalent to a distribution of quadrupole noise sources which have an effective strength per unit volume which is of the order of ρu^2, where ρ is a typical jet density and u is the rms value of a typical fluctuating velocity.

The similarity of aerodynamic noise generation by a jet will therefore be a function of the jet density, intensity of the fluctuating velocity (turbulence), and the distribution of turbulence within the jet. There are three additional effects which influence the intensity and directivity of the noise generation: convection of the sources, shear in the mixing region, and refraction of the noise at the boundaries of the jet.[8,9] The effects of shear can be expected to exhibit similarity due to the strong similarity of velocity profiles of all turbulent jets[24,25] so that the magnitude of the local velocity, U_c, should provide an indication of the shear effect. The effect of convection and refraction at the moving boundary of the jet should be governed by the Mach number of the flow and the ratio of the velocity of sound in the flow to the velocity of sound in the

ambient atmosphere.[9] Thus the necessary and sufficient variables which should define the basic aerodynamic noise generation would be

$$\rho u^2 , \; U_c/c_c , \; c_c/c_o$$

The normalized intensity of turbulence, u/U_c , has been shown to decrease with increasing Mach number.[24]

This simplified consideration of the flow similarity suggests, therefore, that the noise generation should depend primarily on the flow parameters

$$\rho U_c^2 , \; U_c/c_c , \; c_c/c_o .$$

If it is assumed that the sources will be quadrupoles, which have a directivity modified by the effects of convection, shear, and refraction, a general expression for the noise field of the jet is obtained by modifying equation (10) to:

$$p_{r,\theta}^2 \propto \left[\frac{\rho_o}{\rho}\right]\left[\rho U_c^2\right]^2\left[\frac{U_c}{c_c}\right]^4\left[\frac{c_c}{c_o}\right]^4\left[\frac{4\pi}{\beta}\right]\left[\frac{a}{r}\right]^2 G_1\left(\frac{U_c}{c_c}, \frac{c_c}{c_o}, \theta\right) G_2(Kr) \qquad (11)$$

Until the form of this expression had been verified experimentally, there was very little basis for assuming that additional variables were not required. However, evidence[16,27] that has been obtained on jets ranging in size from small cold air jets, less than an inch in diameter, to large rocket engines strongly supports the form of equation (11). It must be pointed out that agreement is obtained between theoretical predictions and observed values of the noise power generated by rockets only when the gross differences in the flow structure of rockets, as compared to simple jets, are taken into account.[16]

The discussion, up to now, has considered an isolated quadrupole noise source of only one frequency. For similarity to be maintained for the noise field of the entire jet, it will be assumed that it is necessary and sufficient to require that a typical linear dimension of the flow be proportional to a characteristic nozzle diameter, provided that the flow parameters of the jet are duplicated. This assumption also implies that the resultant noise field of all the sources in the jet can be predicted if only one so-called "source" at some typical frequency (e. g. - the frequency of highest spectrum level) is defined. It follows then, that the frequency spectrum of the noise from jets of varying diameter but constant flow characteristics would have to be similar. Such a similarity is indeed observed,[16] so that the typical dimension of an individual noise source can now be considered as equivalent to a characteristic diameter, d_c, of the jet nozzle.[24] Two exceptions to this rule will be (a) the physical diameter of a rocket engine nozzle cannot be used for a characteristic diameter if the engine is operating over or under expanded, and (b) the physical diameter of a very small scale model jet may not represent the characteristic diameter due to the finite boundary layer at the exit. This latter problem is evaluated later in this section.

3. Scaling of Turbulent Flow

Similarity Parameters

From the arguments presented above, a suitable non-dimensional form for the noise field of a jet is

$$\frac{p_{r,\theta}^2}{(\rho_j U_j^2)^2} \propto \left[\frac{\rho_o}{\rho_j}\right]\left[\frac{U_j}{c_j}\right]^4\left[\frac{c_j}{c_o}\right]^4\left[\frac{4\pi}{\beta}\right]\left[\frac{d_j}{r}\right]^2 G_1\left(\frac{v_j}{c_j}, \frac{c_j}{c_o}, \theta\right) G_2(Kr) \qquad (12)$$

where the subscript j represents typical values at the center of the noise producing region of the jet and the subscript o refers to ambient conditions.

Inspection of equation (12) reveals that maintaining full scale values of jet Mach number, velocity, and density in a scaled model will result in the same magnitude of acoustic pressures at appropriately scaled observation points. It remains to be seen whether equation (12) can be used as a basis for using flow parameter values in the model which are different from the full scale values, in addition to changing the physical size of the nozzle in the model.[45] It is emphasized that the assumption that a typical jet flow dimension must be proportional to a characteristic jet diameter, as the model diameter is changed, is tenable only if the values of the basic parameters (Mach number, density, etc.) are maintained. This is one of the key points in establishing the validity of an acoustic model jet.

Two significant experimental findings will be cited to further clarify the position taken. Studies of turbulence for cold subsonic jets have shown that at a given position in the mixing region, the scale of turbulence, L, is nearly independent of Reynolds number (for a given nozzle diameter, d), but directly proportional to the axial distance, X, along the jet.[24] Thus, at an axial position X, the scale of turbulence, L, will be

$$L_x \propto d \cdot F\left(\frac{x}{d}\right)$$

where the function $F\left(\frac{x}{d}\right)$ should be linear with $\frac{x}{d}$.

Measurements of the flow boundary of a variety of heated air jets and small solid propellant rockets have shown that the width of the jet, W, in the subsonic mixing region could be defined[25] by

$$\frac{W}{d} \propto \left(\frac{x}{d}\right)^{1.16}$$

which is very nearly the linear relationship required. The constant of proportionality, however, was dependent on Mach number of the jet.

From these same tests it was also established that the axial position of the subsonic flow region, where the majority of the noise is generated, was a predictable function of the exit Mach number.[16,25] Thus, in general, the criterion for flow similarity appears to be approximately true.

In summary, it is readily apparent that a thorough knowledge of the mechanism of noise generation by jets is the ultimate approach to making a scale model of the noise source. The fact is that we cannot define all the characteristics of the noise field in terms of the known or measured parameters of the jet exhaust. Exhaust gas parameters such as viscosity, ratio of specific heats, temperature, velocity, density, diameter, internal energy, Mach number, etc., no doubt all influence the noise produced by the exhaust gas. If the effect of each exhaust parameter were known, it would be very straightforward to use a jet with almost any parameters as a model of some other jet. Employment of such techniques in a completely general manner is not possible at the present time.

From the preceding analysis it has been concluded that for all source mechanisms the density, velocity, and Mach number terms are the most significant. Although other parameters may be important to the fine details of the noise field, it is hypothesized that models which duplicate density, velocity, and Mach number will have considerable usefulness in the study of near field noise. Note that this results in models operating on the basis of constant efficiency (ratio of acoustic energy to kinetic energy) relative to the full scale counterpart, since kinetic energy is proportional to density times the third power of velocity. This is not to say that all jet noise sources have the same efficiency of noise generation, but rather that sources which differ only in diameter have the same efficiency. A small deviation from this, which applies to very small nozzles, is discussed later.

Having decided to consider only the gas flow parameters density, velocity, and Mach number, the question remains as to where each parameter should be evaluated. Any one of these has a wide range of values at different locations within a given exhaust flow. For example, the velocity at the point of origin of a particular octave band of sound, assuming it could be localized, is possibly more important to the generation of that frequency than is the value of velocity at any other point within the exhaust. However, in general, if two similar jets have the same velocity at some characteristic location, then the velocities at all scaled locations within the flow must be similar. To choose a velocity which is easily defined for any jet would appear to be logical. The fully expanded nozzle exit velocity is the velocity which will be chosen for consideration in all jets. Similarly the density and Mach number to be considered will be those present at the nozzle exit of any particular jet.

Providing Necessary Parameters

It is appropriate at this point to consider the practical matter of producing a desired set of nozzle exit conditions. Two general means of accomplishing this will be described.

First, if the model uses the same gases as the full scale jet, it is necessary only to provide the same plenum temperature and pressure in the model as are present in the full scale jet in order to automatically provide proper values of all fully expanded exit conditions. If the model gases are similar to but not identical to the full scale gases, then small adjustments can be made in the plenum temperature and pressure which will result in almost the exact exit conditions desired. An example of this is the use of different fuels, model to full scale, where both fuels are hydrocarbons.

If other means of providing these exit conditions can be found which appear to be preferable on the basis of involving simpler procedures, they should be considered. The use of less expensive facilities or lower gas temperatures, for example, would simplify model testing. A general means of providing the desired exit conditions by using a gas other than that used full scale (a "substitute" gas) will be discussed here.

Tempelmeyer[34] describes an analytical method for doing this. The use of an ambient temperature gaseous mixture, specified by the simultaneous solution of three mixture equations, which has macroscopic properties and flow parameters similar to those of a hot jet engine is suggested. Solutions could not be obtained for simulation of afterburning engines or rockets by this method on the basis of the initial analysis. No experimental verification was attempted by Tempelmeyer. The explosive or toxic nature of all gas combinations for which solutions were found in Reference 34 is perhaps less restrictive for use in aerodynamic measurements in a wind tunnel (the purpose of the reference study) than for making acoustic model jets. However, it should be noted that at present only the exhaust parameters density, velocity, and Mach number are considered significant, and a reasonable mathematical correction can probably be made if density or velocity differ by not more than perhaps 10 or 20 per cent from the desired values for these parameters.

A study of Tempelmeyer's work reveals that if the ratio of specific heats of the model and full scale gases are the same, virtually all other requirements are met by setting the product of gas constant and absolute temperature equal to the full scale product. The observation was then made that steam (a gas not considered by Tempelmeyer, apparently because of its higher temperature) has almost the identical ratio of specific heats as a turbojet exhaust. Steam is of course subject to the criticism that it is really a stream of water particles which will not mix with surrounding air in a realistic fashion. However, this particular objection is removed by using superheated steam. Since the gas constant for superheated steam is about 1.6 times that of a turbojet exhaust, the absolute temperature required by the steam is about 5/8 of the turbojet absolute temperature. With suitable small adjustments in pressure, the steam then does closely match all of the important characteristics of a turbojet exhaust and is still superheated even at the fully expanded temperature. All other individual gases with a ratio of specific heats in the proper range have either a serious handling problem or a gas constant lower than that of a full scale jet exhaust, thereby requiring operation at temperatures higher than used for air and defeating the main purpose of simplifying the model.

One more approximation to Tempelmeyer's more rigorous approach seemed appropriate. If it is assumed that it is not too difficult to mathematically correct the measured values of the noise field when erroneous values of density are used, a gas with the incorrect ratio of specific heats can duplicate exit velocity and Mach number at a low plenum temperature provided that it has a high acoustic velocity. Of the few gases with this latter property, helium is the safest and most easily-handled gas. Far field data from earlier experiments with an unheated helium jet and a cold air jet[47] also encouraged the use of helium. In some respects its usage for this purpose is very restrictive. For example, if exhausted at a typical turbojet Mach number and ambient temperature, its exit velocity is considerably higher than that of a full scale jet. However, depending upon the Mach number employed by the particular engine, a helium jet at ambient temperature can duplicate the Mach number and exit velocity of an afterburning turbojet engine or a rocket

engine fairly well. A small degree of temperature control on the helium flow would improve the flexibility of its use considerably, even permitting its use to simulate a military turbojet condition if the helium flow is cooled. It is unlikely that this latter application will ever be considered practical. For helium simulation of an afterburning engine, the first power density correction required will probably not be greater than 3 db. For simulation of a rocket, this same correction will tend to be larger, perhaps approaching 10 db in some cases.

In practice a great majority of the practical model tests will utilize a gas identical to full scale.

Limitation on Minimum Nozzle Size

Two basic items must be considered in making scale models very small. These are the discharge coefficient and whether the flow is laminar or turbulent.

Figure 1 shows discharge coefficient (actual mass flow divided by ideal mass flow) as a function of Reynolds number (based on throat diameter) as theoretically derived in Reference 35 for a particular nozzle. The nozzle chosen has fundamental geometric characteristics which do not differ greatly from most nozzles in use. Other experimental and theoretical investigations referred to by Reference 35 grouped quite well around Figure 1 with a scatter of ± 1% or less over most of the usual Reynolds numbers. For a model employing the full scale gas at full scale temperature and pressure, the Reynolds number is directly proportional to nozzle diameter. Since typical full scale Reynolds numbers are of the order of a million, reducing the nozzle diameter by a factor as large as one hundred will still usually allow a discharge coefficient greater than 0.90. Since a coefficient less than 1.0 is equivalent to a reduced effective nozzle area, this may be compensated for by making the model throat area oversize by the percentage its discharge coefficient falls below its full scale counterpart. In the case of coefficients above 0.90, the failure to correct for area would theoretically cause an error of less than 1/2 db.

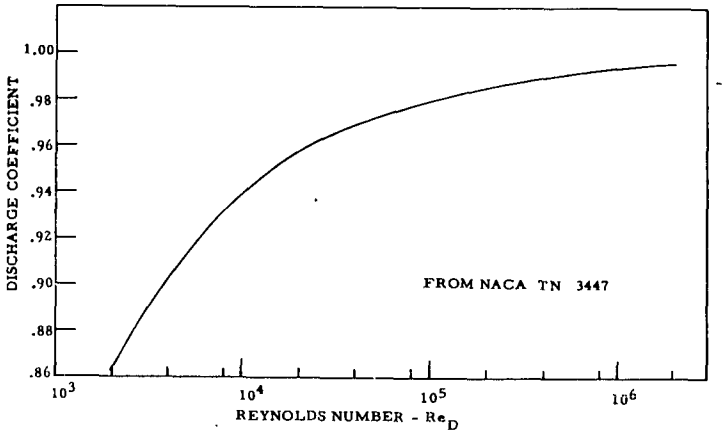

Figure 1. Discharge coefficient as a function of Reynolds number for a typical nozzle.

At Reynolds numbers between 2000 and 3000, flow through a nozzle throat changes from laminar to turbulent. To preserve similarity, all models should fall in the same Reynolds regime (laminar or turbulent) as their full scale counterparts, and therefore all acoustic model jets should have Reynolds numbers greater than 3000. Referring to Figure 1, it is apparent that specifying that Reynolds numbers shall be greater than 3000 also results in nozzle area corrections not greater than 1/2 db.

Accuracy of Flow Measurements

Inaccuracies in construction or operation of a model will result in errors. The effect of these inaccuracies can be estimated easily by assuming that any errors must have an effect on the total radiated power of less than 1/2 db. Since power is proportional to the square of the nozzle diameter, a 6% diameter inaccuracy would be required to produce the 1/2 db error.

The other major error possibility which will be considered is that due to the model operating at some velocity other than that intended, which in turn is a result of inaccurate temperature or pressure instrumentation. If radiated power is assumed proportional to the eighth power of velocity, a 1 1/2% error in jet velocity would change the radiated power 1/2 db. The velocity is proportional to the square root of absolute temperature, so a 3% error in absolute temperature would produce the 1/2 db error. In the case of a military turbojet, this would require a 4 1/2% error in the gauge temperature determination. Jet velocity is dependent upon total pressure in a somewhat more complicated manner than for temperature, but evaluating this dependence for a typical military jet shows that a 4% error in gauge pressure determination would produce sufficient error in the jet velocity to change the radiated power by 1/2 db. For afterburning jets, and especially rockets, these values will be somewhat different. When the velocity exponent is less than eight, the effect of a small velocity error is even less important. The accuracy with which temperature or pressure can be measured is better than the values given above, so it may be concluded, in general, that any errors in a carefully built and operated model due to inaccurate construction or operation will probably produce no more than about 1/2 db error in the total radiated power.

4. Scaling of Other Noise Sources

Other potential sources of aerodynamic noise which must be considered are shock-turbulence noise and combustion noise.

Shock-turbulence Noise

Early studies of supersonic jets demonstrated the importance of noise created by the interaction of convected turbulence and quasi-stationary shock waves in the flow.[17,18] The predominant characteristic of this noise is the presence of an intense high frequency noise source which has the directional characteristics similar to a dipole noise field and has a characteristic frequency and intensity predicted by the following relationships[13,23]

$$f_c = \frac{V}{dN}\left[1 + \frac{2}{\sqrt{P_T - P_c}}\right], \quad N = 6 \text{ or } 7 \tag{13}$$

$$p^2 \propto \left[\frac{P_o^2\, G(P_T/P_o)}{\rho_o c_o}\right]\left[\frac{d}{r}\right]^2 \tag{14}$$

V = flow velocity

f_c = characteristic frequency of shock-turbulence noise

P_T = chamber pressure

P_c = critical chamber pressure

P^2 = mean square pressure in noise field

P_o = ambient static pressure

$G(P_t/P_o)$ = undefined function of the nozzle pressure ratio

r/d = distance to field point in nozzle diameters

The equations above appear to indicate that the intensity and frequency of this noise could be studied on a scale model which duplicated the exit Mach number and ensuing shock structure in the flow. However, there is some question as to the significance of this noise source for high temperature supersonic jets. Noise from supersonic rockets appears to correlate more readily with some modified form of the Lighthill equation without any consideration of the shock-turbulence noise.[13,16] As an indication of the effect of temperature in decreasing the apparent effect of this noise, a brief test was made on a convergent-divergent nozzle over a range of pressure ratios to explore the discrete frequency noise as a function of exit Mach number and temperature. A typical result from this pilot study is shown in Figure 2. For the hot jet, wide band turbulence noise predominates. Where the overall sound level of the cold jet deviates from the trend in sound level versus Mach number shown for the hot jet, a discrete frequency dominates the spectrum. Similar results have been observed for other model tests.[14]

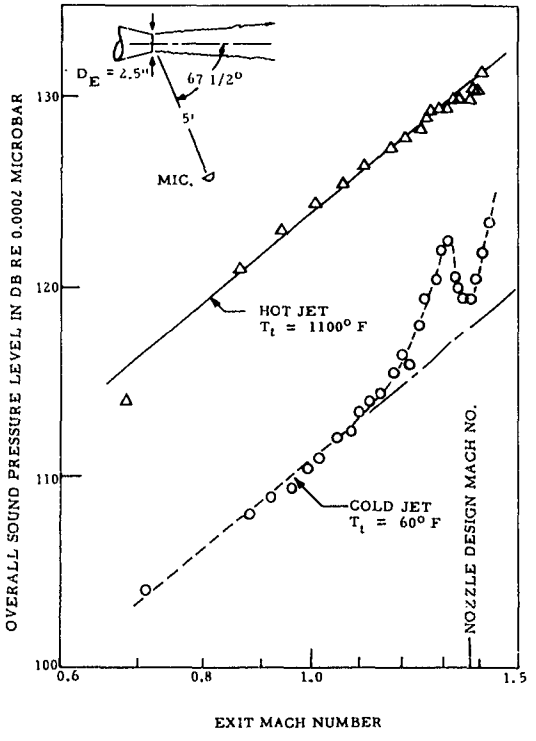

Figure 2. Illustration of cold jet shock-turbulence noise.

Combustion Noise

Another potential source of noise which must be considered in the development of an acoustic model jet is that due to an instability or fluctuation in the combustion process. While this phenomenon is usually confined within the combustion chamber, it can influence the external sound field in a very significant manner. In one well documented case, the instability took place in the flame outside the nozzle and generated very intense pressures in the near field.[3] In general, the engine manufacturer tries to eliminate the instability phenomenon since it can easily cause catastrophic failure of the engine. However, since it may be necessary to attempt to scale this acoustic source or, what is more likely, avoid its occurrence in a scale model, a very brief review of the scaling concepts of the phenomenon is given. It must be emphasized that a far more detailed analysis would be required if this complex phenomenon represented the major noise source which one wished to study on a model scale.[4,5]

Low Frequency Fluctuations.--The most severe combustion instability occurs on full scale liquid rocket engines at low

frequencies (i.e.-below 100 cps) and may generate fluctuating pressures within the combustion chamber of 5 to 30% of the stagnation pressure.[4] The mechanism of this low frequency resonance may be explained as follows: Fuel introduced into the combustion chamber delays its ignition until it has absorbed sufficient energy to support combustion. When this ignition delay time, τ , is of the same order as the so-called residence time, t_r , of the combustion gases within the chamber, then unstable combustion can occur if the reaction processes are properly phased in time. Each of these characteristic times is dependent on certain parameters of the liquid rocket engine so that a criterion for instability may be expressed qualitatively as follows:

$$\tau \approx t_r$$

where

$$\tau = F \left[\begin{array}{l} \text{Pressure drop across fuel injection head,} \\ \text{Combustion chamber pressure,} \\ \text{Fuel composition and mixture ratio} \end{array} \right]$$

$$t_r = \left[\frac{\text{Chamber Volume}}{\text{Throat Area}} \times \frac{1}{\text{Characteristic Velocity}} \right] = \frac{L^*}{C^*}$$

Thus, the ignition delay is primarily a function of the engine design and fuel, and is not strongly dependent on scale, per se, while the residence time is directly proportional to the scale of the engine. Therefore, it is not possible to maintain the same relationship between these characteristic time delays for various scale factors by using any simple linear scaling law. Empirical methods would be required to adjust the ignition delay time if it were necessary to achieve or to avoid a combustion instability. The frequency of oscillation will be inversely proportional to the time delay, t_r . When it does occur, this phenomenon is characterized by fluctuations in the fuel feed system, pressure and temperature fluctuations throughout the combustion chamber, and propellant flow-rate variations. Due to the last mentioned aspect, one would expect the noise field to have the directional characteristics and efficiency of a monopole sound source. A pulse jet is a good example of an engine with a controlled instability of this type and it does indeed exhibit the characteristics of a monopole noise source.[6] For model tests employing heated air jets, a muffler should be used in the line between the burner and exit to prevent any of this low frequency burner noise from appearing in the radiated noise field.

High Frequency Resonance.--A more common form of combustion noise observed on afterburning turbojets and liquid and solid propellant rockets occurs at acoustic resonant frequencies of the combustion chamber. Standing waves in the combustion chamber can have a reinforcing action on the combustion process when they are properly located and phased with respect to the latter.[4,7] While these resonant oscillations are contained within the combustion chamber, they can develop very high sound levels outside the combustion chamber by noise transmission through the walls, noise radiation out the nozzle exit, or by actual modulation of the overall flow.

Like the low frequency phenomenon, a delay time associated with the burning process must coincide with a characteristic time of an acoustic resonant mode

within the chamber in order for the combustion oscillation to exist. Thus, a criterion for such an occurrence can be expressed as:

$$\tau \approx t_n = \frac{1}{f_n}$$

where τ is similar to the characteristic burning time defined above, and t_n is the period of the nth acoustic mode which has a frequency f_n. Experimentally, it has been found[4] that when

$$\text{Chamber Length/Diameter} = L/D > 4$$

then

$$f_1 \approx 0.36 \frac{C^*}{L}$$

and when

$$L/D < 4$$

$$f_1 \approx 0.59 \frac{C^*}{D}.$$

It is clear that proper scaling of the combustion chamber geometry is fundamental to scaling of this phenomenon. In addition to the obvious effect on frequency, it is also reported that for the short engines, $L/D < 4$, the amplitude of the oscillation is less than for the longer engines and is nearly always sinusoidal.

The ability to develop a scale model which duplicates a resonance of this type for a full scale engine has not been established. As with the low frequency instability, the characteristic burning time is more a function of engine design and fuel composition than of scale alone. It should be pointed out, however, that the resonant frequency relationships given above have been observed over a range of diameters of about 2 to 30 inches.

In summary, the minimum requirements which would probably have to be met by a scale model which could simulate a combustion instability would be (1) exact geometrical scaling of combustion chamber, (2) duplication of fuel composition and mixture ratio, and (3) duplication of combustion chamber conditions.

Although there does not appear to be any guarantee that these conditions are sufficient to insure that a valid model can be constructed, consideration of them should enable a model to be constructed which does not produce the high frequency resonance. This latter consideration will generally be the more important to the model designer.

B. Noise Radiation and Propagation

1. Identification of Near and Far Field

The noise field of an extended aerodynamic noise source, such as a jet, can be

broken down into three regions:

a. Near-near field (Region of pseudo-sound)

b. Near field (Region within finite size effects)

c. Far field (Region where source appears concentrated at a point)

In the previous sub-section, the expressions for the pressure in the field of a dipole or quadrupole sound source contained terms involving powers of the distance parameter, Kr. When Kr is no longer large compared to one, the pressure field no longer acts like that of a monopole. Reactive components then appear which exceed the inverse square law pressure field of the equivalent monopole source that exhibits the same level in the far field. To illustrate this effect, the combined inverse square law and near field terms, given by

$$10 \log \left[\left(\frac{1}{r} \right)^2 G_2(Kr) \right]$$

have been plotted on a relative scale in Figure 3 for all four types of sources considered earlier. It is clear that the near field effect for an isolated source is not significant until one approaches within 1/2 wavelength of the source. This region is, in effect, the near-near field mentioned earlier, for the non-linear increase in pressure as one approaches the source can be considered equivalent to the hydrodynamic pressure field (or region of pseudo-sound) generated by the turbulent flow.[20] It has, in fact, been shown that the mean square pressure in this region falls off inversely as the 6th power of the distance from the source, which is precisely the result predicted by the expression for the near field of a quadrupole. The important point is that this near field should be duplicated by a scale model, providing the flow parameters are equivalent.[15] It has been observed that the exit velocity profile and temperature of the jet have a very important effect on this hydrodynamic pressure field, unlike the radiated field for a jet.[15]

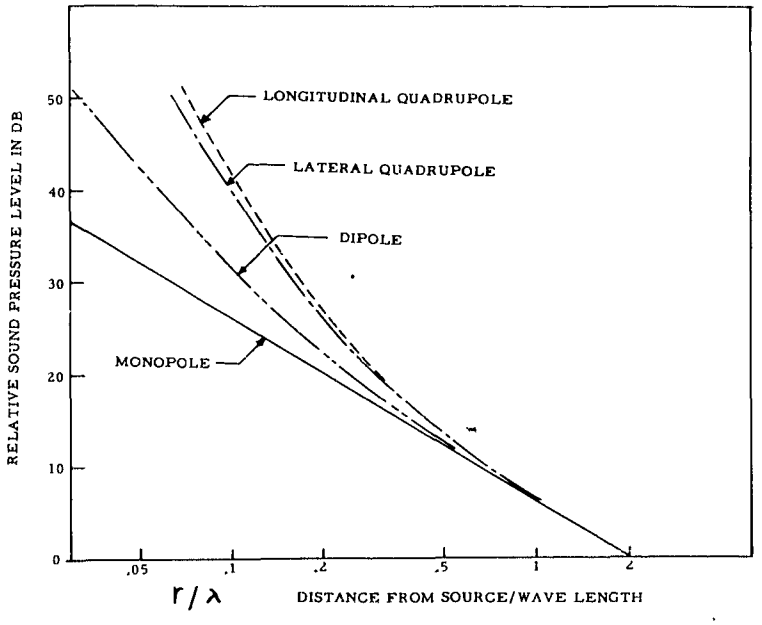

Figure 3. Relative near field sound pressure levels of multi-pole sources compared to monopole source.

Scaling of Radiated Field

The so-called near field of a jet may be described as the area outside the hydrodynamic pressure field (i.e. beyond 1 to 2 source dimensions) and inside of the region where the radiated pressure wave is essentially planar and in phase with the particle velocity. In other words in this area, sound at any given frequency may be arriving at a receiver from many different sources which are spaced along the jet so that the effective direction of the sound field is not readily defined. The mean square pressure in the near field may be considered as the summation of an array of N "sources" of the same frequency as given by:

$$p^2 = \sum_{j=1}^{N} \sum_{k=1}^{N} \left[\frac{P_{oj}\, G(\theta_j)}{R_j}\right]\left[\frac{P_{ok}\, G(\theta_k)}{R_k}\right]$$

where p^2 = Mean square pressure in field

P_{oj}, P_{ok} = rms pressures from the j th and k th source

$G(\theta_j), G(\theta_k)$ = Function of phase angle of j th and k th source

R_j, R_k = Radii to respective sources from a point in the field.

Space correlation measurements made in this area will not necessarily indicate sonic speed of propagation of the pressure disturbance. Again it can be said that this important area of the jet noise field will scale, provided that the relative position and intensity of the distributed noise sources are retained in terms of wavelengths. It is this one fundamental requirement for similarity in the near field which may be the most difficult to achieve if the flow is to be changed in Mach number, density, etc.

The extent of this near field region cannot be defined exactly, but it probably extends to a radius equal to twice the distance between the nozzle and the source of a particular frequency.[26] The outer region, or far field, presents no new problems with a scale model, and, as is the case with all regions closer to the source, the pressure should be the same at scaled positions for jets with the same flow characteristics.

Since the direction of wave propagation is known in the far field, provided there are no reflecting obstacles nearby, the space correlation between two points can be predicted from the following relationship.[30]

$$R_{r,r+\Delta r} = \cos\left[\sqrt{1+\left(\frac{\Delta f}{2f_c}\right)^2}\, 2\pi f_c \tau\right] \frac{\sin\left[\frac{\Delta f}{2f_c} 2\pi f_c \tau\right]}{\left[\frac{\Delta f}{2f_c} 2\pi f_c \tau\right]} \qquad (15)$$

where

Δf_c = bandwidth of noise

f_c = geometric center frequency of band

τ = time delay of sound wave between points

$$= \left(\frac{1}{f_c}\right)\frac{\Delta r \cos\theta}{\lambda}$$

Δr = separation between points

λ = wave length of f_c

θ = angle between sound ray and line joining points

This expression is plotted in Figure 4 for a narrow band (e.g.-sine wave) and for one-third and full octave bands of noise.

2. Scaling of Absorption Losses

The statement made above to the effect that there are no problems associated with scaling in the far field must now be qualified to account for possible scale errors due to atmospheric absorption of the sound.

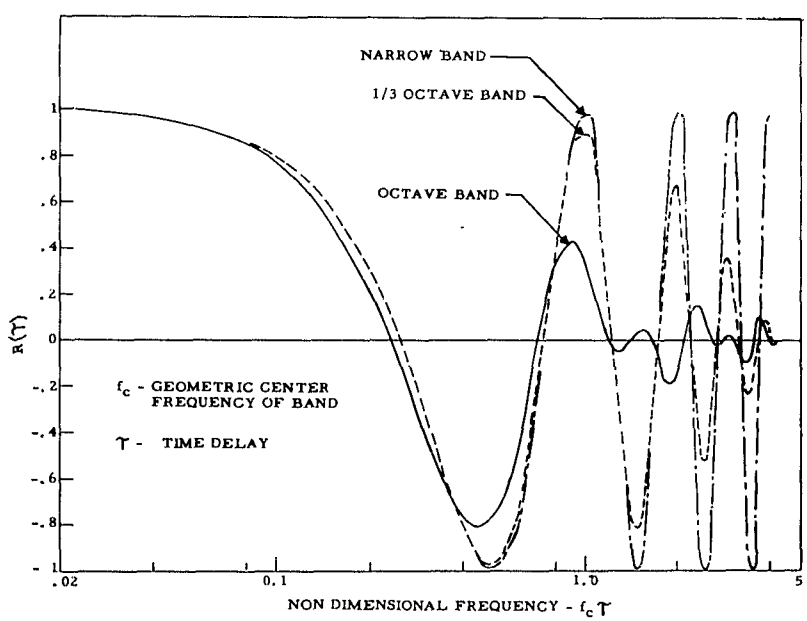

Figure 4. Auto-correlation coefficient of bands of white noise.

Acoustic model studies may involve measurements of frequencies up to 100 kilocycles. At this frequency, propagation losses due to (1) molecular absorption and (2) viscosity and heat conduction can amount to 1 db/foot. Since total power level determinations required for comprehensive model studies are ordinarily computed from sound pressure level measurements made at distances of the order of 10 feet or more from the source, an error of 10 db can be present in the computed power data at 100 kilocycles. The important question, however, is whether this represents a source of error in model versus full scale comparisons. The following shows that this is a significant error, and results are presented which may be used to correct model data for absorption losses.

For illustration of the absorption effects, the mean square pressure in the far field of a simple source may be expressed as

$$P_r^2 = P_o^2 \left(\frac{a}{r}\right)^2 e^{-.23A(r-a)}$$

where P_o = reference pressure at radius a

r = distance to the observation point

A = absorption loss in decibels/unit distance.

If measurements are made in the far field of two sources (1 and 2) which have the same reference pressures at their respective radii a_1 and a_2, the ratio of the mean square pressures will be

$$\frac{P_{r_1}^2}{P_{r_2}^2} = \left(\frac{a_1}{r_1}\right)^2 \left(\frac{r_2}{a_2}\right)^2 e^{-.23\left[A_1(r_1-a_1)-A_2(r_2-a_2)\right]}$$

In general, the absorption loss per unit distance will be a function of frequency, or

$$A = A(f)$$

Furthermore, if the two sources are related in size by a scale factor $F < 1$, and the observations are made at scaled positions (i.e. the same value of r/a), then the ratio of mean square pressures becomes

$$\left(\frac{P_{r_1}}{P_{r_2}}\right)^2 = e^{-.23(r_1-a_1)A(f_1)\left[1-\frac{A(f_2)}{A(f_1)}F\right]}$$

This ratio will be 1 only when the term in brackets is zero. This occurs only when the absorption loss is directly proportional to frequency. Unfortunately, the theoretical and observed values of absorption show absorption loss is more nearly proportional to the square of frequency. Thus, an inherent scale error will occur which can be more conveniently expressed in a decibel form per unit full scale distance as

$$E = -\left(1-\frac{a_1}{r_1}\right)A(f_1)\left[1-\frac{A(f_2)}{A(f_1)}F\right] \quad db/ft.$$

In the far field, $\frac{a_1}{r_1} << 1$, and since for the scale model $f_2 = f_1/F$, the scale error in decibels per unit full scale distance is:

$$E \simeq -A(f_1)\left[1-\frac{A\left(\frac{f_1}{F}\right)}{A(f_1)}F\right] \quad db/ft. \qquad (16)$$

The data in Reference 36 have been used to establish the absorption loss $A(f)$,

which may be expressed in the form

$$A(f) = K_1 \left[A_{Mol} + A_{class} \right]$$

K_1 is an empirical correction term to account for the difference between observed and theoretical absorption, A_{Mol} is the theoretical molecular absorption which depends on moisture content of the air, and A_{class} is the theoretical classical absorption. This expression is shown in Figure 5 for typical conditions.

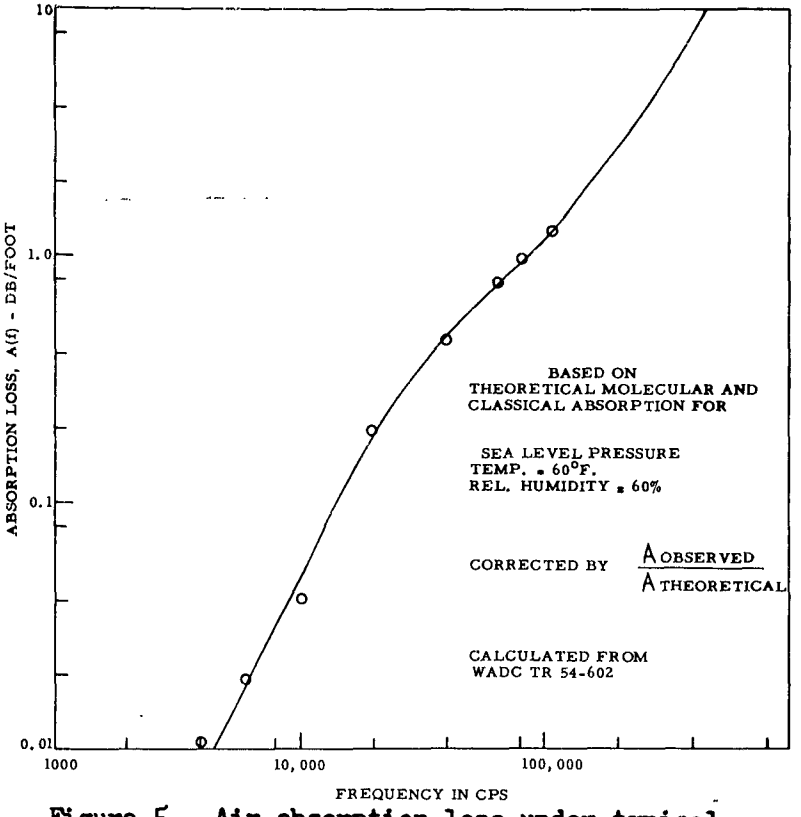

Figure 5. Air absorption loss under typical atmospheric conditions.

To illustrate the significance of this scale effect, the value of $A(f)$ shown in Figure 5 has been used in equation (16) to define the scale error for several scale factors. The results are plotted in Figure 6.

As an example, if power level measurements are made on a 1/10 scale model at a distance corresponding to 200 feet, full scale, the model data would be in error by 12 db at the frequency corresponding to the center of the equivalent full scale 4800-9600 cps octave band. However, a near field measurement at an equivalent full scale distance of 30 feet would be in error by only 1.8 db.

Under these conditions, the scale error due to absorption losses will not be significant for most near field measurements at frequencies below about 3000 cps, full scale. Power level measurements for models, however, may require significant corrections for frequencies above about 800 cps, depending on the scale factor.

In addition to the losses due to molecular and classical absorption, the effects of wind and turbulence must also be considered. In general, model studies should not be conducted under conditions involving appreciable wind or turbulence scattering. Measurements in the far field under such conditions are generally unreliable.

3. Scaling of Finite Amplitude Losses

The non-linear damping of intense sound waves is not ordinarily considered in the analysis of jet noise fields. However, to determine if a source of scale error exists, it is necessary to consider the phenomenon.[27] The predicted attenuation for

plane waves, plotted in Figure 33.6 of Reference 27, can be stated as

$$A' = .0046 \frac{P_I}{P_o} f X$$

A' = Attenuation in db

P_I = Initial peak amplitude of pressure wave

P_o = Atmospheric pressure

f = Frequency, cps

X = Path Length - ft.

This is re-plotted in Figure 7, showing that for plane sound waves the non-linear losses would generally exceed other forms of losses for initial levels greater than about 135 db. For spherical waves, a graphical estimate was made of the losses expected at 1000 cps and 10,000 cps when the level at 1 foot from a point source is 170 db. This is compared in Figure 8 with the losses at the same frequencies for a plane wave. It is apparent that the effects are different for spherical and plane waves, in addition to being frequency dependent. Because the loss is directly proportional to frequency times distance, or distance divided by wavelength, the loss for a model should be exactly the same as for full scale.

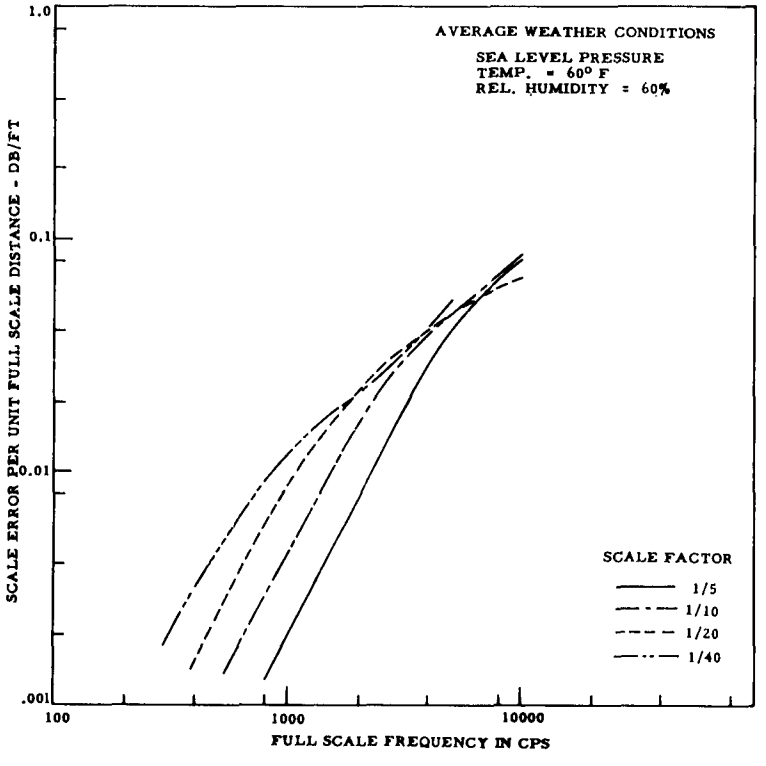

Figure 6. Scale error due to absorption losses in air.

The significance of the shock losses as compared to the molecular losses for a full scale and 1/10th scale model sound source, initally at 170 db, are shown in Figure 9. The pattern that is apparent is that the fixed shock wave losses are overcome by the molecular absorption losses at about 100 to 200 feet. The other effect of the propagation of finite amplitude waves, as shown in Reference 28, is to generate difference frequencies when more than one frequency is involved. This phenomenon has not been explored because it is believed to be relatively unimportant.

4. Multiple Noise Sources

If two or more independent noise sources are present, the rms sound pressure observed at some point will be the square root of the sum of the squares of the pressures propagated from

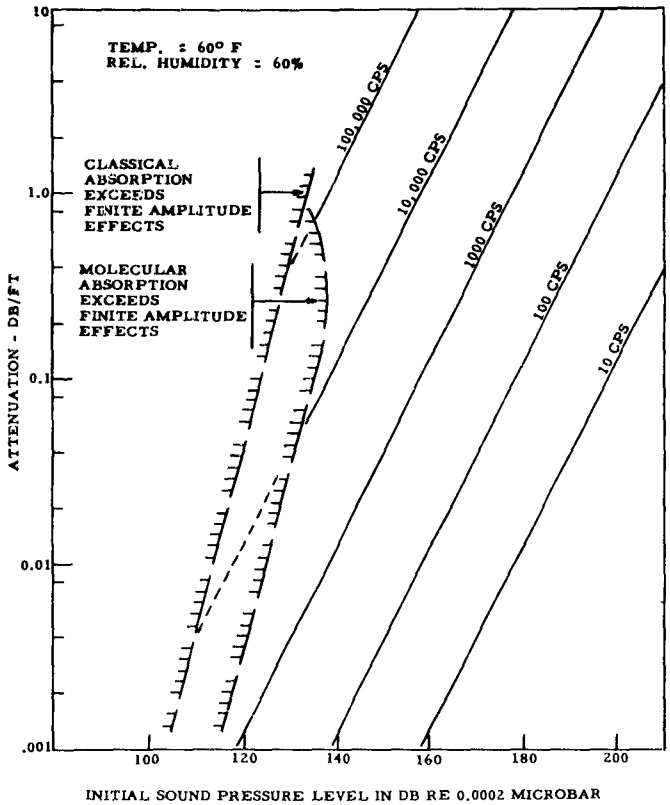

Figure 7. Attenuation rate of finite amplitude plane sound waves.

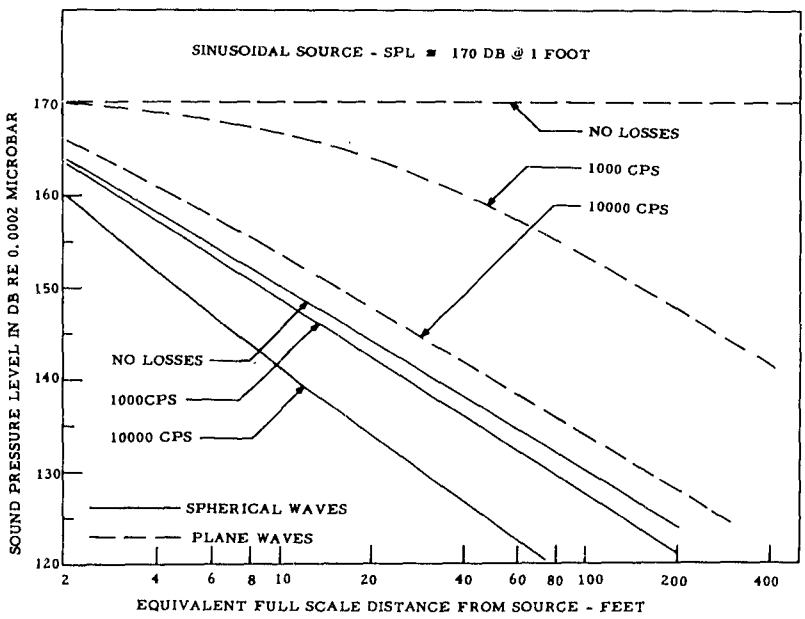

Figure 8. Estimated attenuation of finite amplitude plane and spherical sound waves.

each source. When these noise sources are jet engines the same mathematical computation can be made, except when the geometry is such that the noise from one engine must pass through the exhaust of another to reach the observation point. In this case the nearer exhaust acts as a partial barrier, so that the pressure at the observation point is largely determined by the near jet only. Definition of a limiting path of propagation which is not affected by the intervening jet could probably be accomplished empirically, but for the present purpose it is sufficient to consider only the situations which are clearly not affected by an intervening jet. The problem is then resolved to a question of model simplification, i. e.--can an adequate study of the noise from two or more engines be made by (1) measuring around only one engine, (2) transposing this sound field successively to other engines, and (3) then mathematically summing the fields?

If parallel jets are so close together as to mix a short distance downstream of the nozzle exit, as in clustered rocket nozzles, then they are not independent jets and clearly should all be present when the sound field is measured.

To sum the noise field for two separate jets, the noise field of the engine which has been measured is transposed to the position of the second engine, and the resultant sound levels summed at all points. The corrected sound level in such a case is never greater than 3 db higher than the level which could exist for either engine operating alone,

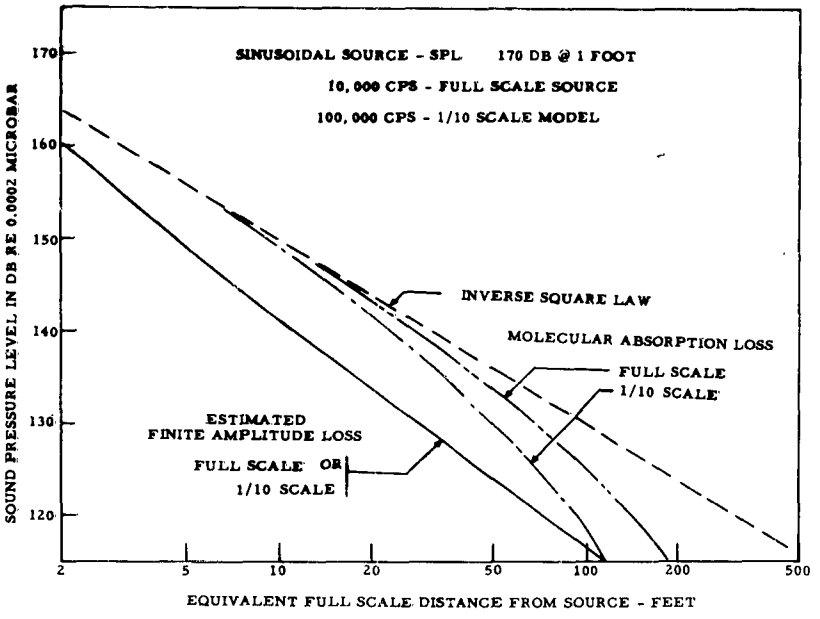

Figure 9. Comparison of effects of estimated finite amplitude losses and molecular absorption losses.

and on this basis the procedure seems acceptable.

At certain spacings, two parallel jets will mix at some downstream distance such that the high frequency sources will be completely separated, but the low frequency sources of the two jets will be mixed. In this case it is expected that the low frequency noise field produced by the pair of jets will not be the sum of the noise fields produced by each jet, but that the summation should still hold for the high frequencies. Experimental verification of these effects would be difficult because the difference between the noise produced by two separate jets and two mixed jets is probably very small throughout most of the frequency range.

5. Partially Bounded Noise Field

Effect of Plane Surface

Effect on Total Radiated Power.--It is not possible to conduct model studies of jet noise fields without a reflecting surface somewhere in the field. Whether the reflecting plane is placed there intentionally or not, its significance for model studies must be recognized. The first effect to consider is the potential influence on the sound power output of a source placed close to a reflecting surface. The change in sound power output of a monopole and longitudinal quadrupole, oriented vertically to the ground,[29,46] is shown in Figure 10. The effect for an octave band noise source has been estimated from the theory in Reference 29, and it is seen that for separation of the plane by 1/2 wavelength or more from the sound source, very little effect is observed. Note that the intensity in the far field is still increased by an additional 3 db due to the smaller total radiating area. Since the increase in power output scales with the height in wavelengths, it can be duplicated on a linear scale model. As an estimate of the effect of a reflecting plane on the octave band power spectrum for a rocket, the data in Figure 10 were applied to the typical power spectrum for a supersonic jet[16] by using the relation

$$\frac{2h}{\lambda} = \frac{2h}{d} \cdot \frac{fd}{c_o}$$

The results are plotted in Figure 11.

Effect on Sound Pressure Level.--Of more general interest than changes in radiated power is the direct effect that a rigid reflecting plane has on the sound

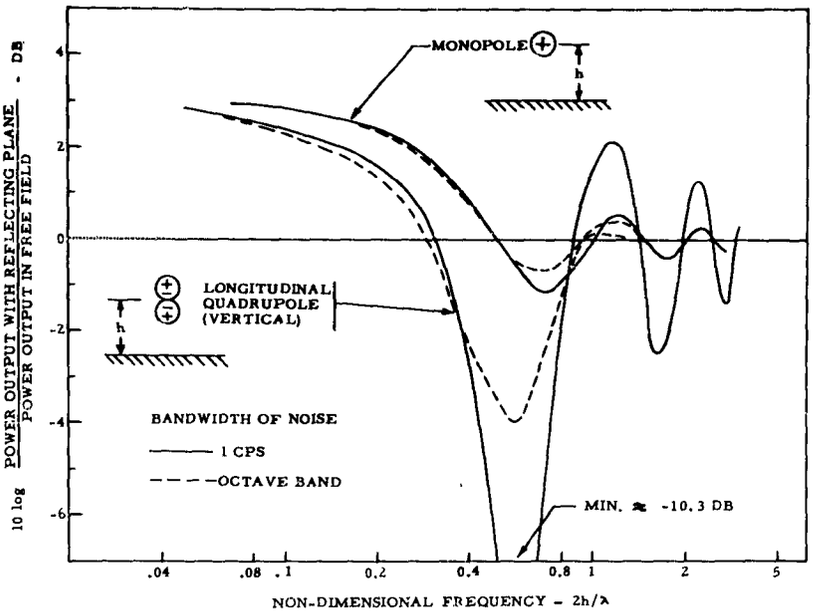

Figure 10. Effect of rigid reflecting plane on acoustic power output of monopole and quadrupole sources.

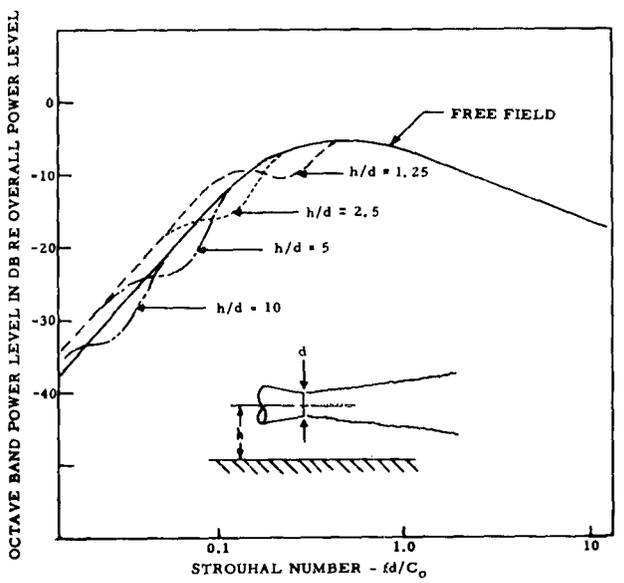

Figure 11. Estimated effect of ground plane on octave band power levels of a horizontal jet.

field observed nearby. A thorough analysis of the problem of ground reflections of noise has been reported in Reference 30. Expanding on the basic approach outlined by this reference, the problem has been analyzed to provide detailed curves of the change in sound level expected over a wide range of frequencies, expressed in terms of wavelengths, for various separations of the source and receiver. Consider the diagram of the problem as shown in Figure 12 (upper left). The ratio of the mean square pressure at the receiver with and without a ground plane is

$$C_R = \left(\frac{P_o}{P_d}\right)^2 = 1 + \left(\frac{P_r}{P_o}\right)^2 + 2\,\frac{\overline{P_{ri}\,P_{di}}}{P_d^2}$$

$$\text{or } C_R = 1 + \left(\frac{P_r}{P_d}\right)^2 + 2\left(\frac{P_r}{P_d}\right)\frac{\overline{P_{ri}\,P_{di}}}{P_r P_d}$$

P_o = rms value of the combined direct and reflected signal

P_d = rms value of the direct signal

P_r = rms value of the reflected signal.

i indicates instantaneous value

Thus, the problem reduces to finding the ratio of amplitudes of the direct and reflected signals and the cross-correlation coefficient between the two signals. The latter has already been discussed in an earlier paragraph. The time delay between the direct and reflected signals is given by

$$\tau = \frac{\Delta r}{c_o} = \frac{1}{f_c}\,\frac{2h}{\lambda}\cdot\frac{1}{2h/r}\left[\sqrt{1+\frac{2h}{r}\left(2\sin\theta+\frac{2h}{r}\right)}-1\right]$$

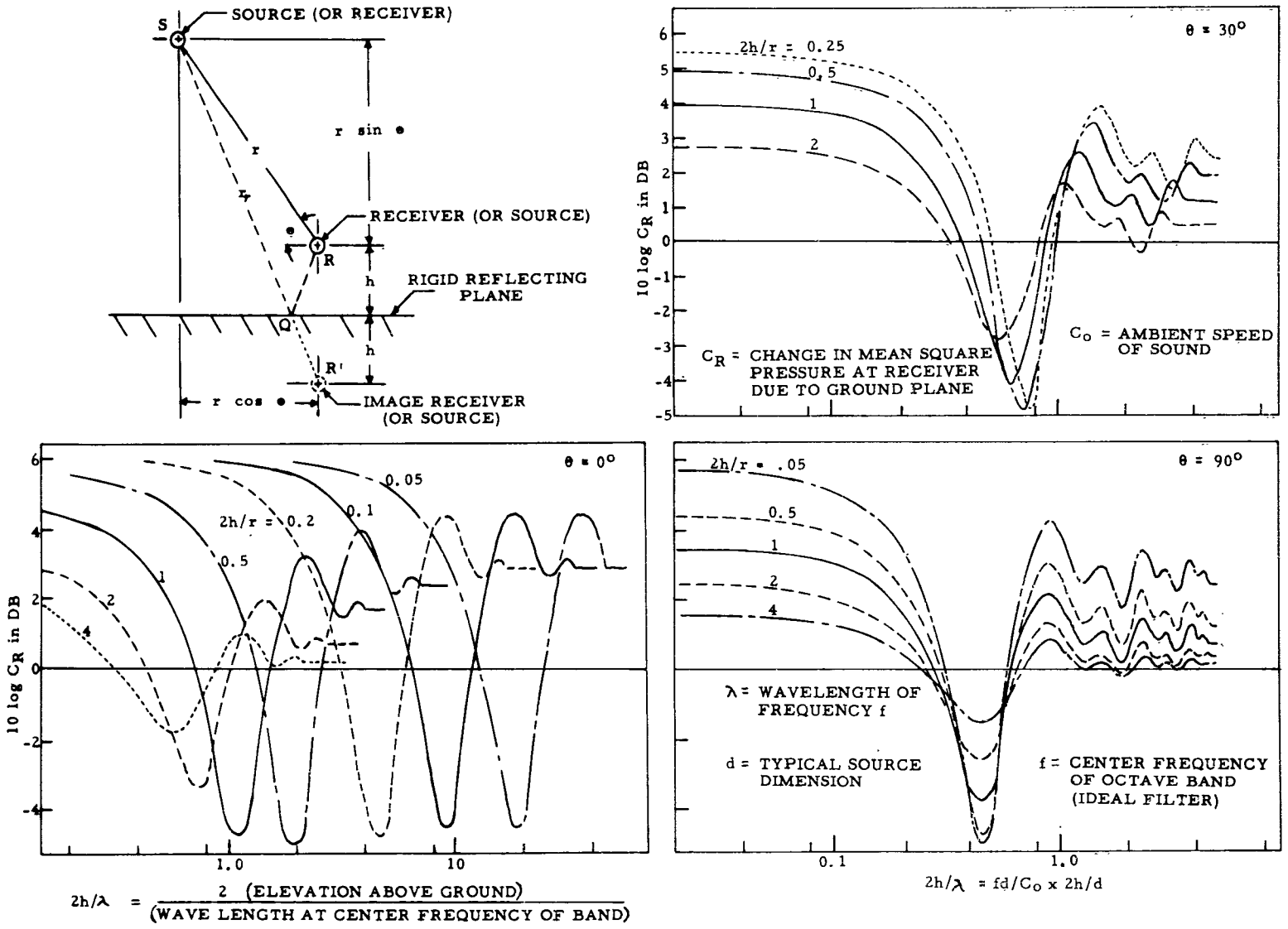

Figure 12. Changes in octave band levels at a point due to the presence of an ideal reflecting surface. Upper left -- Graphical illustration of the reflection problem. Lower left -- Changes for θ = 0°. Upper right -- Changes for θ = 30°. Lower right -- Changes for θ = 90°.

and the ratio of their amplitudes by

$$\frac{P_r}{P_d} = \frac{Q}{\sqrt{1+\frac{2h}{r}\left(2\sin\theta+\frac{2h}{r}\right)}}$$

Thus, a general expression for the effect of a reflecting plane on bands of noise is given by

$$C_R = 1+\frac{Q^2}{Z^2}+2\frac{Q}{Z}\left\{\frac{\sin\left[\frac{\Delta f}{2f_c}\cdot 2\pi\left(\frac{2h}{\lambda}\right)\frac{Z-1}{2h/r}\right]}{\frac{\Delta f}{2f_c}\cdot 2\pi\left(\frac{2h}{\lambda}\right)\frac{Z-1}{2h/r}}\cos\left[\sqrt{1+\left(\frac{\Delta f}{2f_c}\right)^2}\cdot 2\pi\left(\frac{2h}{\lambda}\right)\frac{Z-1}{2h/r}\right]\right\}$$

where

$$Z = \sqrt{1+\frac{2h}{r}\left(2\sin\theta+\frac{2h}{r}\right)}$$

Q = Coefficient of reflection at the surface

Δf = Bandwidth of noise

f_c = Center frequency of filter band

h = Height of source above ground

r = Separation of source and receiver

For Q = 1, values of the correction factor have been determined in decibel form for octave bands of noise for:

a. θ = 0° (Source and receiver in same plane, parallel to ground)

b. θ = 90° (Source and receiver in a line perpendicular to ground)

c. θ = 30° (Source and receiver on a line at 30° to ground).

The results are plotted in Figure 12. The predicted effects are based on the assumption of a white noise spectrum uniform over the pass band and zero outside the pass band. The practical octave band filter will not discriminate noise bands to this extent so that measurements cannot be expected to show the detailed oscillations in the correction beyond the first null. The general trend of the curves is to show an increase in level approaching 2-6 db at low frequencies, a null at $\frac{(2h)^2}{r\lambda}\approx 1$ for $\theta=0°$ or $\frac{2h}{\lambda}\approx 0.5$ for $\theta=90°$, and an increase of 0 to 3 db at high frequencies. Note that for a microphone mounted flush on a surface, h approaches zero, so the increase in level at a surface may be considered a limiting case.

Effect of Obstacles

Reflection of the radiated jet noise by finite-sized obstacles can be a very annoying source of error encountered in model studies. No attempt will be made to consider the details of reflection from a variety of shapes. The problem is

reduced instead to defining the limits on the size of a spherical and a cylindrical obstacle placed in the sound field if the sound levels measured near the obstacle are not to be affected by more than a limiting amount. If the obstacle lies beyond the microphone on an extension of the line joining the microphone and the sound source, the following criteria in Table I can be defined.[31]

TABLE I

The Effect of an Obstacle.

Obstacle	r/r_o	Size of Obstacle in r_o/λ Units		
		Δ db < 0.5	Δ db < 1.0	Max Δ db
Sphere	1	< 0.038	< 0.064	6.0 $r_o/\lambda > 1.0$
	4	< 0.093	< 0.145	1.3 $r_o/\lambda > 0.25$
	10	--	--	0.5 $r_o/\lambda > 0.25$
Cylinder	1	< 0.038	< 0.047	~6.0 $r_o/\lambda > .4$
	4	< 0.025	< 0.038	~4.0
	50	< 0.058	--	~1.0 $r_o/\lambda > .12$
	200	--	--	~0.5

r_o = radius of obstacle; r = radius from center of obstacle to observation point; Δdb = change in sound level due to obstacle; λ = wavelength of sinusoidal signal.

6. Jet Interference

Partial Interference

The discussion of the radiated noise field has assumed up to now that the jet exhaust was free and unhindered by any solid boundaries. To extend the similarity laws for acoustic model jets to include the case of jet impingement on some obstructing surface, consider a jet impinging at some arbitrary angle on a deflector vane. While no attempt is made to predict quantitatively the effects of jet interference on the sound source, a rough qualitative estimate can be made and the relative significance of the geometry and flow parameters defined.

An idealized concept of a deflected jet is illustrated in Figure 13. It is desired to relate the respective values of h_e and ϕ, which define the position of the jet at which a jet noise source is first influenced, to the frequency of the source.

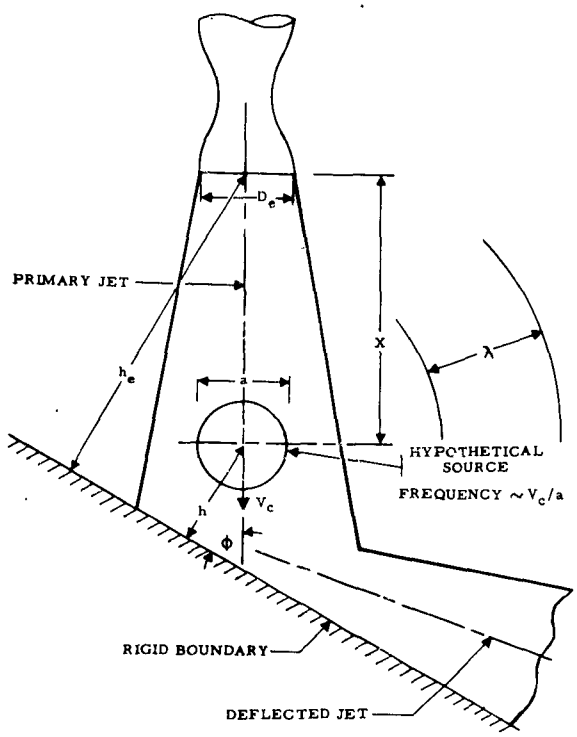

Figure 13. Geometry of deflected jet.

It is assumed that for higher frequencies the boundary has no direct influence on the power output of the source. The ground reflection of sound at the higher frequencies still occurs and in some cases may be the governing factor in defining the effects of the boundary on the radiated sound field. Of primary concern here, however, is the direct effect on the source itself. For lower frequencies the jet structure will be altered so that the relation between source frequency and position may be altered.[41]

The effect of a rigid reflecting surface on the power output of a single source was considered earlier. An approximate criterion for the threshold of influence was that

$$\frac{2h}{\lambda} \approx 1$$

where h = the distance to the ground plane

λ = wavelength of source.

This is accepted as the sole criterion for the minimum distance for a direct effect on the source. This criterion can then be expanded to show the relationship between h_e and f by

$$\frac{2h}{\lambda} = \frac{2h}{h_e} \cdot \frac{h_e}{D_e} \cdot \frac{D_e}{\lambda} \approx 1$$

Since $$\frac{2h}{h_e} = \frac{2(h_e - x\sin\phi)}{h_e} = 2\left(1 - \frac{x}{h_e}\sin\phi\right)$$

and $$\frac{D_e}{\lambda} = \frac{fD_e}{c_o} = \frac{fD_e}{V_c} \cdot \frac{V_c}{c_o}$$

therefore $$\frac{h_e}{D_e} \approx \frac{1}{2}\left(\frac{1}{1 - \frac{x}{h_e}\sin\phi}\right)\left(\frac{fD_e}{V_c} \cdot \frac{V_c}{c_o}\right)^{-1}$$

Now in the mixing region of a jet, where the high frequencies are generated, it is approximately true that:

$$\frac{x}{h_e} = \frac{x}{D_e} \cdot \frac{D_e}{h_e} \approx K\left(\frac{fD_e}{V_c}\right)^{-1} \frac{D_e}{h_e}$$

where k is a constant $\approx$ 0.4

so that the above becomes

$$\frac{h_e}{D_e}\left[1 - K\left(\frac{fD_e}{V_c}\right)^{-1}\frac{D_e}{h_e}\sin\phi\right] \approx \frac{1}{2}\left(\frac{fD_e}{V_c}\cdot\frac{V_c}{c_o}\right)^{-1}$$

or

$$\frac{h_e}{D_e} \approx \left(\frac{fD_e}{V_c}\right)^{-1}\left[K\sin\phi - \frac{1}{2}\left(\frac{V_c}{c_o}\right)^{-1}\right]$$

Thus, an expression is found which relates the position of the jet to the non-dimensional frequency of the source which is just affected at this position. For example, for the peak Strouhal number ≈ 0.25, the following values of h_e/D_e are found for $K \approx 0.4$ and $V_c/c_o \approx 1$

ϕ	0°	45°	90°
h_e/D_e	2	3.1	3.6

The absolute accuracy of the equation derived above will depend on the accuracy with which the noise source can be specified for the undeflected jet. For purposes of scaling, however, the expression may be used as a guide to the sensitivity of the jet noise source to changes in geometry of the deflector or changes in the flow.

For the deflected jet, a new flow structure will be formed. For a rocket fired vertically above the ground, for example, the data in Reference 43 show that the Strouhal number of the pressure fluctuations along the boundary of a radially-spreading deflected jet will vary approximately as $1/R^2$, where R is the distance from the jet impingement.

In general, by choosing new relationships for flow similarity in this "deflected jet" region, the sound generated in this region could be predicted in the same manner as for the free jet. It is important to note that the boundary along which this portion of the jet flows cannot be removed without altering the basic form of the flow, and hence noise generation, in this region.

Enclosed Jet

The extreme case of a bounded jet noise field is represented by the noise field of a jet enclosed in a so-called silo launching device. This case is examined to establish the scaling laws which apply to this unique situation. The analysis considers, first, the initial transient pressure pulse at engine ignition, and then the steady state noise within the silo during a static firing. Both of these phenomena have significance as dynamic loads on the missile structure and equipment.

Transient Pressure.--A typical oscillographic record of the pressure at the base of a missile during the initial firing transient has the appearance of a damped sine wave, suggesting that the pressure pulse may be approximated by the transient response of a lumped-constant acoustical system. Following this line of

reasoning, equations for the pressure and resonant frequency of the pulse may be derived.[42] These equations show that (1) the magnitude of the pressure pulse should be duplicated by a scale model since all dimensions appear as ratios, and (2) the 'resonant frequency', and hence characteristic frequency, of the pressure pulse will be inversely proportional to a typical dimension of the silo configuration. Thus, the basic requirements for a true scale model are satisfied for this transient pressure pulse. It must be emphasized again, however, that unless the model and full scale engine have the same transient ignition characteristics, the magnitude of the pressure pulse cannot be duplicated by a model.

Steady State Sound Field.--Once flow has been established in the silo, the steady state wide band noise is of interest. Only a static firing is considered since it is very unlikely that one would want to launch a model from a scaled silo. More to the point, however, is the fact that if static similarity can be established, then dynamic similarity should also hold for the first few seconds of flight at very low velocities as the missile leaves the silo.

If the fluctuating pressures on the surface of the missile and silo walls are caused by the local turbulent flow, a scale model which duplicates the turbulent flow field of the full scale version should also duplicate the noise field. Thus, the rms sound pressure should scale as

$$p \propto \rho_c U_c^2 \left(\frac{u}{U_c}\right)$$

where

p = rms sound pressure

ρ_c = characteristic density of flow

U_c = characteristic velocity of flow

u = rms velocity of turbulence

The characteristic structure of the flow would be readily duplicated by a geometrically scaled model.

However, from preliminary tests with cold air jets used to simulate a silo noise field, there did not appear to be any direct proportionality between the sound pressure and dynamic pressure of the flow as suggested above. While the evidence is meager, it does suggest that the sound field in the silo is not due primarily to a boundary layer noise phenomenon. The other logical approach is to consider the problem in terms of a reverberant jet noise field.

The sound pressure in the reverberant field of a noise source is defined by,[2]

$$p^2 = \frac{4 W_o \rho c (1 - \bar{\alpha}_T)}{S \bar{\alpha}_T} \qquad (17)$$

W_o = Total power output of noise source

$\bar{\alpha}_T$ = Average absorption coefficient

S = Total surface area of enclosure

If the acoustic power is assumed to be proportional to the mechanical power of the

jet exhaust, and the acoustic absorption is due to both absorption at the walls of the silo and in the gases of the jet exhaust which fill the silo, then:

$$W \propto \rho U_c^3 \cdot d_c^2 \cdot \eta \tag{18}$$

where U_c = characteristic velocity of noise generating portion of jet

d_c = characteristic diameter of this portion of jet

η = efficiency of noise generation

Also,

$$\bar{\alpha}_T = \sum \frac{S_n \alpha_n}{S} + \frac{4mV}{S} \tag{19}$$

where $S_n \alpha_n$ = absorption, in Sabins, of the n^{th} segment of the silo walls

m = coefficient of energy absorption in the gases

V = total volume of silo

To illustrate the scaling concept more clearly, consider two cases: absorption is entirely at the walls, or entirely in the gas. For the first case, the gas absorption is zero, or m = 0. Using the dimensions for the silo and missile defined in Figure 14, the sound pressure in the reverberant field is:

$$P^2 \approx \frac{1}{2}\left(\rho U_c^2\right)^2 \left(\frac{c}{U_c}\right) \eta \frac{\left(\frac{d_c}{l}\right)^2}{\left(\frac{d_1}{l}\right)\left(1+\frac{h}{l}\right)+\left(\frac{d_m}{l}\right)} \left(\frac{1-\bar{\alpha}}{\bar{\alpha}}\right) \tag{20}$$

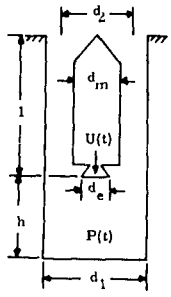

d_2 = equivalent diameter of annulus

$d_2 = d_1\sqrt{1-(d_m/d_1)^2}$

Figure 14. Diagram and dimensions of a missile in a silo

Provided that the efficiency of noise generation is not affected by the scale factor, the above equation indicates that if the flow parameters of the model duplicate the full scale values, then the sound pressures measured in the model should duplicate full scale values since the silo dimensions all appear as dimensionless ratios. This also assumes that the average absorption coefficient, $\bar{\alpha}$, would be accurately duplicated on the model.

For the case of all the absorption taking place in the gases within the silo ($\bar{\alpha}_n = 0$), the sound pressure in the reverberant field sould be given approximately by:

$$P^2 \approx \frac{1}{2}\left(\rho U_c^2\right)^2 \left(\frac{c}{U_c}\right) \eta \frac{\left(\frac{d_c}{l}\right)^2}{d_1\left(\frac{d_1}{l}\right)\left(1+\frac{h}{l}\right)-d_m\left(\frac{d_m}{l}\right)} \cdot \frac{1}{m} \tag{21}$$

While this shows the same dependency on the flow parameters, it is noted that the sound pressure is now a function of the size of the model since the silo dimensions do not all appear as dimensionless ratios. Furthermore, the value of the energy absorption coefficient, m, will vary with frequency, but not necessarily in a linear fashion, so the absorption losses do not scale. Thus, for the case where the majority of the absorption of sound in the silo occurs in the gases, the losses are proportional to the volume of the silo, but the sound power output will scale as the area of the silo. The scale model will not, therefore, reproduce the sound field of the full scale version.

In practice, it is probable that the absorption of sound in a silo firing is due to a combination of absorption at the walls and absorption by the gases. The lack of a better understanding of the absorption of sound in hot, turbulent exhaust gases of a rocket make it impossible to further define the ability to scale the sound field within a silo. Experimental studies are the only practical recourse.

C. Measurement of Noise Field

1. General Instrumentation

If the model results are to be significant, the instrumentation which is used in model work must be of comparable quality to that used in making full scale measurements, but for a higher range of frequencies. With care, items such as amplifiers, tape recorders, and voltmeters are capable of operation up to 100,000 cps as reliably as to 10,000 cps. While this situation does not hold so readily for microphones or the phase matching of components, the objective with regard to these items is the same.

2. Finite Size of Microphone

The methods of microphone calibration are well known and need not be considered here.[31] The particular method employed in this program will be described in Section III -- Instrumentation.

The size of the microphone inherently limits the accuracy of high frequency acoustic measurements and therefore is a significant factor in the accuracy of any acoustic model study. For measurements in the free field, the obstacle effect of the microphone itself causes well known diffraction effects.[22] The measured free field response of one of the small microphones used in this study is shown in Figure 15 for both normal and grazing incidence. Also shown is the theoretical effect for normal incidence. The corresponding theoretical effect for grazing incidence is zero.[22] The observed and theoretical responses have been plotted in terms of ratio of microphone diameter to wavelength for the sake of convenience in interpretation. The fact that the microphone will be essentially non-directional in the plane of the diaphragm for grazing incidence can also be used to considerable advantage. If the microphone is located so that the extension of the plane of the diaphragm contains the sound source, it is not necessary to know the exact direction of the sound source in this plane.

There is one basic limitation to the grazing incidence technique that may be important when measuring pressures on a rigid plate which has a sound field traveling across it. As a simplified illustration, assume that the microphone is represented by a rigid rectangular piston of width d in the direction of the sound wave and located flush with a rigid plate. If a sinusoidal pressure wave is traveling across the microphone, the instantaneous pressure at any point on the piston may be expressed as

$$P_{x,t} = \sqrt{2}\, p_o \sin(\omega t - Kx)$$

where

p_o = rms pressure in the incident wave

ω = angular frequency

$K = \frac{2\pi}{\lambda}$

x = distance from the center of the diaphragm

The average pressure over the face of the piston will be

$$P_t = \frac{1}{d}\int_{-d/2}^{+d/2} p_o \sin(\omega t - Kx)\, dx$$

$$P_t = p_o \frac{\sin \frac{Kd}{2}}{\frac{Kd}{2}} \sin\left(\omega t - \frac{Kd}{2}\right)$$

and the rms pressure on the piston will be related to the rms incident pressure by

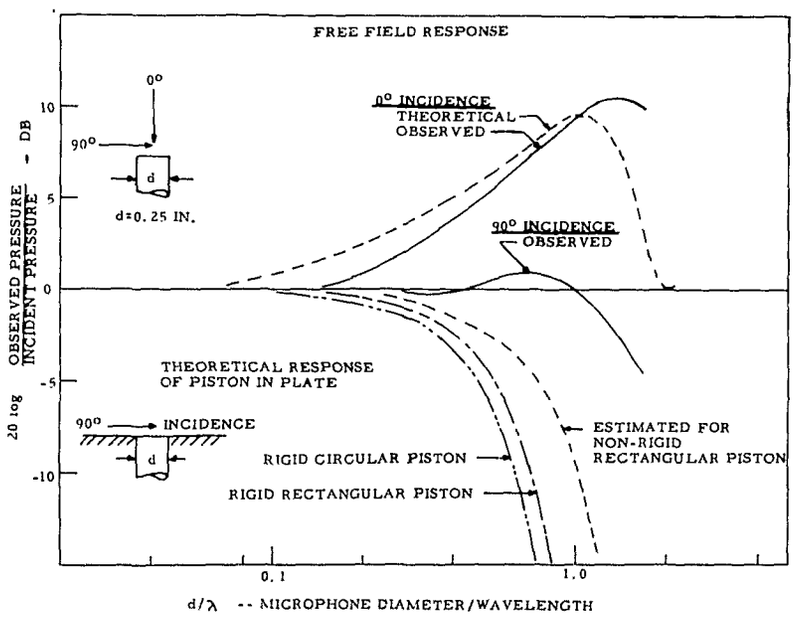

Figure 15. Response of microphone in free field and in a rigid plate.

$$\frac{P}{P_o} = \frac{\sin \frac{Kd}{2}}{\frac{Kd}{2}}$$

When expanded in an infinite series, this becomes

$$\frac{P}{P_o} \approx 1 - \frac{(Kd)^2}{24} + \frac{(Kd)^4}{1920} - \cdots$$

A more detailed analysis of the finite size of a circular microphone of diameter d on measurement of convected pressure fluctuations has been reported in Reference 44. From this latter analysis, it is possible to show that for the case of an acoustic wave traveling across the microphone at grazing incidence, the ratio of observed pressure

to incident pressure can be estimated by the series,

$$\frac{P}{P_o} \approx 1 - \frac{(Kd)^2}{16} + \frac{5(Kd)^4}{3072} - \frac{7(Kd)^6}{294,912} + \cdots$$

This expression for a rigid circular piston is compared in Figure 15 with the previous expression for a rigid rectangular piston; the effect is similar for the two cases. Since the diffraction effect is absent at grazing incidence, identical frequency responses should be observed at grazing incidence whether in the free field or in a plate. However, the computed response for a rigid piston in a plate would suggest a much greater drop in high frequency response for grazing incidence than is actually observed for grazing incidence of a real microphone in the free field. The most probable explanation for this discrepancy is believed to be due to the fallacy of assuming that the microphone diaphragm could be represented by a rigid piston. This assumption implies that pressure at the edge of the transducer is just as effective as pressure at the middle of the transducer. This, of course, is not true for a real microphone since the edges are fixed.

A rough estimate of the response of a flexible diaphragm located in a plate was made by defining an effective pressure P_e on the face of the diaphragm by the relation

$$P_e = P_x \cos \frac{\pi d}{x}$$

$P_x = P_o \sin(\omega t - Kx)$, as before

d = width of rectangular diaphragm

X = distance from middle of diaphragm.

The result is that the ratio of rms pressure averaged over the diaphragm to the incident pressure is proportional to

$$\frac{P}{P_o} \propto \frac{\pi^2 \cos\left(\frac{Kd}{2}\right)}{\pi^2 - \left(\frac{Kd}{2}\right)^2}$$

This expression is also shown in Figure 15, indicating an improvement in high frequency response. This is the expected result since the effective size of the diaphragm which responds to the grazing incidence wave is appreciably smaller than the actual microphone diaphragm size. The actual diaphragm of the microphone used is less than the one-quarter inch outside diameter indicated in Figure 15. Correcting for this would also improve the agreement between the estimated and observed responses. As a tentative procedure, the response in a rigid plate will be considered to be the free field grazing response.

The criterion suggested by the observed response data is that the microphone diameter should not exceed one-half wavelength if large response corrections are to be avoided.

A slightly different requirement is placed on microphone size if space correlation measurements are to be made. If the microphones are placed as close together

as possible, the criterion

$$d < \frac{\lambda}{8}$$

will result in the ability to measure all phase differences greater than 45°. By reviewing measured correlation data, Franklin and Archbold[37] concluded that the largest microphone diameter which could be used with their 2-inch jet was 1/8-inch. A generalization of this conclusion is

$$d < \frac{d_e}{16}$$

where d_e is the nozzle diameter.

The basic elements of the instrumentation system used in the experimental work reported herein are shown in block diagram form in Figure 16. A more detailed description of certain of these elements follows.

The Massa M-213 microphone (ADP crystal) was selected for use in this experimental program primarily because it appeared to satisfy best the requirements of small size (1/4-inch diameter) and useful frequency response up to 100,000 cps. For the special purpose of measuring in high temperature environments, Photocon Research Products' Model 752 water-cooled pressure transducer was used. In all cases this microphone was mounted flush in a surface, which eliminated the problem of diffraction. Its range of useful frequencies nominally is limited to 10,000 cps. Altec 21BR series microphones (5/8-inch diameter) were used to obtain data in those situations for which an insufficient number of Massa microphones were available. The Altec microphone has a useful range up to about 20,000 cps. A detailed description of the use of only the Massa microphone will be presented, as the other two microphones are in widespread use for full scale measurements.

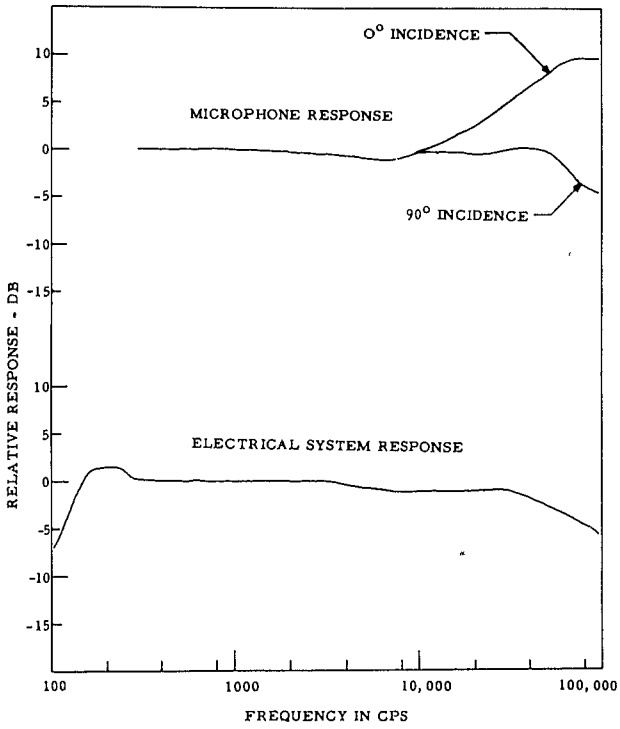

Figure 17. Frequency response of microphone and electrical system.

In Figure 17 the open circuit frequency response of a typical Massa M-213 microphone crystal button is presented. Each microphone button purchased from Massa was accompanied by such a calibration curve. The deviation between buttons is very small. These curves were checked at normal incidence at Boeing by comparison calibration, using a Western Electric 640AA microphone as the standard and a specially built electrostatic speaker as the noise source. In general the agreement with the manufacturer's curves was good. The large difference between normal and grazing incidence sensitivity at the higher frequencies is due to the diffraction pattern of the microphone. Except as noted later, all free field measurements with these microphones were made with grazing incidence. The grazing incidence frequency response indicated by the manufacturer was therefore used in correcting the microphone signal. Immediately before each test each microphone was inserted into a pressure coupler which provided a 1000 cps signal at 150 db, and this reference signal was applied through the entire electrical system to the tape recorder. Later the absolute levels of the signals obtained during the test were established by reference to this 150 db signal. The pressure coupler was qualified by periodic checks with the laboratory standard Western Electric 640AA microphone system. An independent check of this field calibrator was obtained through the use of a pistonphone.

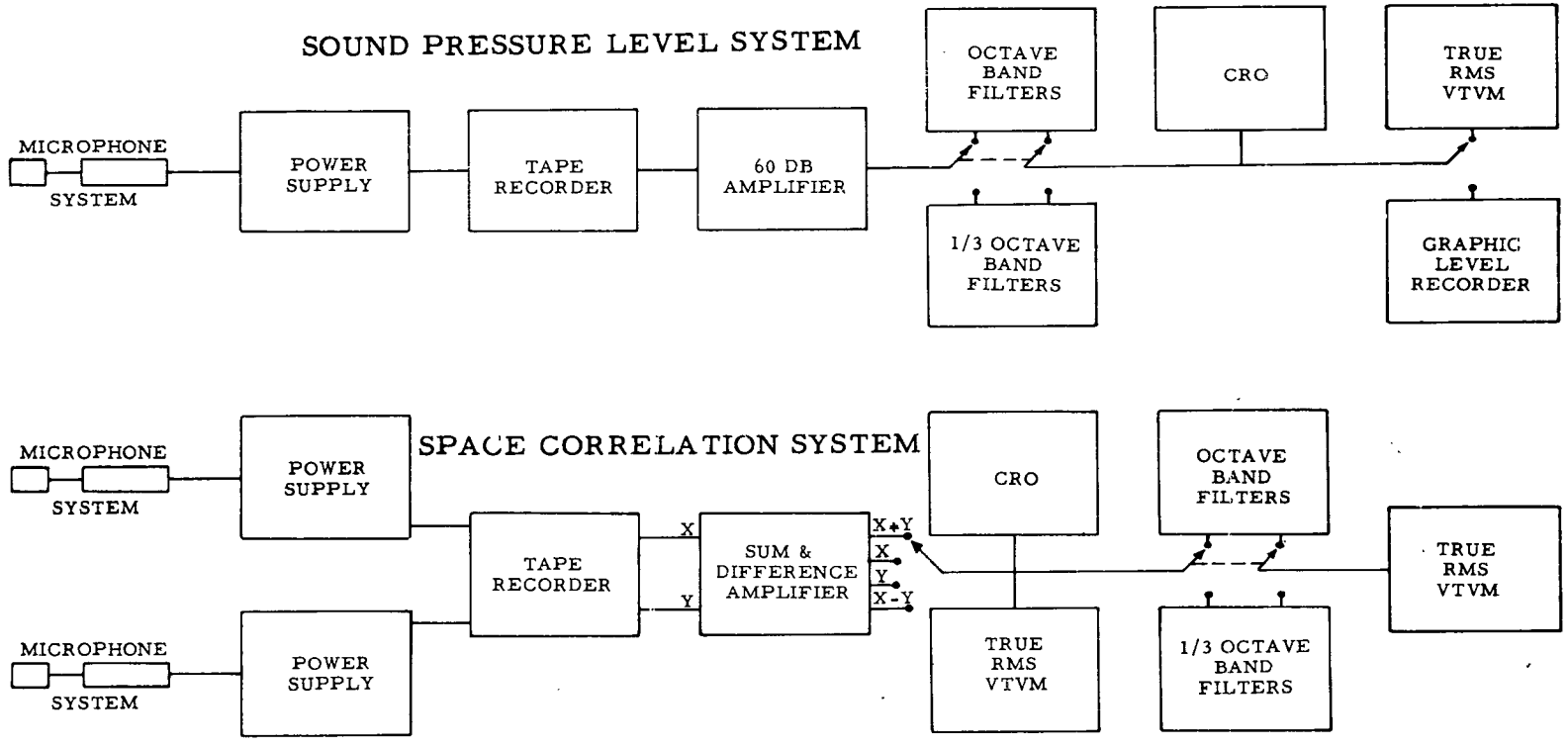

EQUIPMENT	MANUFACTURER	TYPE OR MODEL
TRANSDUCER	MASSA	M213
PREAMPLIFIER	BOEING	
POWER SUPPLY	BOEING	
TAPE RECORDER	AMPEX	FR - 107A
60db AMPLIFIER	MASSA	M185
OCTAVE BAND FILTERS	PACIFIC INSTR. CO.	
1/3 OCTAVE BAND FILTERS	BRUEL & KJAER	2111
OSCILLOSCOPE	TEKTRONICS	515A
TRUE RMS METER	BALLENTINE	320
GRAPHIC LEVEL RECORDER	BRUEL & KJAER	2304
SUM & DIFF AMPLIFIER	BOEING	

Figure 16. Block diagram of complete instrumentation system for measuring sound pressures and space correlation.

An additional problem to be considered in using crystal microphones is their sensitivity to acceleration. Any mechanical connection to the button may transmit motion resulting from vibration of any part of the microphone mount. This motion results in an extraneous signal from the microphone, which may be comparable to or greater in magnitude than the signal resulting from the acoustic pressures at that frequency. By exercising extreme care, it is possible to isolate the button satisfactorily even in environments of rather high vibration levels.

The mount shown in Figure 18 (left) was used for isolating the microphone when free field measurements were required. The entire cathode follower assembly is isolated in this instance, and the microphone button is attached rigidly to it. Figure 18 (right) shows the isolation means used throughout the experimental part of this program when it was desired to measure noise levels flush with a surface. In both types of mounts, resonant frequencies in all directions of motion were 20 cps or less, about 3 octaves below the lowest frequencies to be measured. The distance of the button from the cathode follower assembly was limited to 6 inches because a 6-inch Microdot cable was used to connect the two elements. In the case of the free field mount there is the possibility that reflections from the cathode follower assembly are a source of error on occasion, but a longer cable is undesirable because of its loss due to capacitance.

In summary, the Massa M-213 microphone appears to be suitable for the particular purpose of making high frequency model noise measurements, and if properly used this microphone can result in satisfactory measurements.

Operation of an Ampex FR-107 seven-channel tape recorder at 60 inches per second with direct record electronics provided storage of data over the desired range of frequencies. The entire electrical system except the microphone button was daily checked at all frequencies by inserting a sweep frequency oscillator signal at the cathode follower. Variable attenuation was possible at each filter, and the frequency response of the system was adjusted at that point. The frequency response of the entire electrical system except microphone is plotted in the lower part of Figure 17. Data reduction normally involved the use of octave band filters from 150 to 80,000 cps and a true rms voltmeter. Alternate use was made of a one-third octave band filter set between the center frequencies of 100 cps and 32,000 cps in place of the octave band filters as the occasion demanded. Usually a one-minute data sample was obtained, but when less than about 15 seconds of data were obtained, reduction of data was by use of a graphic level recorder in place of the voltmeter. The graphic level recorder was also used in a few other appropriate instances. With either device, the absolute level of the data was obtained by referring to the 1000 cps 150 db calibration signal.

Space correlation data were obtained over a limited frequency range compared with the range used for sound level measurements. The various pairs of Massa microphone buttons used for correlation measurements were observed to be matched in phase to within 2° between 200 and 2000 cps. The pressure coupler used to observe this phase relationship was not suitable for such use above 2000 cps, but theoretically the crystal microphones used should be in phase to fairly high frequencies. The pairs of tape recorder channels which were used matched in phase to within 3° from 100 cps to 5000 cps, diverging to a mismatch of as much as 10° at 10,000 cps. It may be noted in Figure 16 that the sum and difference amplifier was used in a manner which avoided any requirement for phase matched filters.

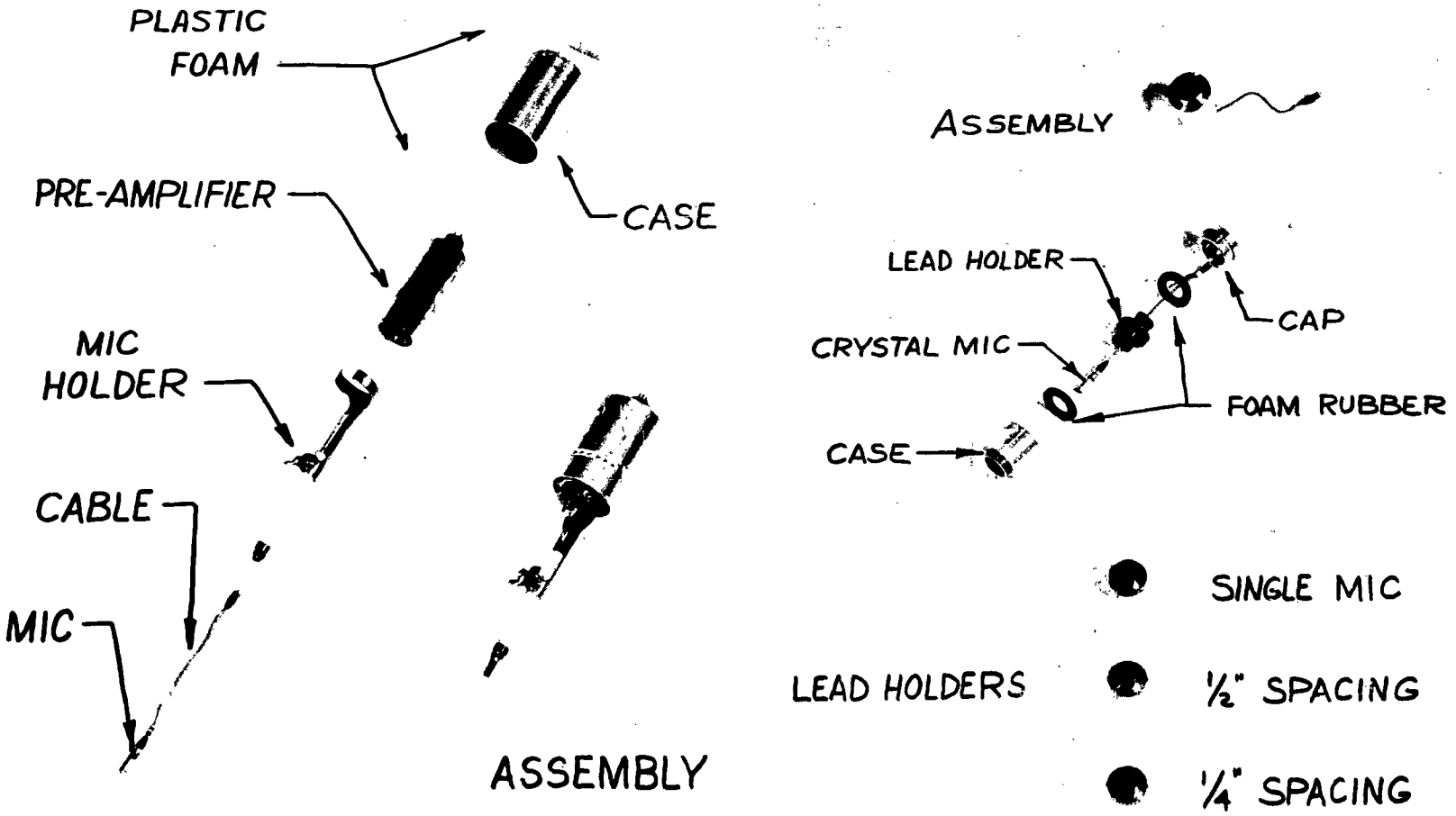

Figure 18. Crystal microphone vibration isolating mounts.
(Left) free field mount; (right) flush mount.

IV. TEST FACILITIES AND PROCEDURES

Each model test performed in connection with this program was planned so as to provide experimental data pertaining to one or more of the items covered in Section II. Details such as exact test point locations and plenum conditions will be presented only in Appendix A. The model data were obtained by octave bands between 150 and 80,000 cps, except as noted.

The basic considerations in the design of a nozzle are exit diameter, area ratio, and shape of inlet and outlet sections. The maximum diameters of nozzles used in this scale model program were dictated by the capacity of the particular gas source to be used. For those model nozzles which were designed to simulate a full scale engine, area ratios were set to be identical to the full scale nozzle. In other instances area ratios were set to match the exit Mach number. Nozzle inlets were all bellmouth in shape, designed by the method of Smith and Wang[32] to provide not over 1% variation in velocity across the nozzle throat. To simplify fabrication the downstream one-third of the ideal bellmouth was approximated by a conical shape. Divergent sections were made conical in shape with a 3° half angle of divergence, except that rocket nozzles used a 10° half angle of divergence.

A. Heated Air Jets

Several tests utilized air heated to temperatures up to 1000°F. To obtain these temperatures a burner using kerosene and compressed air was used. The hot gas was then led through appropriate sections of steel pipe until it was finally exhausted through the nozzle. Total pressure and total temperature probes were installed in the flow a few nozzle diameters upstream of the nozzle. The flow at the measurement station was generally less than Mach 0.3. Desired values of temperature and pressure were obtained by controlling the flow of compressed air and fuel.

1. Surface Effects

To investigate the effects of surfaces, the experimental setup shown in Figure 19 was used. The vertical exhaust was chosen to simplify the process of varying the distance between an exhaust axis and a parallel surface as well as to provide a free exhaust when no reflecting surface was desired. The 90° turn required for the vertical exhaust was obtained through a plenum rather than an elbow. Heat radiation from the vertical stack to nearby microphones was minimized by use of an asbestos wrapping. The movable surface shown in Figure 19 is a steel plate, 8 feet square, made of 1/4-inch steel with a cross network of angle iron stiffeners on the reverse side. In addition, a 1/4-inch layer of Aquaplas damping material was applied to the back surface.

Two types of experiments to investigate the effects of reflecting surfaces were performed with the arrangement shown in Figure 19: changes in sound levels at the surface, and changes in sound levels at points near the surface.

To investigate the sound levels at a surface the microphones were mounted flush with the surface of the plate at several locations, and the plate was positioned successively 2, 4, 8, and 16 nozzle diameters from the nozzle axis. A hot exhaust condition of a 3-inch nozzle was used as a noise source for all measurements. The same measurements were then repeated with the surface removed. Each microphone was in the identical position in space and at the same incidence relative to the noise source as before. A similar series of tests was performed with the surface placed parallel to and one nozzle diameter upstream of the nozzle exit plane. Fewer microphone locations were used, but all measurements were made for three different exhaust conditions of a 3-inch nozzle.

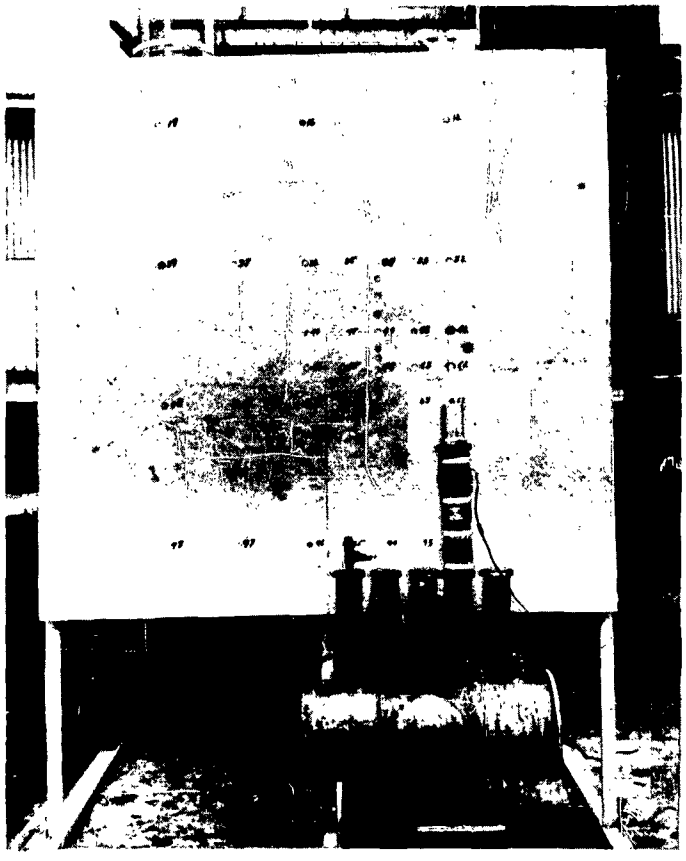

Figure 19. Vertical heated air exhaust near 8-foot simulated ground plane.

To investigate the change in the sound fields caused by the presence of a nearby reflecting surface, five microphones were used. All microphone buttons were located in a plane parallel to and five diameters downstream of the nozzle exit plane. Four of the microphones were kept at a constant relationship to the exhaust, either 4 or 16 diameters from the jet axis, and the fifth microphone was located a constant 1-1/2 diameters from the surface. The incidence of each microphone was chosen so as to minimize the interference of that microphone assembly to either the direct or reflected noise as seen by another microphone. The incidence was then unchanged as the surface was placed at 2, 4, 8, and 16 nozzle diameters from and parallel to the jet axis. A hot exhaust condition of a 3-inch nozzle was used as a noise source for all measurements. The same measurements were then repeated for identical conditions except that the surface was removed. One-third octave band data were obtained from all microphones. The free field data for the four microphones which were fixed relative to the exhaust were obtained three times. These data were then averaged to provide a better free field sound level reference.

2. Two Engines

The plenum shown in Figure 19 was built with several exhaust stacks so that two nozzles could be operated simultaneously at various spacings relative to each other. A 3-inch nozzle on each stack was preceded by total pressure and total temperature indicating devices. In actual operation the temperature was found to be the same in each line, and the total pressure varied by not more than 1-1/2% between lines, indicating that the exhaust velocity from one nozzle was within 1% of the exhaust velocity for the second nozzle.

Microphones were flush mounted in the plate as shown in Figure 19, with the plate positioned 2 and 4 diameters from the nozzle axis. Measurements were made for a single nozzle source, and for two nozzles spaced 2, 4, and 8 diameters apart.

Space correlation measurements were also made for each of the three nozzle spacings. One face of a 2 x 2-inch angle was placed in the nozzle exit plane, on the perpendicular bisector of the line connecting the centers of the two nozzles. Microphones were then mounted flush on the angle, utilizing the mounts shown in Figure 18. The reference microphone was placed 4 nozzle diameters from the line connecting the two nozzles, and the other microphones, three at a time, were placed at distances of from 1/4 to 36 inches from the reference microphone, away from the nozzles. After a measurement was made using two nozzles, one of the nozzles was capped off, and a measurement was made with just one nozzle as a source. Correlation reduction was by octave bands from 150 to 10,000 cps. The same hot exhaust condition was used for all measurements in the series, both for sound level and correlation data.

3. Nozzle Size

Convergent nozzles with exit diameters of 3/8, 3/4, 1-1/2, and 3 inches were exhausted vertically with no reflecting surfaces nearby. Microphones were placed at 15 test points ranging from the nozzle exit plane to 16 diameters downstream, and up to 16 diameters away from the exhaust axis. Any given test point was described in terms of nozzle diameters from the exit, so that the test point appeared to be in the same place for each nozzle.

4. Vertical Take-off

Figure 20 shows an arrangement for discharging a jet exhaust down on a flat surface. The elevation of the nozzle exit was adjustable from 2 to 16 nozzle diameters above the ground by using different lengths of pipe between the plenum and nozzle. Microphones, located upstream of the nozzle, recorded the sound levels produced by 3-inch nozzles operated at three plenum conditions. The microphones were kept at a constant location relative to the nozzle as the nozzle elevation was changed. Free field base line data were obtained with the plenum mounted as in Figure 19, except that the reflecting surface was absent.

5. One-tenth Scale B-52

An extensive 1/10 scale model program of B-52 near field noise levels was conducted in connection with development of a noise suppressor for the B-52 engines. Reference 33 summarizes the model B-52 program. This B-52 program was completed

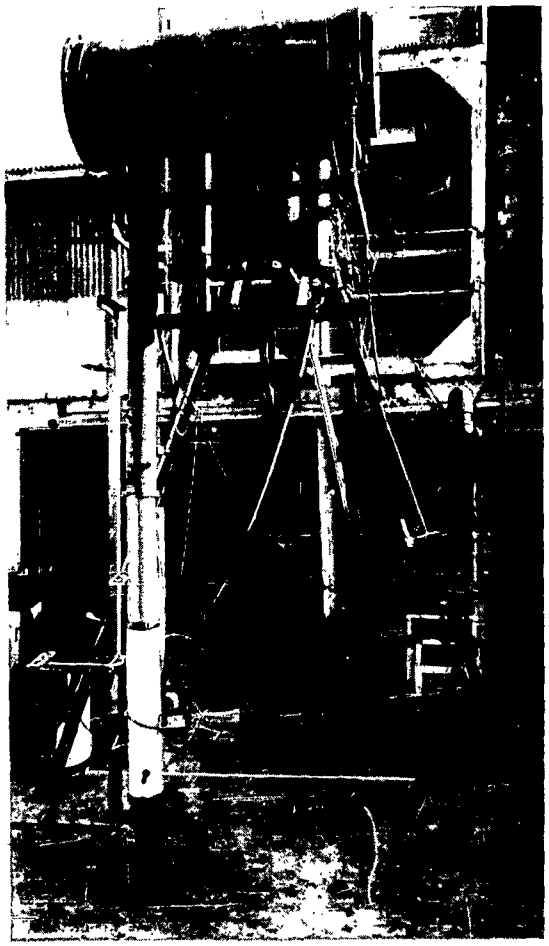

Figure 20. Test apparatus simulating vertical take-off.

before the present studies were undertaken, but it is included here for completeness. The model wing and fuselage used are shown in Figure 21. A pair of the B-52 engines were simulated by the model, and sound levels were measured at many locations on the under wing surface and fuselage. Basic techniques were the same as for the other models described here, except that an Altec condenser microphone was used to provide direct octave band read-out from 150 to 10,000 cps.

6. One-eighth Scale J-57

An eighth scale model of a single J-57-P3 engine was made by using a 3-inch convergent nozzle. This was exhausted horizontally 8 inches above a ground plane. Microphones were placed at 25 test points in the horizontal engine plane, from the nozzle exit to 25 diameters downstream, and up to 10 diameters sideways from the engine.

7. One-eighth Scale J-79 (Military)

The J-79 engine has a variable orifice exhaust nozzle which gives it considerable flexibility of operation. Figure 22 (left) shows the model nozzle which was built to simulate the full scale nozzle. The full scale engine obtains cooling air of about 8% of the primary flow through scoops on the side of the engine. The plant compressed air system provided the model nozzle with this cooling air. The nozzle exhaust was horizontal, 7-1/2 inches above a ground plane. Microphones were placed at about 50 locations in the horizontal engine plane, from 5 diameters forward of the nozzle exit to 25 diameters downstream, and up to 20 diameters to one side of the engine axis.

B. Afterburning Air Jets

Model simulation of afterburning engines was accomplished by use of a kerosene burner in basically the same manner as for the models described above. The difference lies entirely in the range of temperatures required and the techniques for coping with the extremely high temperatures. The burner which was used was of conventional design except that it was made entirely of stainless steel, and a water jacket about one inch thick surrounded all heated sections. All piping

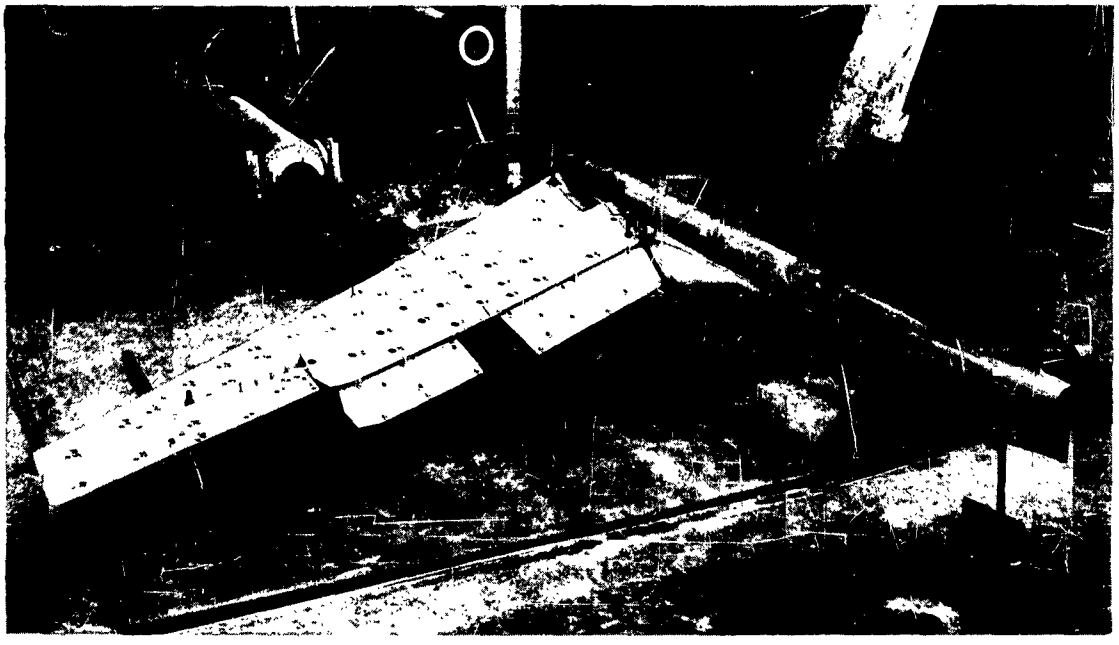

Figure 21. One-tenth scale model B-52 with inboard engines in position.

downstream of the burner was water cooled, as was the total pressure pickup. The thermocouple used was of Platinum--Platinum-10% Rhodium construction and required no cooling. Temperatures up to about 3400°F. are obtainable with this apparatus under optimum operation. Cooling of the exhaust nozzles is necessary for any operation above about 1000°F.

1. One-eighth Scale J-79 (Afterburning)

Figure 22 (right) shows the model J-79 afterburning nozzle which was used. In the full scale operation the angle of convergence of the primary and secondary nozzles is varied between military and afterburning engine conditions. This was accomplished on the model by providing two nozzles. The increased diameter of the afterburning nozzle relative to the military nozzle compensates for the increased temperature of operation so that the same primary mass flow is obtained at about the same pressure. The sound level survey made with this nozzle was identical to that described above for the J-79 model at military operation.

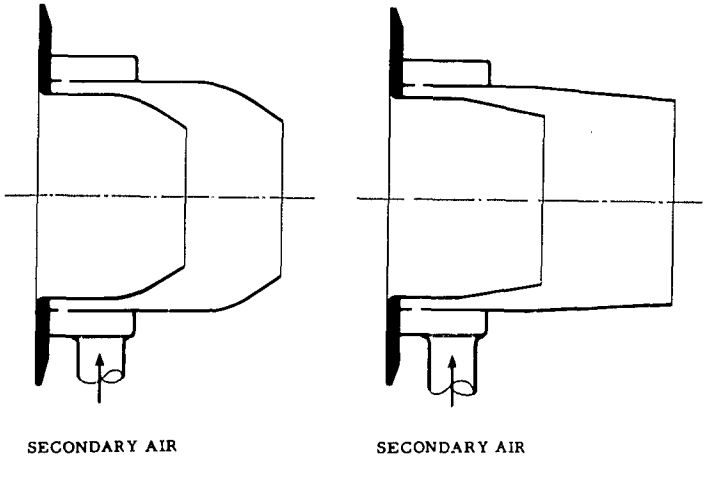

Figure 22. One-eighth scale model J-79 nozzles, (left) for military operation, (right) for afterburning operation.

2. High Pressure Afterburning Model

A water-cooled nozzle with an exit diameter of 1-1/2 inches was built for operation at Mach 1.6 over a temperature range of 2000° to 3000°F. The model afterburning engine was placed in its usual horizontal attitude, but 8 feet above ground. Exhaust was direct from the burner through the nozzle. This provided an essentially free field exhaust without the need for either turning the extremely hot gases or mounting the burner vertically. Octave band spectra were obtained at test points in the horizontal engine plane, from the nozzle exit to 16 diameters downstream, and up to 16 diameters sideways.

C. Helium at Ambient Temperature

Use of helium at ambient temperature to obtain near field sound level data for an exit Mach number of 1.6 required solving a series of practical problems. The cost of the gas is considerable, but not prohibitive if efficient use can be made of it. The only sources which could be conveniently provided were bottles containing three pounds of helium under 2200 psi pressure. Twelve cylinders of helium were manifolded together, and connected to the pressure regulator, plenum, and nozzle as shown in Figure 23. The plenum was used to minimize shock noise, valve noise, and line noise, as well as to provide a settling chamber.

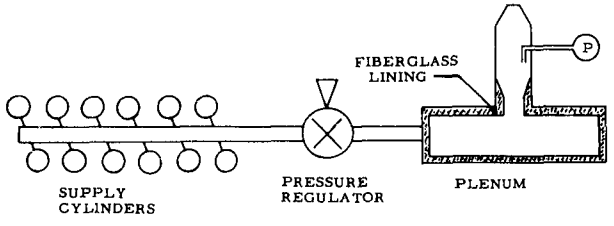

Figure 23. Schematic diagram of helium test apparatus.

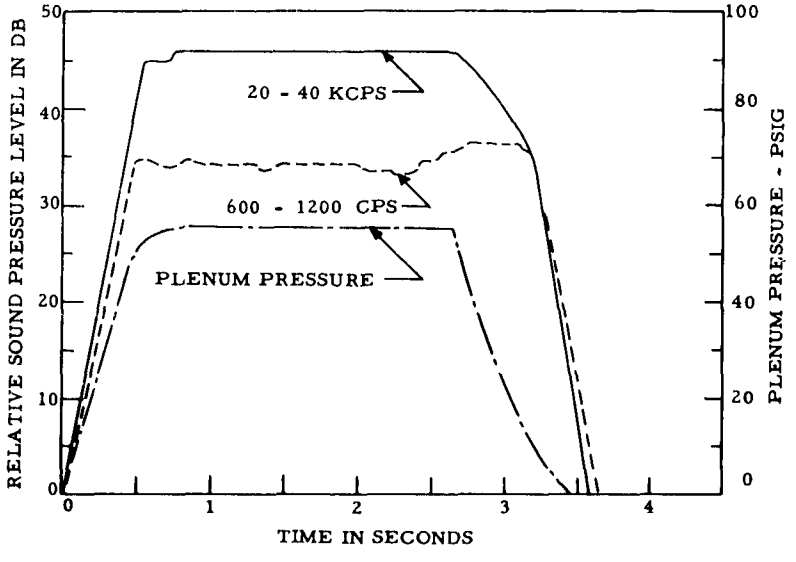

Figure 24. Time plot of plenum pressure and sound pressure level during a helium test.

Manual control of the plenum pressure was considered to be not feasible because of the high waste during the interval of pressure adjustment. A 3/4-inch nozzle was used, requiring a mass flow of about 1/4 pound per second. The flow was controlled by a Futurecraft Model 40079 pressure controlled pressure regulator. Satisfactory operation was achieved for 6 bursts of about 3 seconds duration each. Figure 24 presents sample time records of the plenum pressure and exhaust noise. It may be seen that the proper pressure

was achieved quickly and maintained steadily. The same observation applies to the time history of noise. For the particular source and plenum pressures used, the temperature change due to the throttling process across the pressure regulator was estimated to be negligible. The adiabatic expansion in the cylinders resulted in a temperature drop in the cylinders and plenum, but the duration of individual bursts was limited so that this effect was also negligible.

Noise level data were obtained for test points in the near field at the same scaled locations as used with the high pressure afterburning model described above. Octave band data were read out with the graphic level recorder for both of these test series.

D. Steam

A four-inch branch line was taken from a main plant steam line, supplying steam to the plenum shown in Figure 19, exhausting vertically into a free field. Up to 30 minutes were required to stabilize the temperature and pressure in this plenum, this operation consisting of adjustments to the valve at the branch line and adjustments of the steam superheater controls. The same test point locations as described earlier in this section for the heated air tests employing various sized nozzles were used. The general arrangement is shown in Figure 25. The first plenum condition used provided superheated steam even at the fully expanded temperature. An additional plenum condition provided saturated steam in the plenum and fully expanded steam with 4% water content at the nozzle exit.

Figure 25. Apparatus using steam as a substitute gas.

E. Liquid Rockets

A 140-pound thrust rocket motor was used for all scale model liquid rocket tests. A wide variety of chemicals could be used for suitable operation of this rocket motor. During operation, measurements of chamber pressure, oxidizer and fuel weight flows, and engine thrust were routinely obtained. Combined with knowledge of the nozzle geometry, all other rocket performance data could be calculated. All sections of the motor were water cooled.

1. AR-1 Rocket Model

A fuel of 75% ethyl alcohol-25% water was combined with gaseous oxygen to simulate an AR-1 rocket. The rocket was fired horizontally, 10.5 inches above the ground plane. Initial firings were at an equivalence ratio (ratio of fuel to oxidizer relative to the stoichiometric ratio) of 1.6. This ratio was then changed, maintaining the same total weight flow and chamber pressure, and additional firings were made at an equivalence ratio of 1.15. Figure 26 shows the test set-up. The two rows of microphones were placed nominally in the horizontal engine plane, but actually the elevations were adjusted somewhat so that the outer row would not suffer from any shadowing by the inner microphones. As the firings were each of one minute duration, direct read out with the true rms voltmeter was performed. Sound levels were essentially constant throughout each run, and octave band levels at any given test point were nearly always within one decibel for repeated firings.

Figure 26. Near field acoustic measurement of 1/8 scale model AR-1 rocket.

2. Jupiter Rocket Model

The Jupiter model rocket utilized kerosene as a fuel and gaseous oxygen as an oxidizer. The rocket was fired vertically downward onto a scaled bucket deflector, with the subsequent deflected exhaust being approximately horizontal, 10 inches above the ground. Figure 27 shows the test set-up. The bucket was water cooled. Erosion of the bucket surface occurred in spite of this cooling, and as a result the firings were limited to approximately 15 seconds duration. The sheet aluminum wrapped around the rocket motor provided a reasonable simulation of a missile skin, at least when compared with the highly irregular surfaces of the model rocket motor itself. The rocket motor's water cooling lines were grouped as well as possible to eliminate shadowing of any of the microphones. Data obtained for three firings of this configuration repeated in almost all instances to within one decibel. Data reduction was performed by one-third octave bands, and after observing the basically regular spectra which were obtained, octave band reduction from 150 to 80,000 cps was performed using the true rms voltmeter.

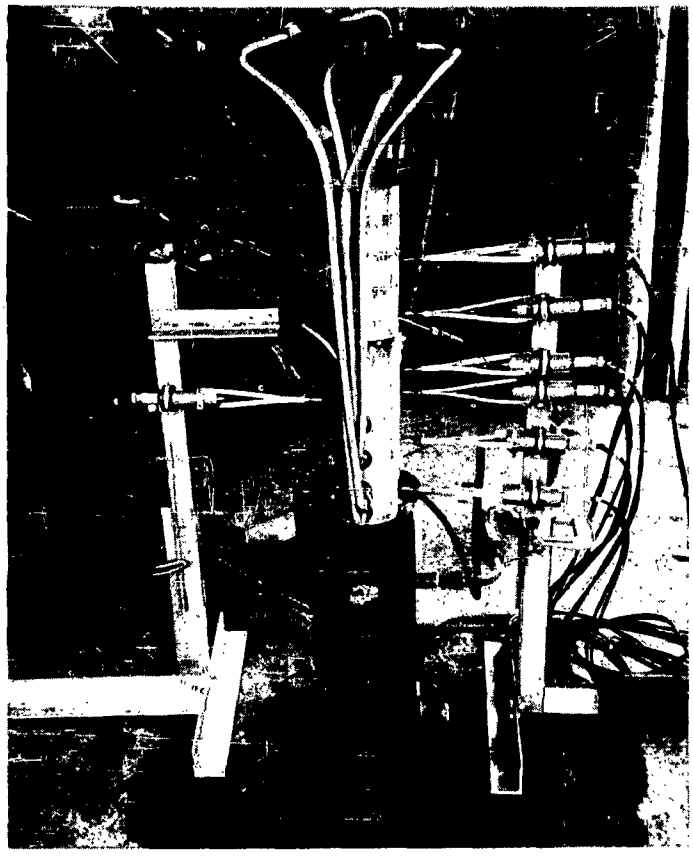

Figure 27. Near field acoustic measurement of 1/36 scale model Jupiter rocket.

F. Solid Propellant Rocket

Sound level data for 1/20, 1/3, and full scale Minuteman rockets, all utilizing essentially the same solid propellant grain, were obtained during a Minuteman development program. The 1/20 scale and 1/3 scale firings were for fixed positions in a silo, with firing durations of one second and three seconds, respectively. The full scale firings were "tethered" launchings from a silo. Water cooled Photocon microphones were mounted at a number of locations flush with missile and silo surfaces.

The 1/20 scale cold flow tests used Massa M-213 crystal microphones mounted flush with the silo wall. The duration of each test was 30 seconds. Two types of models were used in the cold model tests, providing full scale Mach number and pressure ratio, respectively. Various emergence conditions were used for both models to simulate the full scale missile motion and the other two subscale test programs. The nozzles for the subscale cold flow tests had area ratios less than the full scale nozzles so as to produce the same nozzle exit pressure. The exit diameters of all of the subscale cold flow nozzles were approximately 1/20 of the full scale exit diameter. The pressure ratio model mass flow was approximately 3/4 of the Mach number model mass flow.

V. DISCUSSION OF RESULTS

A. Duplication of Full Scale

The most important question concerning the use of acoustic scale models for near field investigations is "Do they work?" An attempt to answer this question will be made by comparing the noise fields of various types and sizes of full scale engines with the noise fields measured for models of these engines. Some of these engines are exhausting in free field situations, and others are in the presence of various reflecting and interfering surfaces. As far as possible microphone positions in the model surveys were chosen to duplicate exact full scale positions.

The method which has been chosen to compare the model and full scale results is to obtain the differences in sound level, octave by octave, between model and full scale measurements at each scaled microphone location. Before making this comparison an octave measured with the model is normalized by multiplying its center frequency by the scale factor. The datum at the normalized frequency can then be compared directly with the measured full scale datum. The resulting differences are averaged, producing the average agreement between model and full scale in any octave. Naturally, averaging differences which have a wide ranging scatter about the full scale data must be avoided, as the average could result in a misleading appearance of excellent agreement. To present these results a full scale spectrum which is typical in shape and level is chosen, and then a model spectrum is plotted alongside, separated from the full scale spectrum in each octave by the amount of the average agreement previously obtained.

Prior to these averaging operations the model data were examined carefully, considering (1) spectrum shape, (2) level at any point relative to nearby points, and (3) repeatability of data measured more than once. When significant deviations were observed by any of these check methods, the irregular data were deleted, and measured again if possible. This approach to qualifying data assumes only that the noise field of a jet engine or its model is continuous in frequency and space, that the source is repeatable, and that measurements are made at more than one point.

1. J-57 Engine

Reference 38 contains results of a complete sound level survey of a J-57 P-3 engine. To simplify the process of comparing these sound levels with the levels measured with a model of this engine, the sound level contours of the reference report were evaluated at each of 25 positions for each one-third octave band. By this means an octave band spectrum was reconstructed for each of the 25 test points, and direct comparisons were made with the model data measured at these same 25 test points. Figure 28 presents model to full scale comparisons for four areas of the J-57 sound field. Each area represents about six microphone locations grouped by their similarity in spectrum shape and intensity. In general good agreement is observed, with the model appearing consistently high in the highest frequencies.

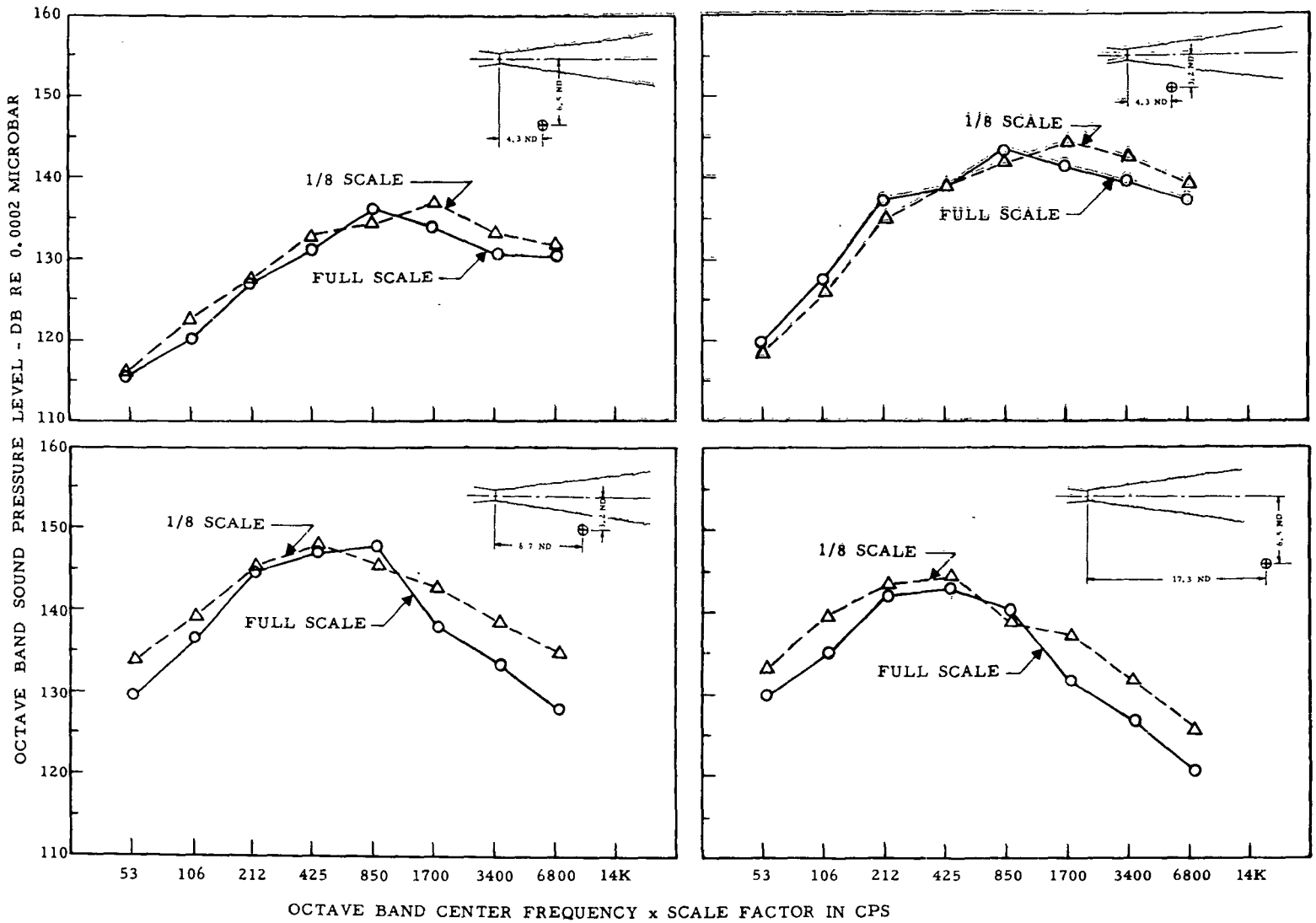

Figure 28. Comparison of model and full scale sound level measurements for a J-57 turbojet engine at four locations. Each of the comparisons shown is representative of the average agreement for an area centered about the point shown in the diagram. Full scale plenum conditions were duplicated by the model.

2. J-79 Engine

Reference 39 includes sound level measurements of a YJ-79-3 engine operating at both military and afterburning conditions. Again the full scale levels were presented in the form of sound level contours, requiring reconstruction of octave band spectra. As the levels obtained by the model, both for military and afterburning operation, were observed to be consistently much higher than the full scale levels, the usual averaging process was bypassed. Instead Figure 29 presents model and full scale spectra, military and afterburning, for a test point near the nozzle and for another point downstream. The test points shown are typical in that they show the range of differences observed. The magnitude of the model to full scale sound level differences shown in Figure 29 is a unique result. The nozzle of the J-79 (see Figure 22) is a complex variable orifice, primary-secondary nozzle arrangement, with cooling air being drawn in between the primary and secondary nozzles. Because of the possibility that this arrangement might have a significant effect on the exhaust noise produced, it was duplicated in the model nozzles, instead of using just a convergent nozzle. Further, model investigations were made a step at a time to delete the cooling air and the secondary nozzle. These changes, combined with adjustments in the plenum conditions to account for possible errors at that point, affected the noise field a small amount, but not nearly enough to account for the large differences observed. It was also observed that the 1/8 scale model J-79 at military condition produced a noise field similar to that of the 1/8 scale model J-57 described above, as would be expected in view of their comparable sizes and exit velocities. The full scale data for J-57 and J-79 military engines are significantly different however. A possible explanation for the lack of agreement by the 1/8 scale J-79 models is the failure of the model to duplicate some dimension or flow between the primary and secondary nozzles.

3. AR-1 Liquid Rocket

Measurement of the AR-1 rocket noise field is reported in Reference 40. This rocket uses a JP-type fuel and hydrogen peroxide oxidizer. The model facility which was to be used could not conveniently handle hydrogen peroxide, so 75% ethyl alcohol-25% water and gaseous oxygen were used instead. This combination generates approximately the same specific impulse as does the full scale combination. An additional specification for the model was that it operate at about 1.2 equivalence ratio to simulate the full scale rocket. This resulted in model sound levels in very good agreement with the full scale sound levels, as shown in Figure 30 (upper).

The model was also operated at an equivalence ratio of 1.6 to provide a check of the sensitivity of the noise field to equivalence ratio. Slightly higher sound levels resulted in this case, as shown in Figure 30 (lower). An additional observation was made that the total radiated power level was about 5 db greater when the higher equivalence ratio was used. It was concluded that re-ignition of the surplus fuel which is present when using high equivalence ratios was responsible for these observations. The location of this re-ignition noise source, and its directivity, could account for the different effects on near field and far field sound levels. Apparently, then, equivalence ratio of a model should duplicate that of its full scale counterpart quite closely.

4. B-52 Airplane

Figure 31 shows the results of extensive B-52 testing, 1/10 scale model and

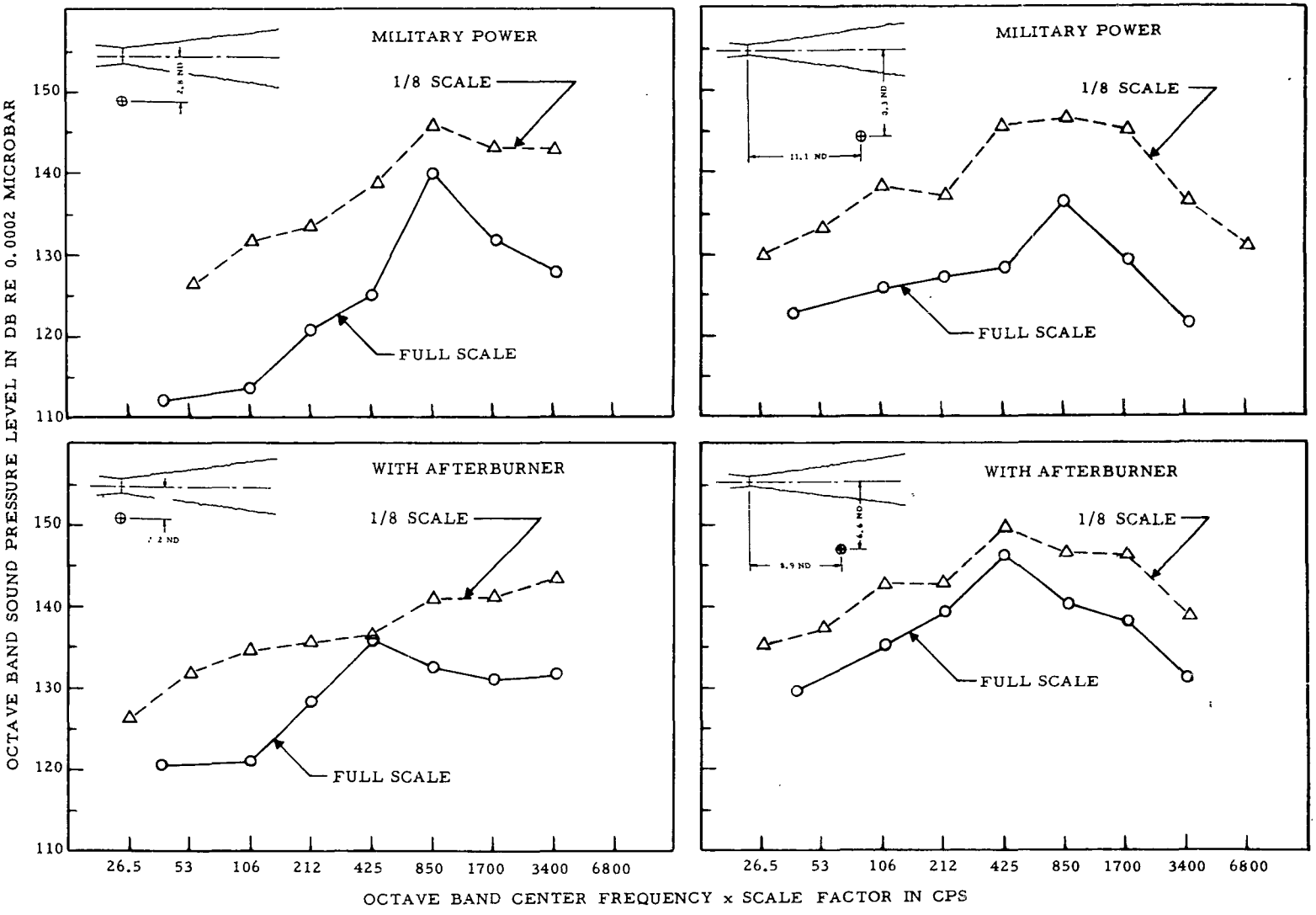

Figure 29. Comparison of model and full scale sound level measurements for a J-79 engine at two power conditions. Sound levels at microphone locations near the nozzle exit (left) and downstream (right) are shown. Full scale plenum conditions were duplicated by the model.

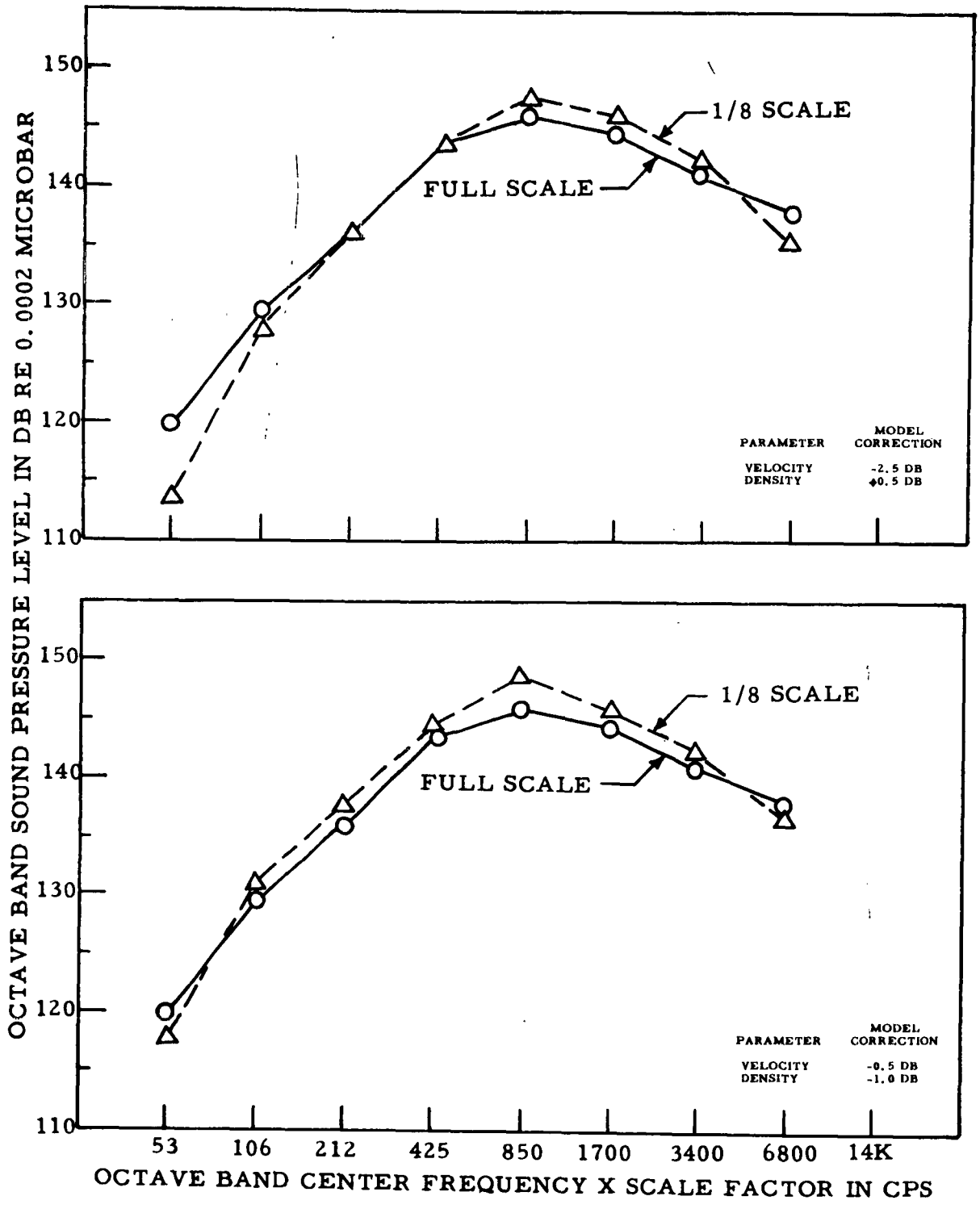

Figure 30. Comparison of model and full scale average sound levels measured for an AR-1 liquid rocket. The model liquid rocket utilized a different fuel and oxidizer than the full scale rocket. Two model rocket conditions were used, differing in exit velocity and amount of downstream re-ignition. The re-ignition is believed responsible for the slightly higher model data in the lower set of curves.

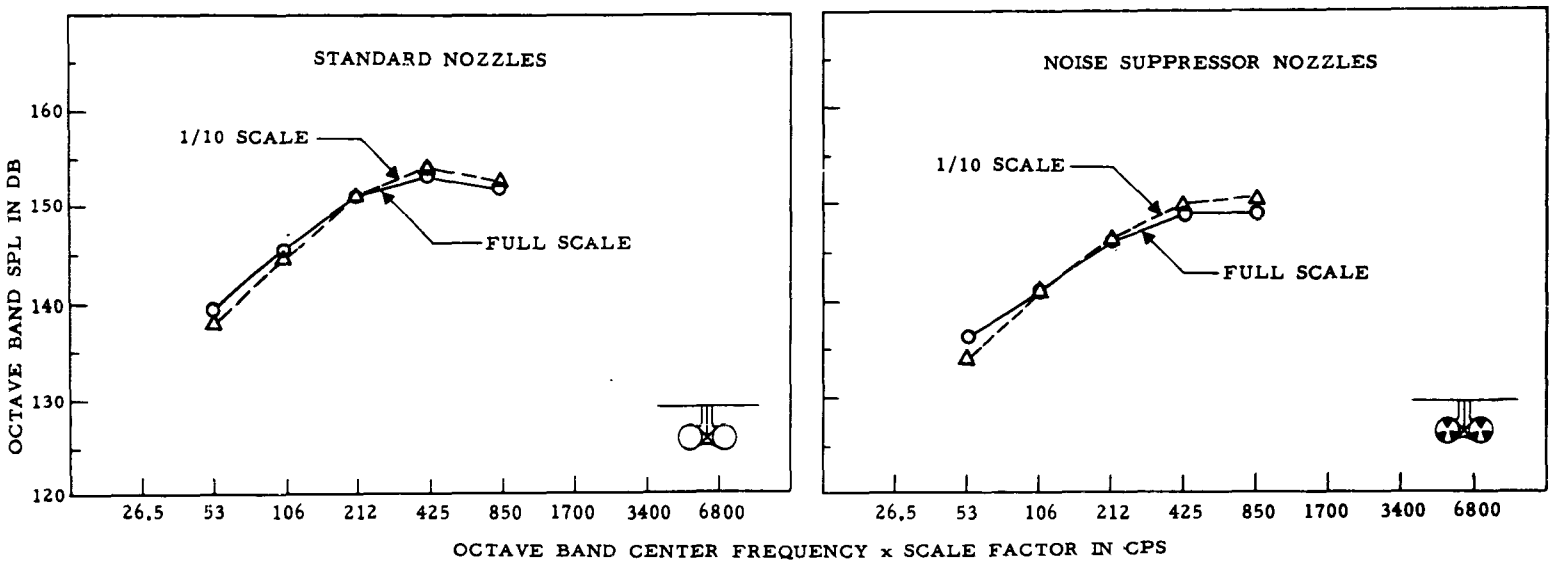

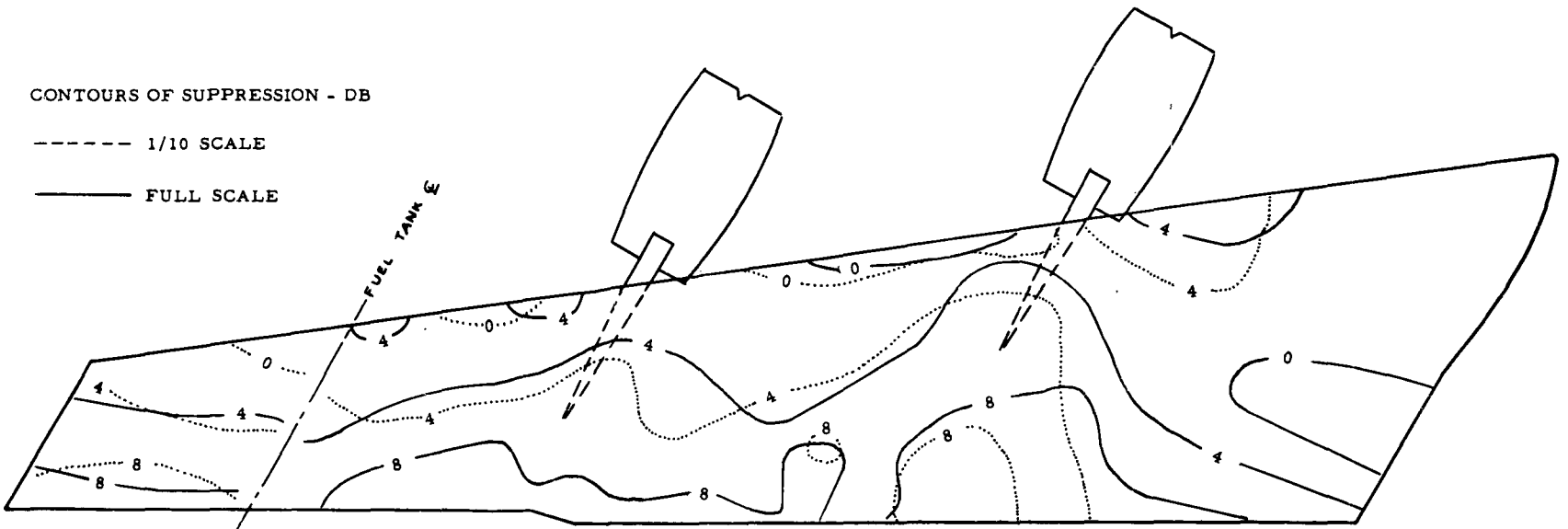

Figure 31. Upper--Average sound level measurements for model and full scale B-52 wing with standard nozzles (left) and suppressor nozzles (right). Lower--Contours of suppression in the 150-600 cps band as determined by model and full scale engines. The model used only two engines simultaneously, duplicating full scale plenum conditions. Successive measurements with the model engines at inboard and outboard locations were summed to establish four engine sound levels.

full scale. Since testing resulted from the process of designing a noise suppressor, data are available for two completely different nozzles on the same engines. With both types of nozzles the resulting sound levels on the under surface of the wing show good agreement model to full scale. Contours of suppression (the differences between standard and suppressor sound levels) on the underside of the airplane wing for the frequency band of 150 - 600 cps are also shown in Figure 31. In this respect also, good model to full scale agreement is evident.

5. Jupiter Liquid Rocket

Sound level data measured near 1/36 scale model and full scale Jupiter missiles are presented in Figures 32 and 33. This model was built to a smaller scale factor than any other model described in this report. The full scale data are from Reference 41. In Figure 33, octaves of frequency above and below the spectrum peak frequency are plotted versus position along the missile for model and full scale measurements. The low frequencies match quite well, diverging somewhat toward the top of the missile. In the higher frequencies there is a consistent difference between model and full scale levels. At a scaled elevation of 25 feet the model was measured on both sides of the missile. Whereas good agreement between opposite sides of the missile was observed full scale, the corresponding agreement was obtained only in the lower frequencies for the model. Inaccurate placement of the model bucket deflector could be responsible.

Correlation data were also obtained with the model Jupiter. Model and full scale results are plotted in Figure 34. Considering that the most important purpose of model correlation data probably will be to establish the first zero crossing, the agreement shown is good. In the lower part of Figure 34, significant differences in the correlation curves in the region of 200 cps are apparent. However, on the basis of the analysis given in Reference 41, a frequency of oscillation and a symmetry about zero correlation similar to those shown for the model data are to be expected. Three repeated firings of the model rocket produced this part of the curve with negligible variation in frequency or magnitude.

6. Minuteman Solid Propellant Rocket

Sound level data measured for 1/20, 1/3, and full scale solid propellant Minuteman firings in a silo are shown in Figure 35. In each chart a test point at a specific location on the missile has been selected for a particular emergence of the missile. Each spectrum is the average of two or more determinations. In contrast to most other model tests the same type of microphone (with limited high frequency capability) was used for all three missile sizes. This accounts for the lack of high frequency model data in Figure 35. The full scale sound levels in many cases varied rapidly in time due to the missile motion. It was necessary to read these data at estimated positions on the time scale in order to permit comparison at the specific emergences used by the static subscale models.

Sufficient data were obtained on each of the three test programs to enable sound level versus position on the missile to be established at all frequencies and missile emergences. A sampling of these data is presented in Figure 36.

The magnitude and time duration of the transient pressure pulse which occurs immediately following ignition of the solid propellant rocket in the silo is shown for 1/3 and full scale firings in Figure 37. The similarity of

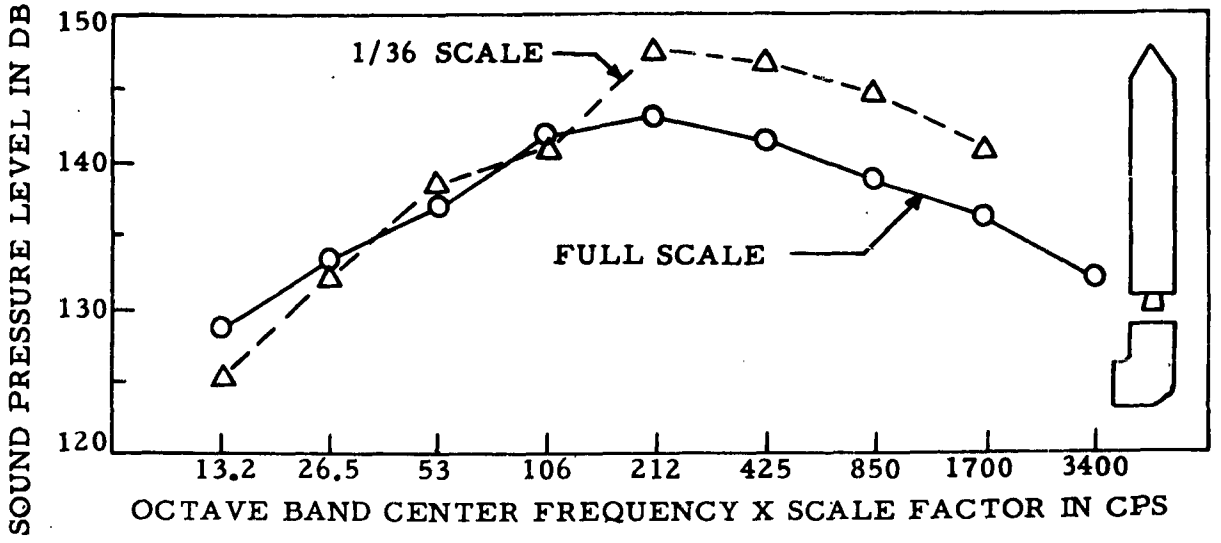

Figure 32. Model and full scale sound level measurements for the Jupiter liquid rocket. Results represent the average agreement observed at six elevations along the missile.

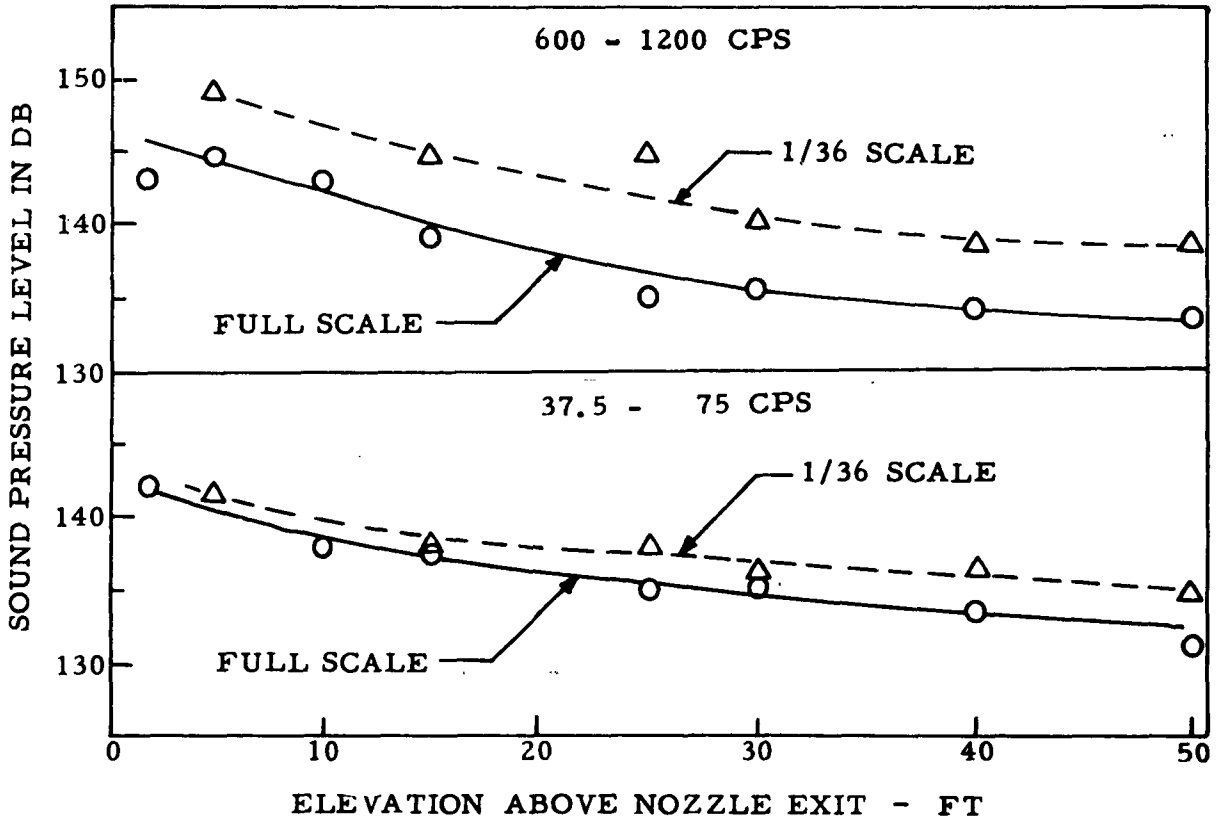

Figure 33. Sound level versus elevation for the model and full scale Jupiter missiles exhausting over a bucket deflector.

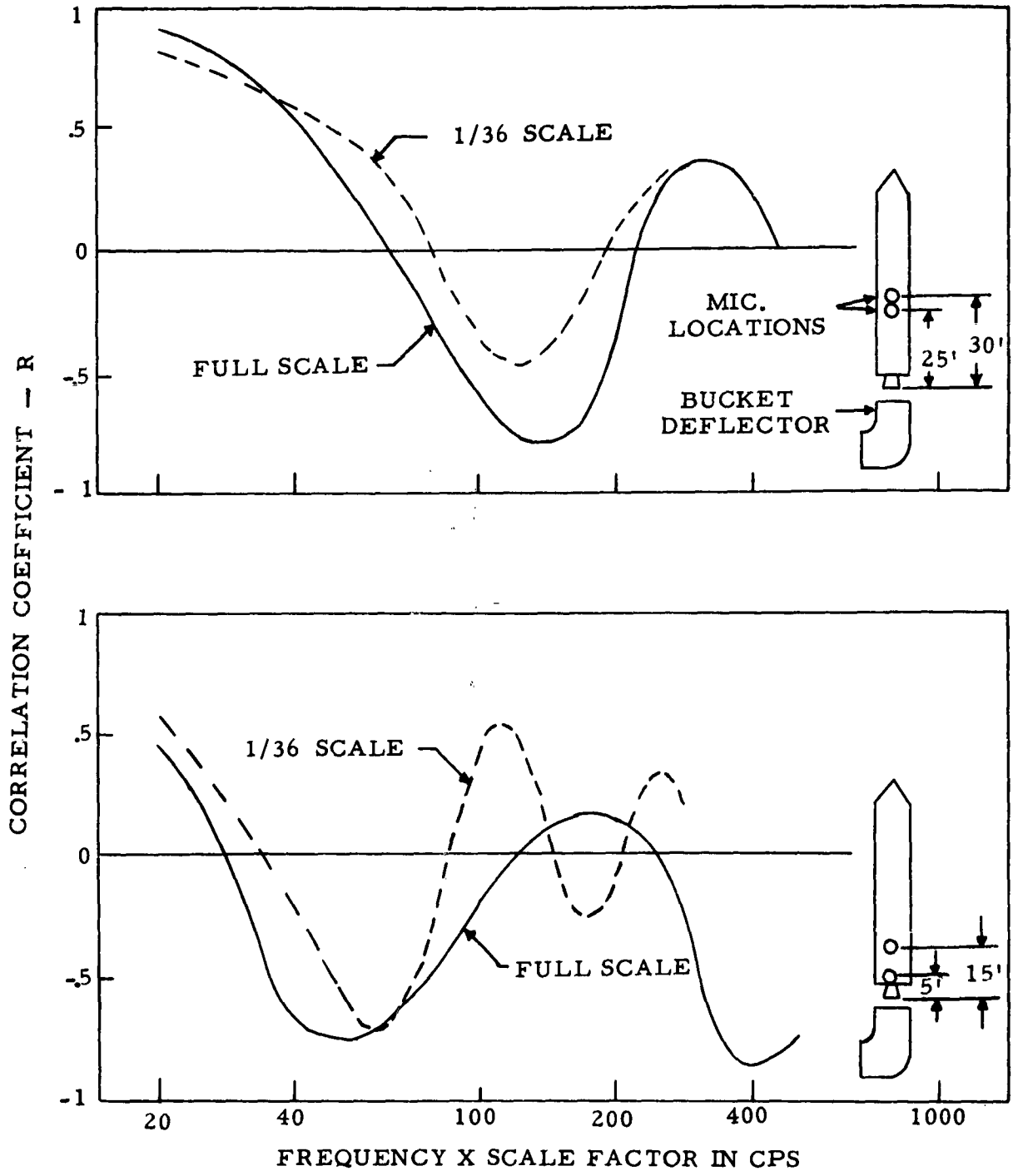

Figure 34. Model and full scale determinations of correlation coefficient for the Jupiter liquid rocket.

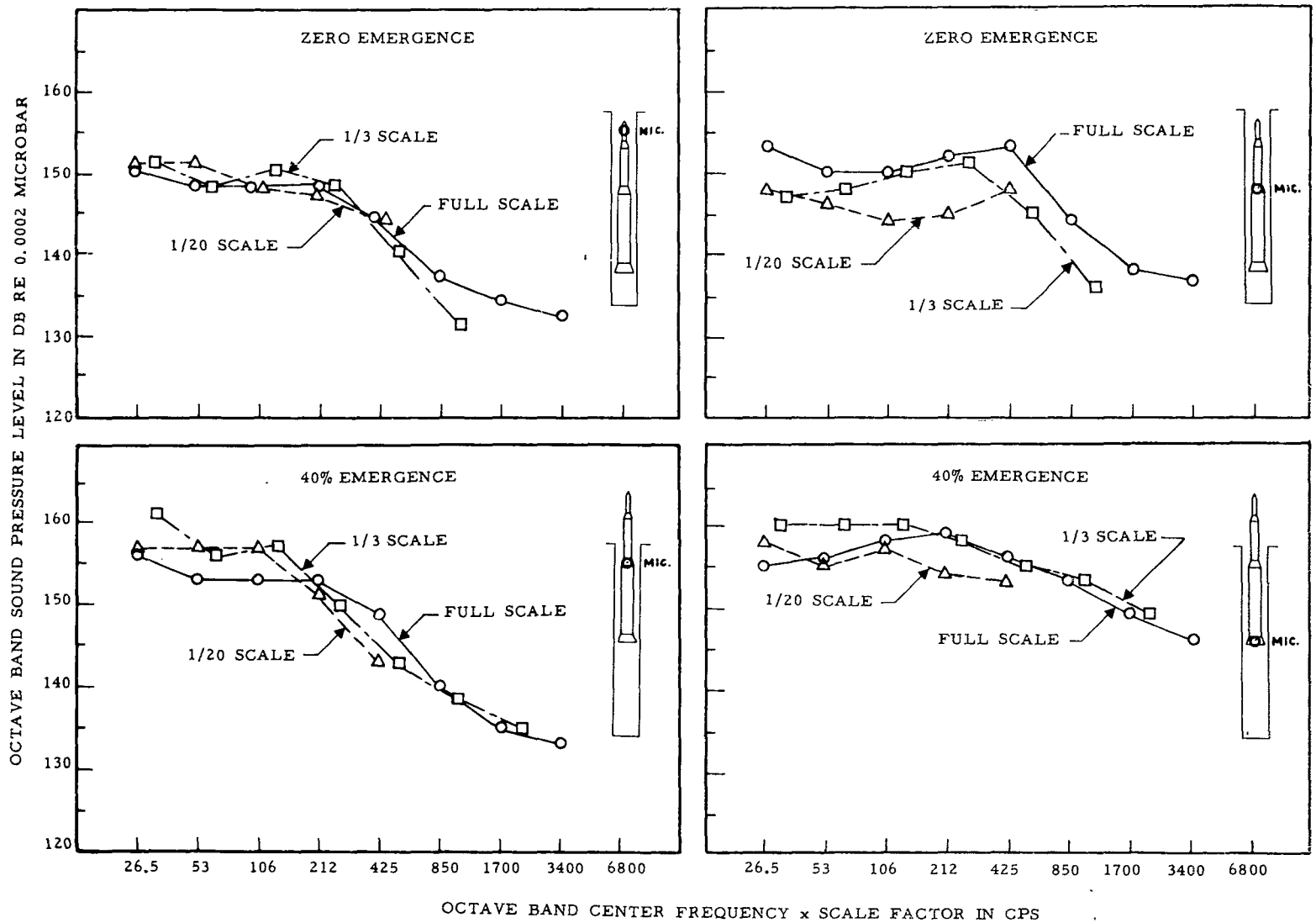

Figure 35. Comparison of sound level measurements for two sub-scale models and a full scale Minuteman missile during silo launch. Results for various microphone locations and missile emergence conditions are shown. Any given spectrum is the average of two or more repeated measurements. The model and full scale rockets are all solid propellant grain of essentially the same composition.

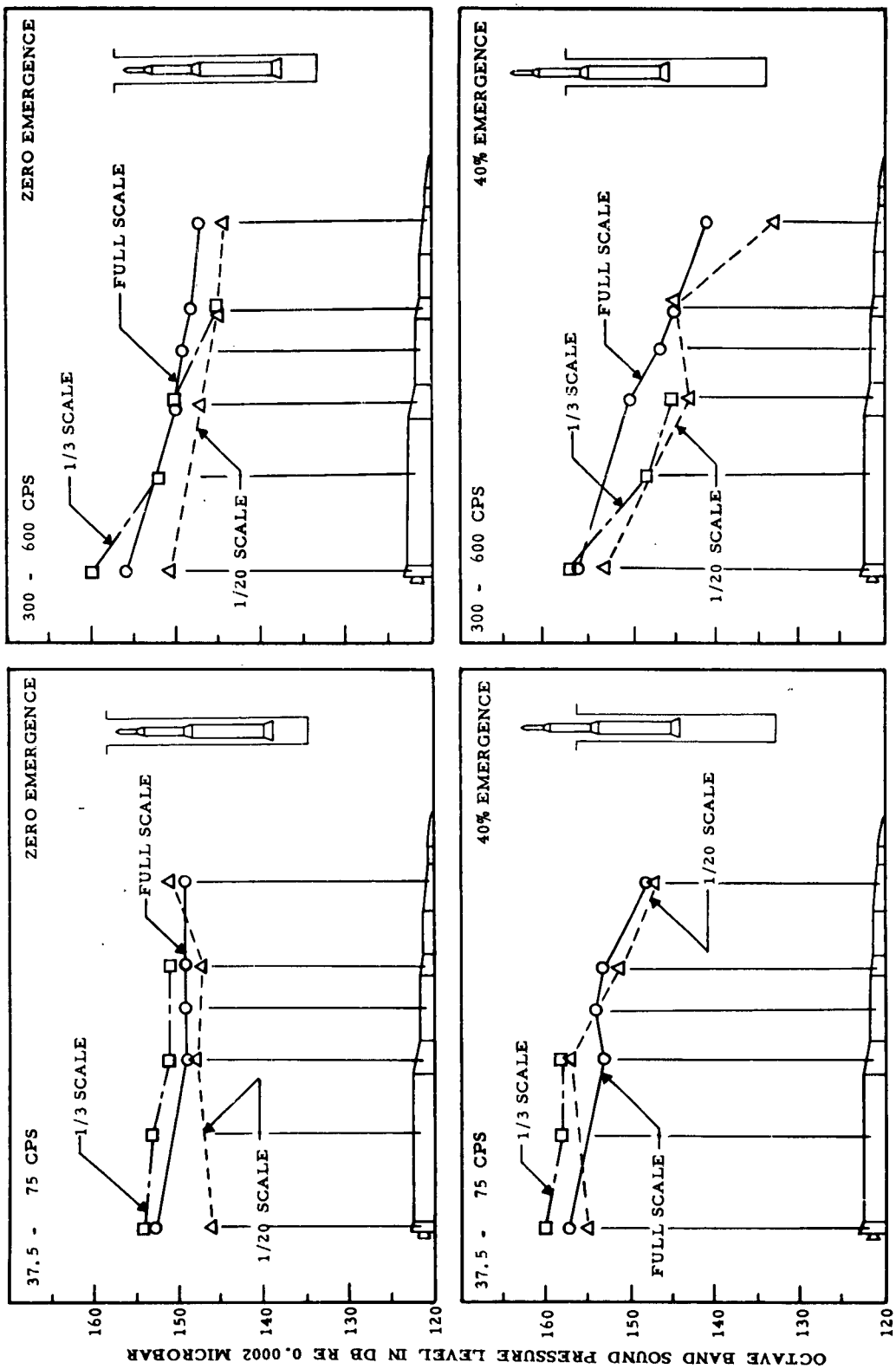

Figure 36. Sound levels versus position along the missile at two missile emergences are shown for two sub-scale models and a full scale Minuteman missile. The frequency bands indicated are equivalent full scale frequency. All of these rockets are solid propellant grain.

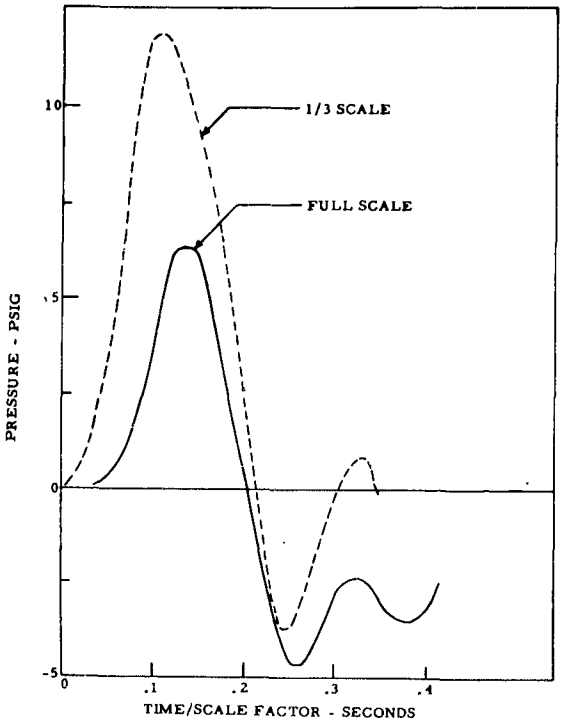

Figure 37. Minuteman transient pressure pulse.

the pressure pulses is apparent. Comparable data were not obtained with the 1/20 scale model because of detailed differences in instrumentation techniques. Pressure pulse data obtained on the 1/3 scale model program for two silo diameters permit an experimental check on the theoretical trend in pulse magnitude relative to silo diameter, as discussed in Section II. The results are shown in Figure 38.

It is concluded that the model techniques used in this unusual environment produced satisfactory results.

B. Simplification of Models

Having established that the noise field of a model fairly well matches the noise field of its full scale counterpart, it is appropriate to consider possible model simplifications, most of which result in reduced costs. Aspects of models which hold promise for simplification are reduced model size, use of lower temperatures, elimination of complex surfaces (or compatibility with existing surfaces), and use of less than the full number of engines.

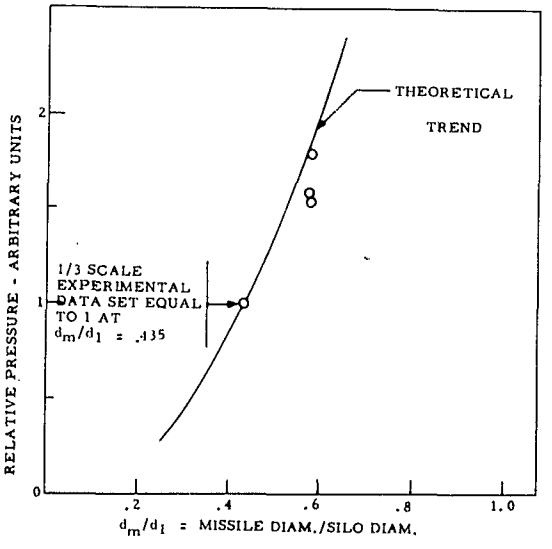

Figure 38. Experimental and theoretical trends in Minuteman transient pulse magnitude.

1. Model Size

Because of its direct bearing on costs, the suitability of using smaller models is the most important simplification to consider. This would be particularly important when a cluster of nozzles is required. The results of tests using a model turbojet military condition with four sizes of nozzles are shown in Figure 39. It appears that no limiting size has been reached by these nozzles. The only problem which appeared in using these nozzles is the limited high frequency capability of the instrumentation. If the data for the smallest nozzle could have been measured at all of the scaled frequencies used for the largest nozzle, a correction for absorption coefficient would have been necessary.

The critical nature of the microphone positioning is brought into perspective by

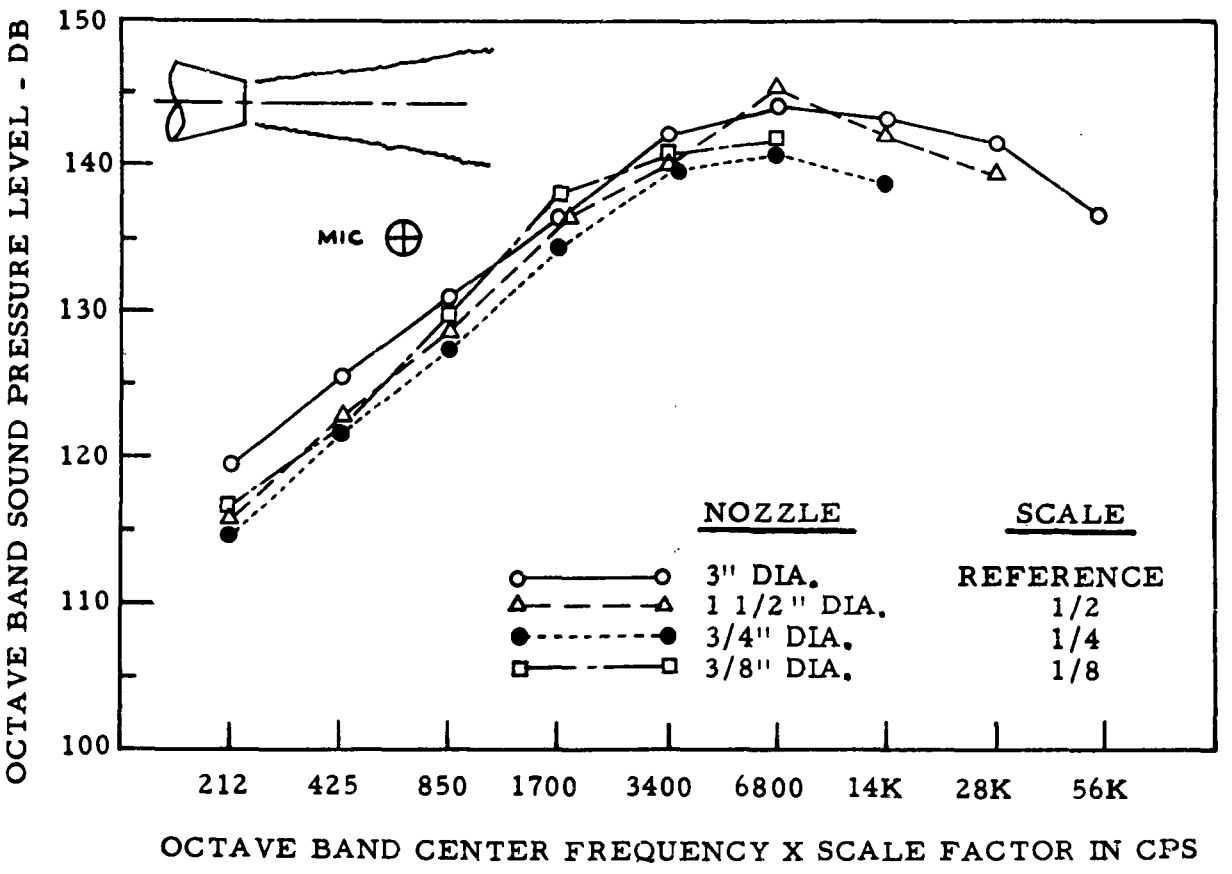

Figure 39. Similarity of noise produced by four nozzles varying in diameter by a factor of 8, all operating at the same plenum condition. Results are averages for a number of test points at scaled locations.

pointing out that for the smallest nozzle, microphones positioned one inch apart observed sound level differences as large as 10 db in some frequencies, whereas for the largest nozzle this 10 db difference was observed by microphones eight inches apart. Since the noise field for each nozzle was measured just once, relatively small errors in positioning the microphones relative to the jet exhaust for the smallest nozzles rapidly results in sound level differences of the order of 2 db.

2. Use of Air at Reduced Temperature

Cold Minuteman

The use of cold air is the simplest type of model which one can consider. A number of cold air model tests had been performed in the early development of the Minuteman missile; these tests were intended to show qualitative differences in effects of silo diameter, base shape, level versus location on missile, and level versus emergence of the missile. After comparing results of these tests with the hot model test results, it was concluded that the cold flow data were not too meaningful. However, the early cold flow tests used air at much lower pressures, and therefore lower Mach number, than full scale values. The result of the analytical studies indicated that use of such a model at full scale Mach number would at least be an improvement, if not a completely valid technique. In addition, since the exhaust gas flow is at high velocity on the silo surface, duplication of the dynamic pressure in the silo might yield full scale sound levels. Models for performing these types of tests were available, and so acoustics measurements with them were made to see if improved results could be obtained.

A sampling of the data obtained is presented in Figure 40. Neither the model which duplicated dynamic pressure, ρV^2, nor the model which duplicated exit Mach number, produced sound levels very close to full scale values. Although some characteristics of the full scale data such as changes in level with position or emergence are observed, these results were not consistently obtained.

Simulation of Vertical Take-Off

If the changes in level for a particular change in geometry are expected to be dramatic, as with an engine in vertical take-off, a useful simplification would be to use a model which operated at a lower temperature. Results of such an experimental investigation are shown in Figure 41. One exhaust condition corresponds to a turbojet military condition, and the other two conditions duplicate Mach number or velocity of the first condition, but operate at a lower temperature. While similar characteristics are observed for different exhausts at some frequencies, in general the changes in sound level are dependent upon which exhaust is being used. These observations are supported by other data not reported in Figure 41. It may be concluded that the sound level changes during a vertical launch of any type of engine will not be reliably duplicated by a model operating at significantly different nozzle exit conditions.

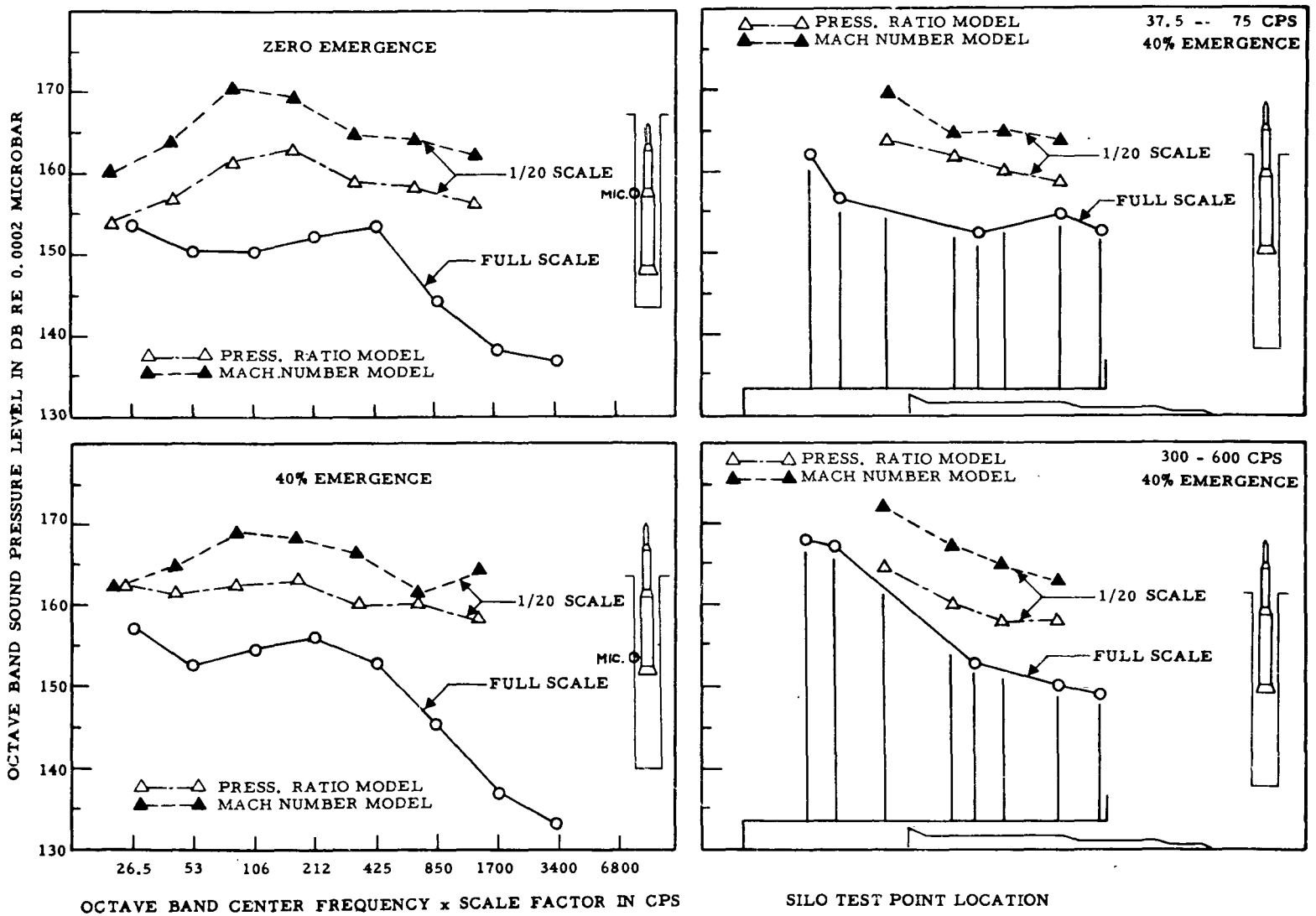

Figure 40. Sound level data for 1/20 scale models utilizing high pressure cold air are compared with data from full scale Minuteman firings. The Mach Number model simulated full scale pressure on the base of the missile, and the pressure ratio model simulated the full scale pressure on the silo wall. The pressure ratio model mass flow was approximately 3/4 of the Mach Number model mass flow. The frequency bands for the curves at the right are equivalent full scale frequency.

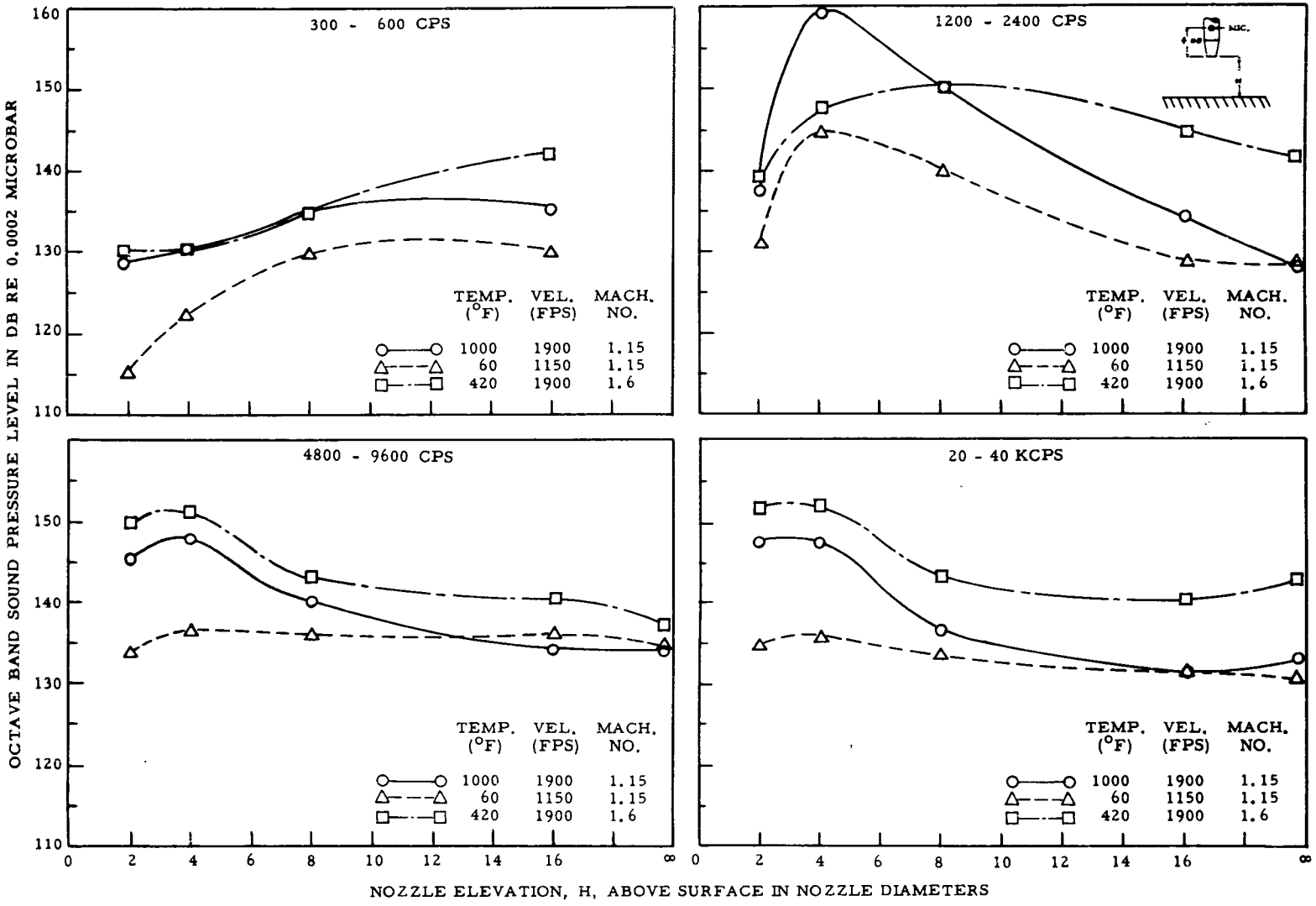

Figure 41. The change in sound level at a point on a simulated vehicle exhausting vertically downward against a plane surface is plotted versus vehicle elevation. Considering the complete spectrum, it is apparent that the rate of change of sound level is dependent upon the particular plenum condition used.

3. Use of a Substitute Gas

Helium

Figure 42 compares near field sound levels measured with a 3/4-inch helium jet, and a 1 1/2-inch high pressure afterburning-type jet. These two sources operated at the same exit Mach number and at nearly the same exit velocity and density. Plenum and exit conditions are tabulated below.

TABLE II

Plenum and Exit Conditions for Helium and Heated Air Models					
	GAS	TOTAL TEMP.(°F.)	MACH NO.	VELOCITY (FT/SEC)	DENSITY (LB/CU.FT)
(a)	Hot Air	3070	1.6	3860	.015
(b)	Helium	60	1.6	3860	.0195
(c)	Hot Air	2320	1.6	3440	.0195
(d)	Hot Air	2800	1.6	3720	.016

Conditions (a) and (c) above were planned to duplicate the exit velocity and density of the helium exhaust, respectively, and therefore, the initial plans were that two experimental checks would have been available, each requiring correction for only one parameter. However, for the particular combination of mass flow and pressure required by the 1 1/2-inch nozzle, it was found that the burner could not be operated at temperatures above 3000°F. This required substituting condition (d) for condition (a), so that the velocity of the helium was not matched exactly.

In order to compare the sound levels between the helium and hot air, it is necessary to evaluate the small sound level corrections necessary to account for the differences in density and velocity. Since the difference in level between conditions (c) and (d) was approximately 2 db at all near field test points and frequencies, the assumption of a first power correction for density as indicated in equation (12) enables an experimental determination of the velocity exponent to be made. This method avoids the necessity of arbitrarily selecting exponents which might not apply to the particular velocity range and near field test point locations used. An even more accurate determination of the velocity exponent could be made by obtaining data at additional plenum conditions in the same range. The velocity exponent calculated by this experimental comparison of (c) and (d) is about 7.

The spectra plotted in Figure 42 are for conditions (b) and (d) tabulated above, with appropriate corrections included. A similar comparison of (b) and (c) (not shown) yields an almost identical plot. Use of different exponents to establish the corrections would have resulted in agreement nearly as good as that

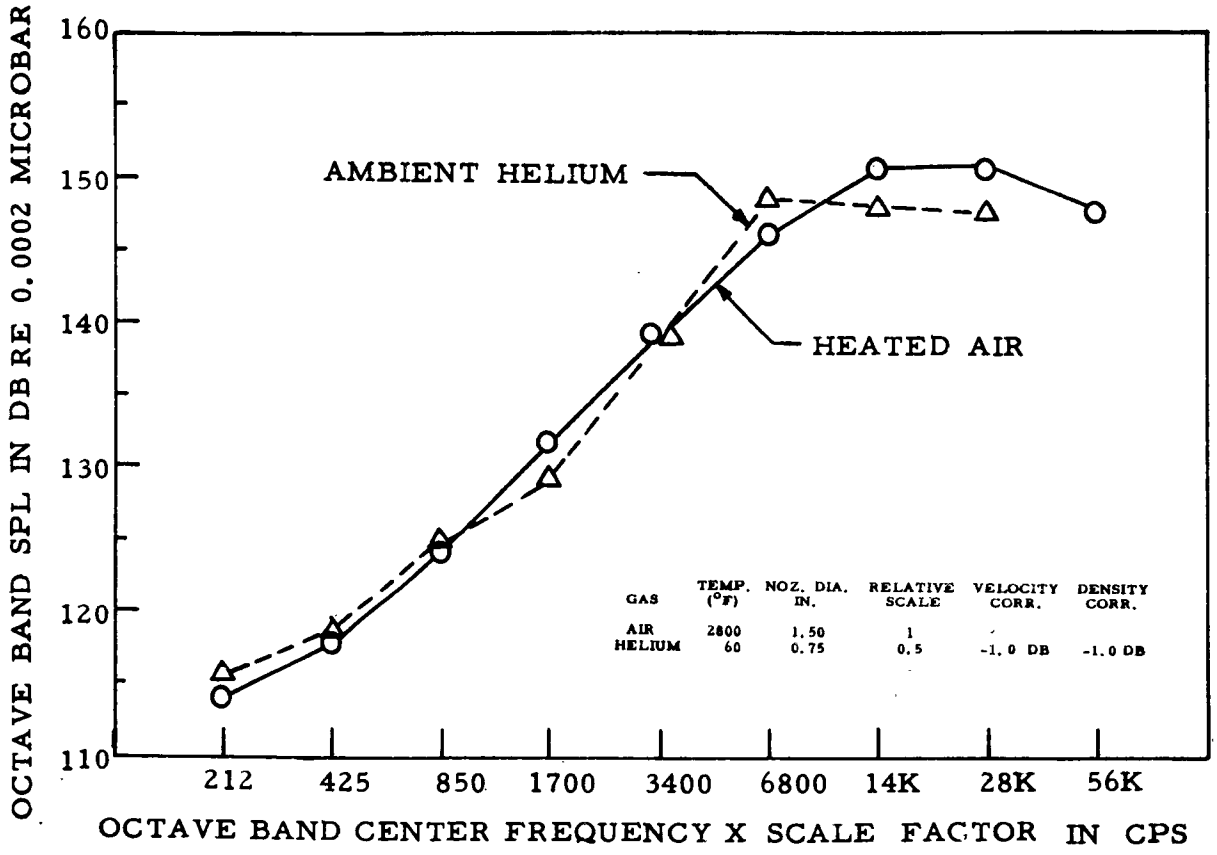

Figure 42. Comparison of sound levels measured using a high temperature air jet and an unheated helium jet. Exit parameters of the jets were chosen to nearly match velocity and density. Results are averages for a number of test points.

presented. The reason of course is that the velocities and densities for conditions (b), (c) and (d) are all fairly close to each other.

Steam

The near field data obtained for 20 test points in the near field of comparable heated air jets and superheated steam jets are summarized in the upper part of Figure 43. The Mach number, exit velocity, and exit densities of both types of jets were virtually identical, so no mathematical corrections were necessary as with the helium-heated air comparison. The agreement on the basis of all 20 data points is perhaps misleading. In tabulating the differences between the sound levels measured at each test point with each source, it was observed that the agreement for a test point tended to be either quite close at all frequencies or considerably different at all frequencies. The data were then divided into two groups: eleven points showed agreement of the data measured by the steam jet relative to the heated air jet to be within about 3 db at all frequencies; the remaining nine test points were different by about 5 to 10 db at all frequencies. These latter nine points were not located in any particular geometric pattern which would permit a difference in directivity by the two jets to account for their lack of agreement. Neither was there the possibility of ruling them out on the basis of an octave band level comparison with the nearby test points. In spite of this, results for the eleven test points chosen solely on the basis of their good agreement have been plotted in the lower part of Figure 43. The fact that 11 of these 20 points show very good agreement is believed significant, as it appears that basically dissimilar noise sources could not coincidentally produce the same noise field at half of the test points for which data were obtained. It is concluded that superheated steam is deserving of further consideration as a possible useful substitute to heated air in modeling turbojet exhausts.

One additional set of data obtained in the investigations with steam should be mentioned. Near field measurements with saturated steam for a model exhaust, rather than superheated steam as above, were compared with measurements at the same test points for a heated air jet operating at the same exit Mach number, velocity, and density. In this situation the sound levels produced by the steam jet were comparable in the low frequencies, but 6 to 10 db less in the high frequencies when compared with the levels produced by the heated air jet. This tends to confirm the general opinion that saturated steam does not possess sufficient similarity to a turbojet exhaust to permit its use as an acoustic scale model. It should be noted that the relationship between temperature and pressure for saturated or wet steam is such that Mach number, velocity, and density of any realistic engines cannot be duplicated.

4. Reflection

Observations at a Surface

The results of measurements which were made in the presence and absence of a solid surface are tabulated in Table III.

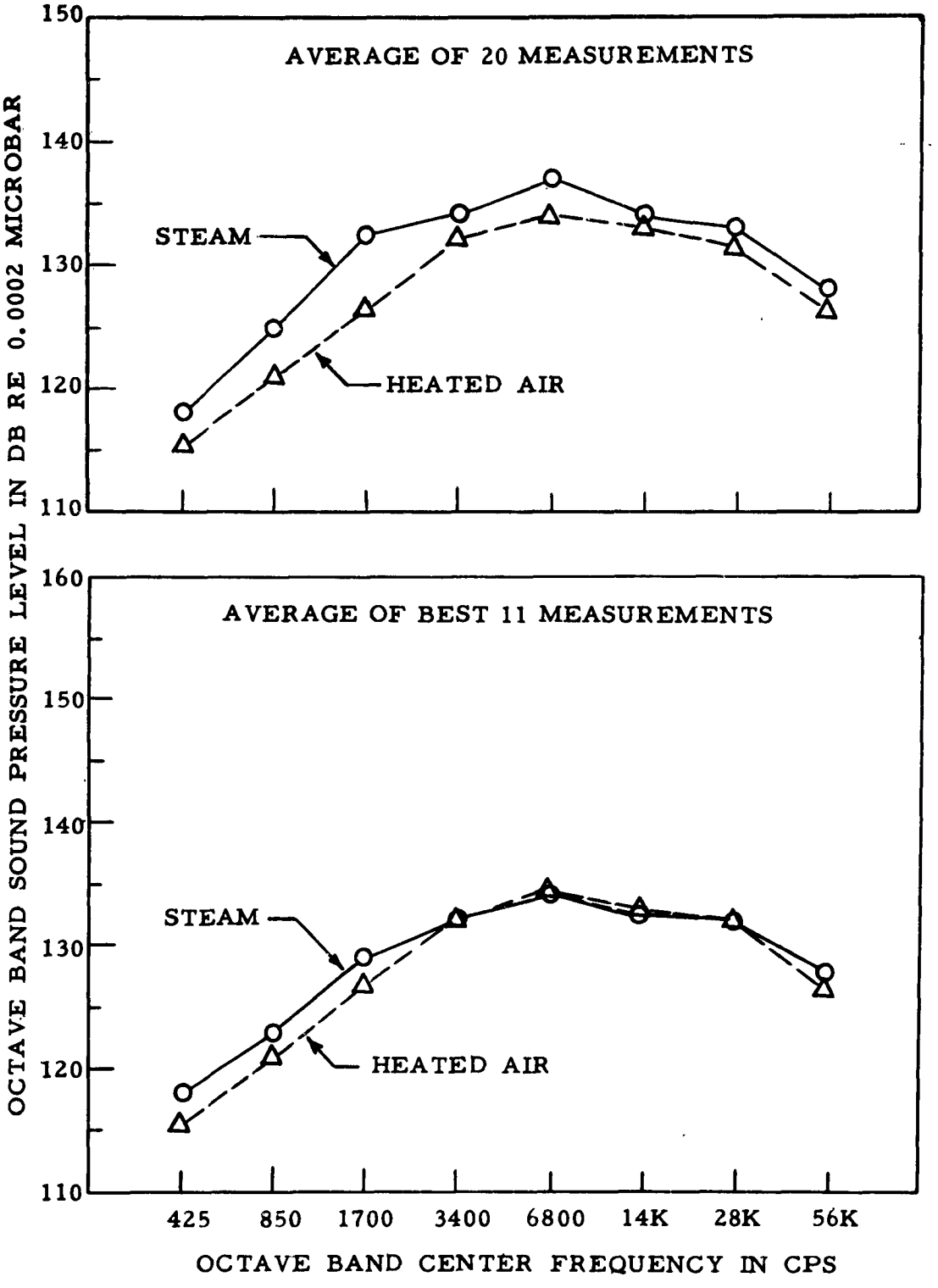

Figure 43. Comparison of sound levels measured using superheated steam and heated air jets at the same exit Mach number, velocity, and density.

TABLE III

Increase in Sound Levels[a] Measured Flush with a Solid Surface Relative to the Levels Measured at the Same Place in the Absence of the Surface.

Octave Band (CPS)	300-600	600-1200	1200-2400	2400-4800	4800-10K	10-20K	20-40K	40-80K
Measurement Plane Parallel to Nozzle Exit Plane	5.4	5.2	2.4	1.1	1.9	0.8	1.3	1.5
Measurement Plane Parallel to Jet Axis	3.8	5.0	3.7	2.2	1.5	1.3	2.1	1.9

[a]Values tabulated are averages of about 20 determinations, in db.

The main conclusion which may be drawn from these experimental results is that the levels at a surface are consistently higher than in free field, regardless of position in the field or plenum condition, and further, the amount of this increase is not readily predictable. Being in the near field makes it impossible to exactly define the location of a source, and therefore incidence corrections applied to a microphone will have limited accuracy. In such cases an actual measurement at the surface is to be preferred over a free field measurement which is corrected for the surface effects.

Observations Near a Surface

Figures 44 and 45 show the results of measurements made near a jet noise source, with and without a reflecting surface nearby. For comparison a curve showing the form of the effect to be expected theoretically is included in each chart. These latter curves are taken from Figure 12. An interpretation of a theoretical curve is that it shows the effect to be expected with a simple noise source if a frequency sweep were to be made with a bandwidth of one octave. Similarly, by referring to Figure 4 it is apparent that a similar frequency sweep with a bandwidth of one-third octave would, for a simple source, result in an effect with major maxima and minima at about the same dimensionless frequency as for the octave band situation, but with increased amplitude. Since the jet noise source is much too complex to qualify as a simple source, it is to be expected that octave band experimental results will not be as clearly defined as are the theoretical curves. Therefore, the experimental data were reduced by one-third octave bands. A comparison between the experimental and theoretical amplitudes of the maxima and minima are then valid only so far as to indicate order of magnitude. The frequencies at which the first few oscillations occur should be the same however.

In Figure 44 the receiver which shows the better agreement with theory is the receiver between the source and surface (No. 1). Receiver No. 2 was separated from

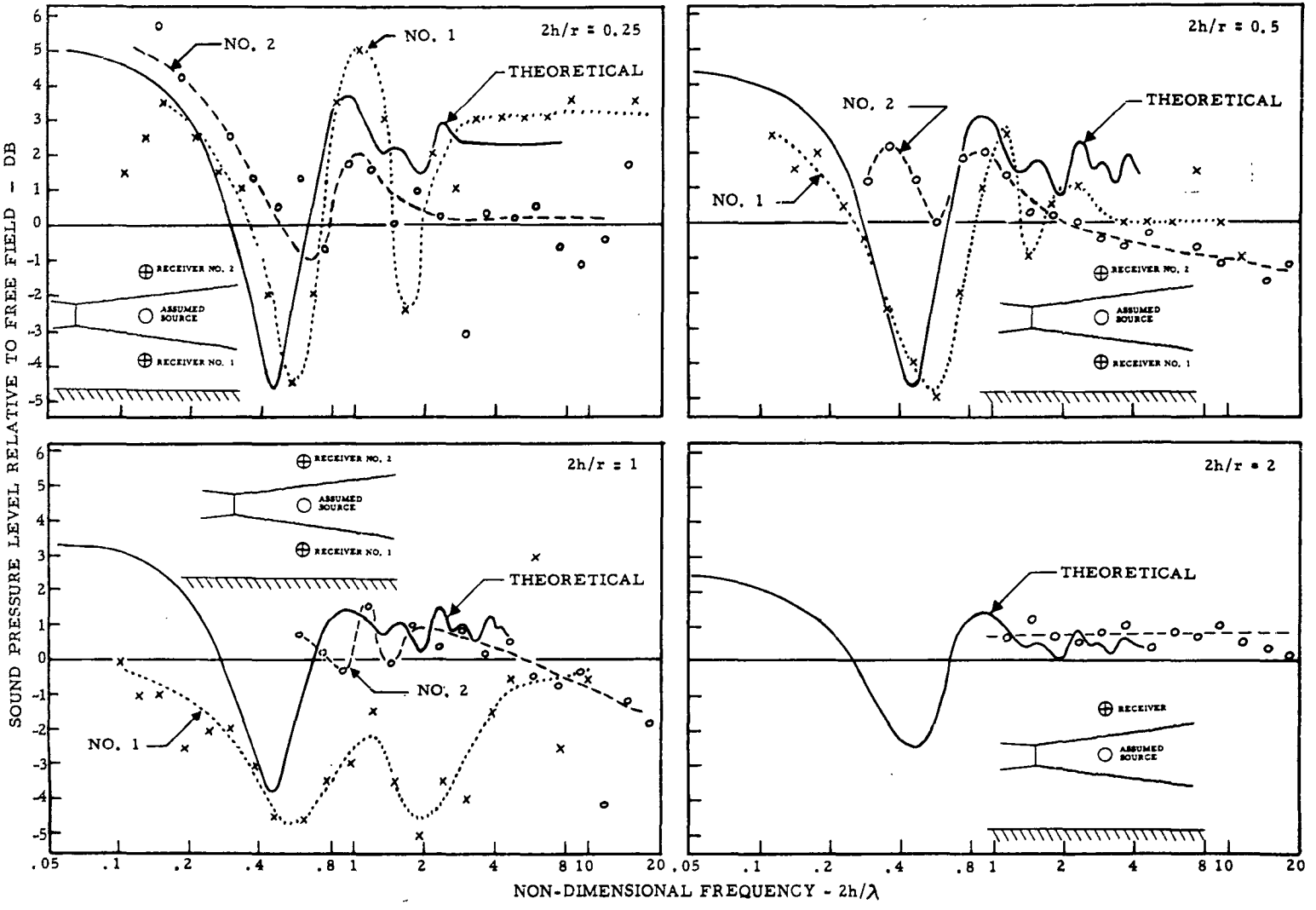

Figure 44. Effects of a reflecting surface on the sound levels observed at locations near the surface are compared with the theoretical effects. The source-receiver relationship is $\theta = 90^{\circ}$ (see figure 12). The reflected noise arriving at Receiver No. 2 passed through the jet exhaust.

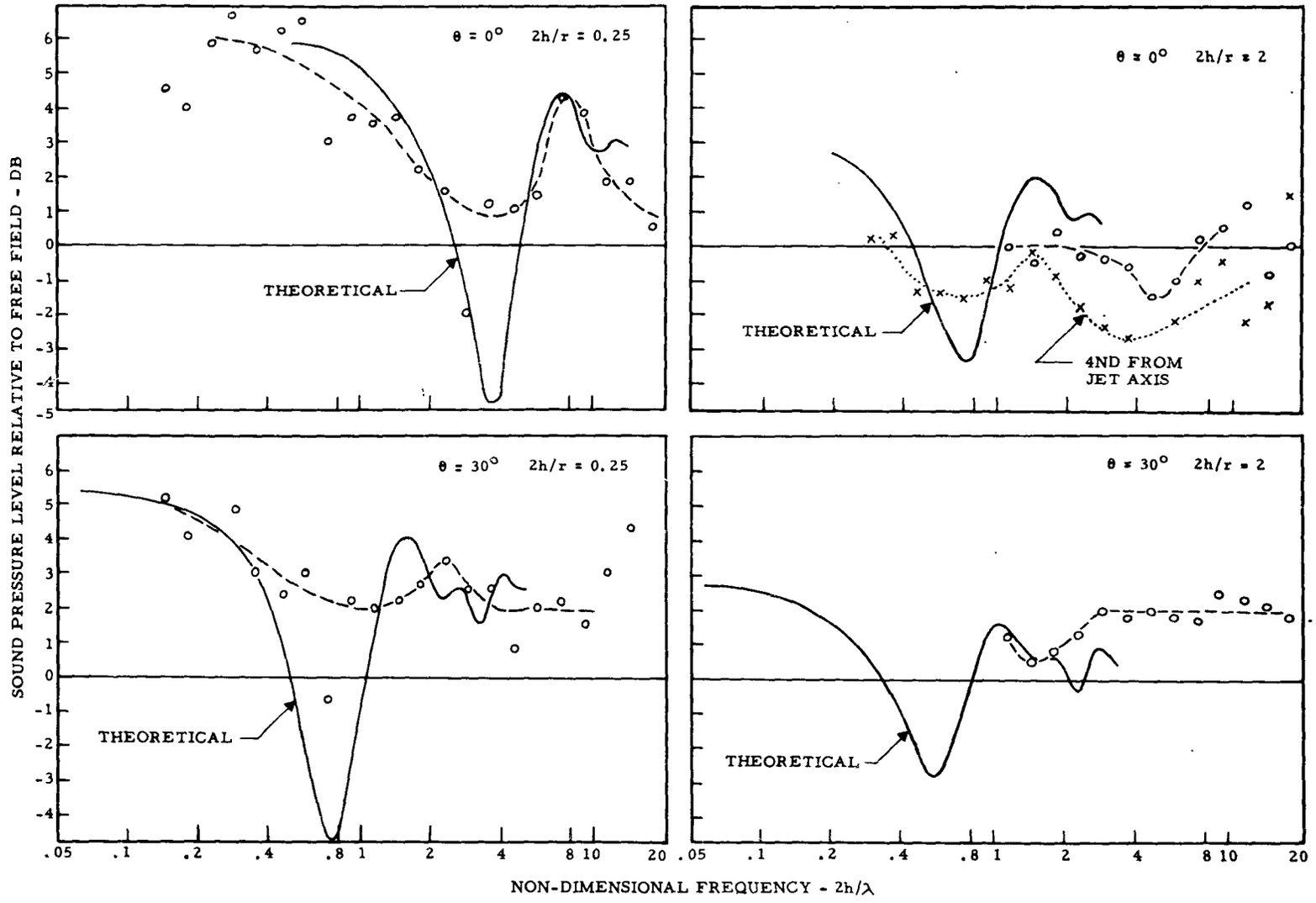

Figure 45. Effects of a reflecting surface on the sound levels observed at locations near the surface are compared with the theoretical effects. The source-receiver relationships are $\theta = 0^{\circ}$ and $\theta = 30^{\circ}$ as described in Figure 12. The lowest frequency for which experimental data are plotted in all cases is for an equivalent full scale frequency of about 20 cps. Except as noted, r = 16 nozzle diameters.

the surface by the exhaust, so any noise reflected to it had to pass through or around the exhaust. In Figure 45 the experimental effects are less pronounced.

As the value of the parameter 2h/r is increased, the magnitude of the effects decreases as expected. Examination of the data in Figures 44 and 45, as well as data for other values of 2h/r not included here, indicates that the effects are relatively small for values of 2h/r of about 2 or greater. The importance of a nearby reflecting surface may be estimated on the basis of the results reported here. If a preliminary calculation indicates that some effect of reflection might occur in a given situation, considering frequency as well as geometry, it is recommended that the surfaces be included in the model.

5. Multiple Sources

Sound Levels

Figure 46 presents a sampling of the types of data obtained from a pair of model jet engines. Included is a comparison of the average octave spectra obtained at any specific point (1) by measuring with two engines and (2) by summing two measurements from one engine. The data in the upper part of Figure 46 are for two engines separated by two nozzle diameters, very nearly the minimum spacing attainable with jet engines. The intersection of the velocity boundaries of these two engines (if this boundary is assumed to diverge at 8° from the nozzle lip[38]) is 3 1/2 nozzle diameters downstream from the nozzle exit. The major part of the noise generated by these nozzles is probably generated downstream of this point. The data in the lower part of Figure 46 are for two engines separated by eight nozzle diameters. If the same 8° divergence of the velocity boundary is assumed to hold, the two exhaust streams will intersect about 25 diameters downstream. Actually such an angle of divergence is probably only realistic for a few diameters downstream. In any event the noise-producing portion of each exhaust stream is clearly separated from that of the other nozzle.

The left side of Figure 46 shows typical data obtained for test points which receive comparable amounts of energy from each engine. In one case the test point was symmetrically located, so the measurement from each engine was assumed to be identical, and the sum of the two separate outputs at this point is just 3 db higher than the output for one of the engines. The data in the right side of Figure 46 are for test points for which considerably higher sound levels are measured from one engine than from the other. In this case the sum is only slightly higher than the contribution from the closer engine.

In general it appears that data measured for two engines operating simultaneously are somewhat higher in level than the levels calculated on the basis of two measurements from one engine. This result seems to be independent of the location of the test point in the noise field. As shown in Figure 46 the relationship between levels measured and calculated was closer for the wider spacing of the two engines, but only by a small amount. In addition, the measured and calculated values are in slightly closer agreement at the higher frequencies than at the low frequencies. Data obtained for engines spaced four nozzle diameters apart (not shown) tend to agree with these observations.

It appears that the technique of calculating the levels from two engines operating simultaneously by measuring only one engine is useful in the event that

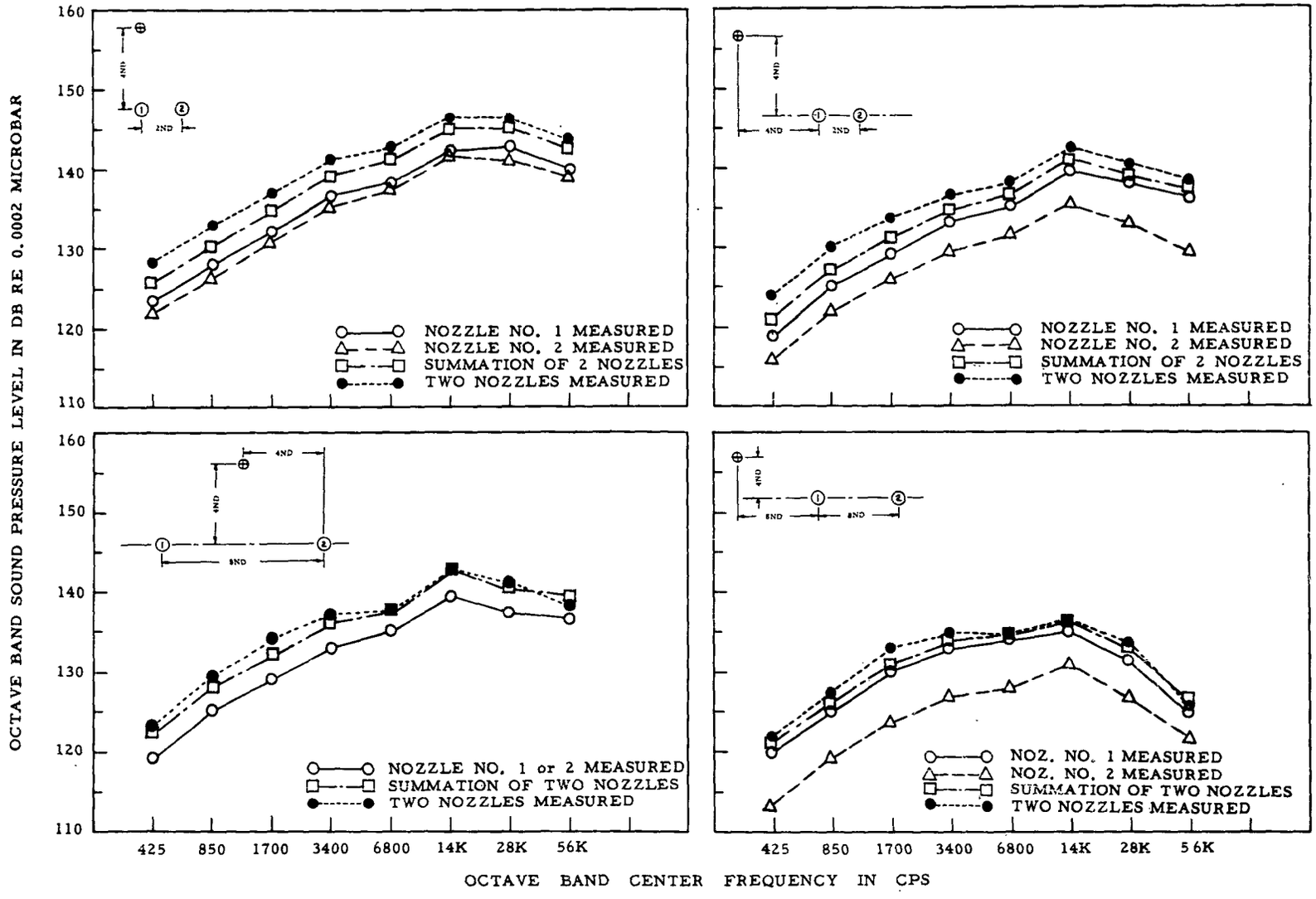

Figure 46. Comparison of sound levels measured for two engines operating simultaneously and sound levels calculated by summing two measurements each from a single engine.

two engines cannot be provided. The technique becomes less suitable as the engines are placed closer together. These results are in agreement with the B-52 model test technique which duplicated both engines spaced very close together, but summed mathematically the noise fields from nacelles (pairs of engines) which were widely separated (see Figure 31).

Space Correlation

Coefficients of space correlation measured in the nozzle exit plane for pairs of model engines are plotted in Figure 47. In each case the coefficients obtained when operating only one engine of the pair are also plotted. It is concluded that two independent sources produce nearly the same plot of correlation coefficient as does one source, for a symmetrical situation. For the two-nozzle-diameter spacing of engines, the higher frequency sources, if assumed to be no more than about five diameters downstream, are still fairly well separated. The low frequency sources, being ten or more diameters downstream, more nearly appear to be a new complex source. This could account for the greater difference between one and two engine results indicated in the upper left chart. The possibility is suggested that measurements of space correlation could serve to establish whether it is appropriate to sum sound levels for particular spacings and frequencies of a pair of engines. It is possible that detection of such effects would be simpler for spacings as close as those used in nozzle clusters, or for a correlation determination along some other symmetrical line, such as parallel to and close to the exhaust axes.

C. Measurement Repeatability

Data were obtained more than once for a number of the model tests. The standard deviation of the difference between any given measurement value and the average value obtained for that test point and specific noise source has been calculated for a sampling of different types of tests. Table IV shows these values.

Repeated firings of the model Jupiter rocket were all accomplished within a few hours, and the positions of the microphones and rocket were undisturbed during that interval. The statistics presented below for Jupiter then indicate that the repeatability of the model rocket as a noise source was very good. The measurements presented for flush-mounted microphones were separated by several weeks; therefore, these measurements include (1) the effects of any long term instabilities in the measurement electronics, (2) the lack of repeatability of the noise source, and (3) inability to exactly position the measurement locations relative to the noise source at some later date. Differences involved in the free field statistics were from data obtained on a given date. The variations indicated under "fixed microphones" are due then primarily to minor variations in the noise source at a slightly later time and to the random differences in reading the sound level indicating meter. The "re-positioned microphones" data were measured a short time after the "fixed microphone" data were taken, but in the meantime all of these microphones had been removed from their mounts and then replaced; this required that the location in space for each microphone be established a second time. The data under "different microphones" were obtained on a given date by placing three

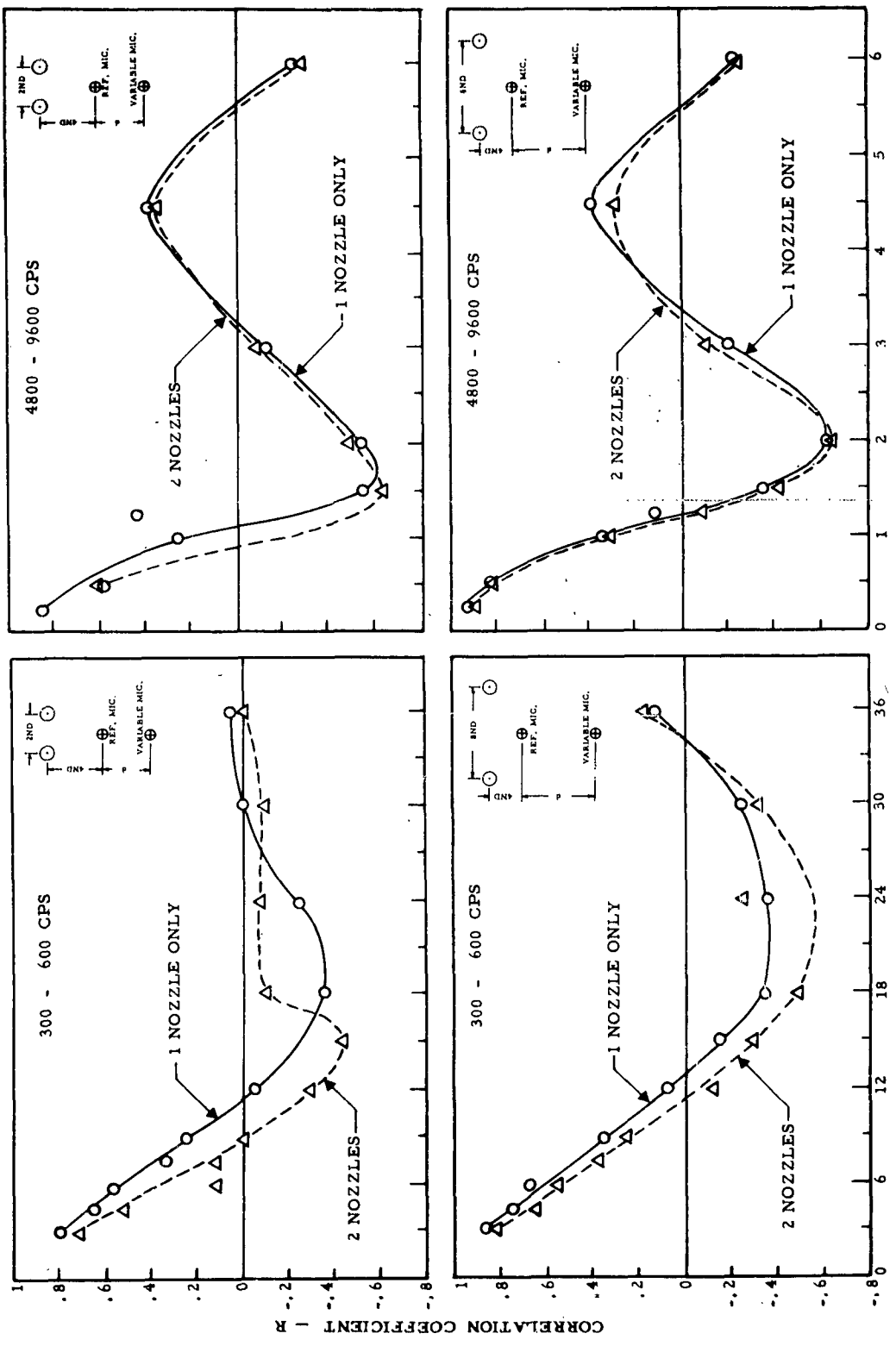

Figure 47. Space correlation measured on a line of symmetry between two nozzles operating simultaneously, compared with the space correlation measured at the same place with only one of these nozzles operating.

TABLE IV

Standard Deviation of the Difference in DB between Repeated Determinations of Octave Band Sound Levels at a Point and the Average Value Obtained for that Octave and Point

Octave Band (cps)	(1) Jupiter model rocket	Heated Air Jet Source			
		(2) Flush mounted microphones	Free Field Measurements		
			(3) Fixed microphones	(4) Re-positioned microphones	(5) Different microphones
150-300	0.9	---	0.5	0.4	1.5
300-600	0.5	0.7	0.6	0.4	1.1
600-1200	0.3	0.7	0.3	0.4	0.9
1200-2400	0.4	0.6	0.3	0.4	0.8
2400-4800	0.4	0.7	0.5	0.6	1.1
4800-10K	0.9	0.8	0.5	0.6	1.4
10K-20K	0.7	0.6	0.5	0.7	2.0
20K-40K	0.4	0.7	0.5	0.7	1.6
40K-80K	0.4	0.8	0.3	0.9	2.6

Sample sizes: Jupiter - 7 points, 3 times; flush microphones - 34 points, twice; fixed microphones - 23 points, twice; re-positioned microphones - 23 points, twice; different microphones - 17 points, 3 times.

microphones successively at a given test point. Thus in this case calibration errors are added to the causes of differences already stated.

Although the size of the samples is not as large as is required for complete interpretation, for columns (1) through (4) it is apparent that there are no large variations in repeatability with type of repetition scheme or frequency band. One possible exception to this is the highest frequencies in column (4), for which the microphones were re-positioned in free space. It is to be expected that the accuracy of microphone positioning is more critical for measurement of the highest frequencies, and a trend substantiating this is indicated in column (4). The increase in the standard deviation with frequency in column (5) reflects the increasing difficulty of obtaining accurate microphone calibrations at these frequencies. The data for the 150-300 cps band are probably not especially significant because the sound levels measured were in many cases very close to the background noise of the electronics.

To give added information about the data from which the standard deviations were calculated, the differences in measurements which resulted in a standard deviation of 0.6 db at 10 - 20 kcps for the flush-mounted microphones will be discussed as being typical. Of the 34 test points measured twice, 15 of these were measured 1/2 db lower on the second test, so the mode is -0.5 db. The median is also -0.5 db, and the mean value of the differences is -.94 db. Seventy percent of the values obtained on the second test were within ± 1 db of the values obtained on the first test, and 97% were within ± 2 db.

VI. CONCLUSIONS

A model noise source which is identical to a full scale source except in linear dimensions will scale the near field noise to a reasonable accuracy. Proper model gas flow is readily obtained by using the full scale gas at full scale values of plenum temperature and pressure. Experimental support of this conclusion has been demonstrated for a wide variety of nozzle exit conditions, from turbojet through rocket exhausts, and whether in the free field or in the presence of a variety of objects which interfere with the flow, such as shaped nozzles and flame deflectors.

It has been analytically derived that provision of full scale values of the Mach number, velocity, and density at the nozzle exit is an adequate criterion for the model flow. This can be provided through a "substitute" gas using a lower temperature and appropriately adjusted pressure. While this method shows promise, adequate supporting experimental data have yet to be obtained.

Aside from the "substitute" gases, it is sometimes useful to use fuels other than the exact full scale fuel. If entirely different chemicals are used, the plenum conditions may need to be changed considerably to maintain the desired exit conditions. This will probably constitute a valid model provided that the combustion is at a similar location on the stoichiometric scale. An excessive amount of fuel will cause re-ignition downstream, resulting in noise levels significantly higher than would otherwise be expected on the basis of the nozzle exit conditions only.

The use of cold air jets to establish absolute values of a full scale noise field is considered not feasible. Although cold air jets can be used to determine differences in a noise field due to geometrical changes such as a repositioning of surfaces bounding the flow, no formula is available which will assure that the success will be comparable to that achieved with a properly scaled jet.

The size of the nozzle used does not appreciably influence the ability of the model to produce a scaled noise field. However, since a smaller model produces a higher frequency noise field, the accurate measurement of this noise field becomes increasingly difficult as the nozzle size is reduced. Nozzles as small as 3/8 inch diameter have a limited usefulness, but in general nozzle diameters of 1 inch and larger will prove to be more satisfactory.

The noise field determined by transposing the field measured for one jet to a position occupied by a second identical engine, and then adding the two fields together, will reasonably approximate the noise field produced by the two engines operating simultaneously. For accurate determination of the noise field, direct measurement of the pair of engines is preferable. The need for providing each engine increases as the engines are placed closer together.

Air absorption of sound produces a small error in the scaling of the propagation of sound. With rare exceptions this error is negligible for near field measurements, but it becomes significant for many far field measurements such as those required to determine power levels. A mathematical correction may be readily determined.

It can be analytically predicted when a surface or other obstacle in the noise field will significantly affect the noise levels in that field. This prediction is not sufficiently accurate to evaluate the exact effect; rather it will indicate whether or not it is important to include such surfaces or other obstacles in a model, and whether undesired surfaces or obstacles which are unavoidable near a model will have a significant effect on the noise field. A general conclusion covering most situations is that the presence of a surface is significant for points in the noise field which are closer to the surface than to the source.

Using commercially available instrumentation, satisfactory measurements of scaled noise fields can be made when reasonable care is exercised. However, in some cases it may not be possible to measure all of the high frequency bands. If a sufficiently small microphone with high frequency capability were available, measurement errors could be significantly reduced.

LIST OF REFERENCES

1. Terman, F. E., Radio Engineer's Handbook, McGraw-Hill Book Co., Inc., New York, 1943.

2. Beranek, L. L., Acoustics, McGraw-Hill Book Co., Inc., New York, 1954.

3. Cole, J. N., et al, Noise Radiation from Fourteen Types of Rockets in the 1,000 to 130,000 Pounds Thrust Range. WADC Technical Report 57-354. Wright Air Development Center, Wright-Patterson AFB, Ohio. December 1957.

4. Barrere, Marcel, et al, Rocket Propulsion, English edition, Elsevier Publishing Co., Amsterdam, 1960. (Distributed in the U. S. by D. Van Nostrand Co., Inc., New York.)

5. Putnam, A. A., et al, Final Report on Studies of Turbulent Premixed Flames and Methods of Suppressing Combustion Oscillations. WADC Technical Report 56-583. Wright Air Development Center, Wright-Patterson AFB, Ohio. December 1956.

6. Oleson, S. K. and Ingard, U., "Acoustic Characteristics of Model Pulsed Jets." J. Acoust. Soc. Am. Vol. 29. October 1957. p. 1145.

7. Crump, J. E. and Price, E. W., "'Catastrophic' Changes in the Burning Rate of Solid Propellants During Combustion Instability." ARS Journal. Vol. 30, No. 7. July 1960. pp. 705-707.

8. Lighthill, M. J., "On Sound Generated Aerodynamically. I. General Theory." Proc. Roy. Soc. (London). Vol. 211, A. March 1952. pp. 564-587.

9. Powell, A., "Concerning the Noise of Turbulent Jets." J. Acoust. Soc. Am. Vol. 32. December 1960. pp. 1609-1612.

10. Ribner, H. S., "Energy Flux from an Acoustic Source Contained in a Moving Fluid Element and Its Relation to Jet Noise." J. Acoust. Soc. Am. Vol. 32. September 1960. p. 1159.

11. Cheng, Sin-I, On the Aerodynamic Noise of a Jet. GASL Technical Report No. 148. General Applied Sciences Laboratories, Inc., Westbury, L. I., New York. April 1959.

12. Mollo-Christensen, E. and Narasimha, R., "Sound Emission from Jets at High Subsonic Velocities." J. Fluid Mech. Vol. 8, Part 1. May 1960. p. 49.

13. Howes, W. L., Similarity of Far Noise Fields of Jets. NASA Technical Report R-52. National Aeronautics and Space Administration, Washington, D. C. 1959.

14. Tyler, J. M. and Perry, E. O. Jet Noise. Report No. PWA Inst. 451. Pratt & Whitney Aircraft, Division of United Aircraft Corp. 9 April 1954. (Preprint of a report prepared for presentation to S. A. E. meeting, New York, 14 April 1954.)

15. Howes, W. L., Distribution of Time-Averaged Pressure Fluctuations Along the Boundary of a Round Subsonic Jet. NASA Technical Note D-468. National Aeronautics and Space Administration, Washington, D. C. October 1960.

16. Eldred, K., Roberts, W., et al, Structural Vibration in Space Vehicles. Phase I Report. Investigation of Structural Vibration Sources and Characteristics. NOR-60-26. Progress Report of the Dynamics Branch, Northrop Corp. and Western Electro-Acoustic Laboratories. January 1960.

17. Powell, A., On the Mechanism and Reduction of Choked Jet Noise. Part 1. ARC 15,623 FM 1858. Aeronautic Research Council, Dept. of Aeronautics and Astronautics, University of Southampton, England. December 1952.

18. Ribner, H. S., Shock-Turbulence Interaction and the Generation of Noise. NACA Report 1233. National Advisory Committee for Aeronautics, Washington, D. C. 1955.

19. Lord Rayleigh, Theory of Sound, Vol. II, First American Edition, Dover Publications, New York, 1945. p. 113.

20. Westervelt, P. J., Aerodynamic Noise, Its Generation and Suppression. General Engineering Lab. Report 57GL222. General Electric Co., Schenectady, New York. 1 July 1957.

21. Morse, P. M., Vibration and Sound, Second Edition, McGraw-Hill Book Co., Inc., New York, 1948.

22. Olson, H. F., Elements of Acoustical Engineering, Second Edition, D. Van Nostrand Co., Inc., Princeton, N. J., 1955.

23. Merle, Marie, "Etude Experimentale des Ecoulements Gazeux." Publications Scientifiques et Techniques de l'Air. No. 308. January 1956.

24. Laurence, J. C., Intensity, Scale and Spectra of Turbulence in the Mixing Region of Jets. NACA Technical Note 3561. National Advisory Committee for Aeronautics, Washington, D. C. September 1955.

25. Anderson, A. R. and Johns, F. R., "Characteristics of Free Supersonic Jets Exhausting into Quiescent Air." Jet Propulsion. Vol. 25. January 1955. pp. 13-15, 25.

26. Doelling, N., Mercer, D. M. A., et al, A Compilation of Turbojet Noise Data. WADC Technical Report 54-401. Wright Air Development Center, Wright-Patterson AFB, Ohio. July 1956.

27. von Gierke, H. E., "Aircraft Noise Sources." Handbook of Noise Control ed. by C. M. Harris, McGraw-Hill Book Co., Inc., New York, 1957. Chap. 33.

28. Oda, F. and Ackerman, E., Propagation Distortion of Bands of Large Amplitude Acoustic Noise. II. An Experimental Investigation of Certain Plane Wave Cases. WADD Technical Report 60-233. Wright Air Development Division, Wright-Patterson AFB, Ohio. May 1960.

29. Ingard, U. and Lamb, G. L., "Effect of a Reflecting Plane on the Sound Power Output of Sound Sources." J. Acoust. Soc. Am. Vol. 29. June 1957. p. 743.

30. Howes, W. L., Ground Reflection of Jet Noise. NASA Technical Report R-35. National Aeronautics and Space Administration, Washington, D. C. 1959.

31. Beranek, L. L., Acoustic Measurements, John Wiley & Sons, Inc., New York, 1949.

32. Smith, R. H. and Wang, Chi-Teh, "Contracting Cones Giving Uniform Throat Speeds." J. Aeronaut. Sci. Vol. 11, No. 4. October 1944. p. 356.

33. Sutherland, L. C. and Morgan, W. V., "Use of Model Jets for Studying Acoustic Fields near Jet and Rocket Engines." Noise Control. Vol. 6, No. 3. May-June 1960. p. 6.

34. Tempelmeyer, K. E., An Analytical Study of Hot Jet Simulation with a Cold Gas Mixture. AEDC-TN-58-54. Arnold Engineering Development Center, ARO, Inc., Tullahoma, Tenn. September 1958.

35. Simmons, F. S., Analytical Determination of the Discharge Coefficients of Flow Nozzles. NACA Technical Note 3447. National Advisory Committee for Aeronautics, Washington, D. C. April 1955.

36. Nyborg, W. L. and Mintzer, D., Review of Sound Propagation in the Lower Atmosphere. WADD Technical Report 54-602. Wright Air Development Division, Wright-Patterson AFB, Ohio. May 1955.

37. Franklin, R. E. and Archbold, R. B., "A Small-Bore Pick-up for Measurement of Fluctuating Pressures." Aeronaut. Quart. Vol. XI. November 1960.

38. Howes, W. L. and Mull, H. R., Near Noise Field of a Jet Engine Exhaust. I. Sound Pressure. NACA Technical Note 3763. National Advisory Committee for Aeronautics, Washington, D. C. October 1956.

39. Cox, R. J., et al, A Study of the Characteristics of Modern Engine Noise and the Response Characteristics of Structures. Report 13,700. Lockheed Aircraft Corp. (Preliminary copy - release as a WADD Technical Report pending.)

40. Steed, C. N., Temperature, Sound, and Vibration Survey. Rocketdyne Technical Report 57-48. Rocketdyne Division of North American Aviation, Inc. 17 July 1957. (CONFIDENTIAL Report).

41. Staff of Bolt, Beranek and Newman, Inc., The Noise Field of Jupiter Missiles. BBN Report No. 659. Bolt, Beranek and Newman, Inc. 28 December 1959.

42. Sutherland, L. C., Unpublished notes on the Transient Pulse of an Enclosed Jet. Boeing Airplane Co., Seattle, Wash. 1961.

43. Lilley, G. M. and Hodgson, T. H., On Surface Pressure Fluctuations in Turbulent Boundary Layers. CoA Note No. 101. College of Aeronautics, Cranfield, England. April 1960.

44. Corcos, G. M., et al, On the Measurement of Turbulent Pressure Fluctuations with a Transducer of Finite Size. Univ. of California Institute of Engineering Research, Series No. 82. November 1959.

45. Howes, W. L., Similarity of Near Noise Fields of Subsonic Jets. NASA Technical Report R-94. National Aeronautics and Space Administration, Washington, D. C. 1961.

46. Bies, D. A., "Effect of a Reflecting Plane on an Arbitrarily Oriented Multipole" J. Acoust. Soc. Am. Vol. 33. March 1961. p. 286.

47. Hubbard, H. H., Unpublished data. National Aeronautics and Space Administration, Langley Research Center, Langley Field, Virginia.

APPENDIX A

GAS FLOW PARAMETERS, ACOUSTIC POWER LEVELS, AND SOUND PRESSURE LEVELS OF MODEL JETS AND ROCKETS

TABLE V

GAS FLOW PARAMETERS OF MODELS

Plenum Reference Number	Gas	Total Temp.(°F)	Exit Conditions			Model
			Mach No.	Velocity Ft/Sec	Density Lb/Ft^3	
1	Kerosene/Air	1000	1.15	1900	.033	J-57
2	Cold Air	60	1.15	1145	.096	----
3	Kerosene/Air	420	1.6	1900	.066	----
4	Kerosene/Air	1070	1.17	1990	.033	J-79 Mil
5	Kerosene/Air	3040	1.14	2920	.013	J-79 A/B
6	Kerosene/Air	2800	1.6	3720	.016	----
7	Kerosene/Air	2320	1.6	3440	.0195	----
8	Helium	60	1.6	3860	.0195	----
9	Steam	450	1.15	1900	.032	----
10	Steam	250	1.15	1680	.042	----
11	Kerosene/Air	670	1.15	1680	.043	----
12	Alcohol-H_2O/O_2	---	2.8	7990	.010	AR-1[a]
13	Alcohol-H_2O/O_2	---	2.8	6850	.013	AR-1[a]
14	Kerosene/O_2	---	2.85	9400	.0085	Jupiter[a]

[a]Calculated for fully expanded flow

TABLE VI

OCTAVE BAND POWER LEVEL[a] SPECTRA MEASURED AT RADII OF 100 NOZZLE DIAMETERS

Plenum Reference Number[b]	Radius of Measurement Sphere, Ft.[c]	Over-all	Octave Pass Bands - cps								
			150-300	300-600	600-1200	1200-2400	2400-4800	4800-10K	10K-20K	20K-40K	40K-80K
1	25	159.5	133.0	144.0	150.0	153.5	153.5	153.5	150.5	142.0	138.5
1[d]	25	164.0	139.0	146.0	151.5	155.0	157.0	158.5	157.5	152.0	142.5
1[e]	25	164.5	138.0	146.5	154.0	159.0	158.5	158.5	155.5	148.5	141.0
1[f]	25	164.5	138.0	148.5	154.5	157.5	158.0	158.0	156.0	149.0	141.5
2	25	151.0	129.5	134.5	139.5	140.0	143.0	147.5	141.5	138.0	139.0
3	25	163.5	136.0	146.0	152.0	155.5	157.0	158.0	157.0	149.0	141.5
6	12.5	165.5	134.5	147.0	149.5	156.0	160.5	158.0	159.0	155.5	152.0
7	12.5	164.0	134.5	146.5	148.0	153.0	157.0	157.0	158.5	155.0	151.0
8	6.2	—	—	—	136.0	144.0	147.0	151.5	155.0	150.5	146.5
9	25	163.5	138.5	145.5	154.0	161.0	155.5	153.5	151.0	146.5	143.0
9	12.5	155.5	129.5	132.0	141.5	146.0	152.0	149.0	144.0	141.5	138.0
10	12.5	150.5	126.0	128.0	140.5	145.5	146.5	141.0	137.0	130.5	132.0
4[g]	25	159.0	142.5	146.5	151.0	150.5	152.5	152.5	149.0	143.0	136.0
5[g]	25	164.0	154.0	156.0	156.5	155.5	157.0	155.0	151.0	147.5	141.0
12[g]	12.5	—	149.5	155.0	158.0	157.0	155.0	156.0	—	—	—
13[g]	12.5	—	152.0	159.0	162.5	161.0	160.0	159.0	—	—	—
14[h]	10.5	—	138.5	145.5	151.5	154.5	156.5	158.5	—	—	—
14[g]	10.5	—	151.5	157.5	161.5	164.0	165.0	165.0	—	—	—

[a] Acoustic power levels in db re 10^{-13} watts.

[b] See Table V.

[c] Spherical radiation assumed except as noted.

[d] Two nozzles at 2 N.D. separation.

[e] Two nozzles at 4 N.D. separation.

[f] Two nozzles at 8 N.D. separation.

[g] Horizontal exhaust, hemispherical radiation assumed.

[h] Bucket deflecting horizontally, hermispherical radiation assumed.

TABLE VII

ONE-EIGHTH SCALE MODEL J-57 SOUND LEVELS[a]

Distance of Test Point From Nozzle Exit, N.D.[b]		Octave Pass Bands - cps								
Axial	Radial	150-300	300-600	600-1200	1200-2400	2400-4800	4800-10K	10K-20K	20K-40K	40K-80K
0	2.2	111.0	114.0	119.5	125.5	132.5	134.0	136.0	132.5	130.5
0	3.2	110.0	113.0	119.5	125.5	131.5	134.5	135.0	132.0	129.0
0	4.3	109.5	113.0	119.5	125.5	130.5	134.0	135.0	132.5	130.0
4.3	6.5	112.5	117.0	121.0	127.0	132.0	134.5	137.5	137.0	133.0
4.3	10.8	110.0	116.0	120.0	123.5	130.0	130.5	133.0	132.5	128.5
8.7	10.8	113.0	119.0	124.0	126.0	134.5	135.5	137.0	134.0	129.5
2.2	2.2	112.5	116.5	124.0	130.0	137.0	138.5	144.0	144.0	141.0
2.2	3.2	112.0	114.5	121.0	127.5	134.0	137.0	141.0	141.0	139.0
4.3	2.2	122.5	128.5	136.0	141.5	146.5	150.0	147.0	143.0	138.5
4.3	3.2	117.5	123.0	128.5	136.0	141.0	145.0	145.5	143.5	139.0
4.3	4.3	115.5	119.5	124.0	131.5	136.5	140.0	141.5	140.5	136.5
8.7	6.5	118.5	124.5	129.0	135.5	142.0	143.5	142.5	138.0	134.0
6.5	2.2	134.0	138.5	141.5	147.0	147.5	146.0	145.0	140.0	136.5
8.7	2.2	139.0	142.0	144.5	149.0	150.0	147.0	145.5	141.5	139.5
8.7	3.2	130.5	135.5	139.5	147.0	148.0	146.0	143.5	139.0	135.5
8.7	4.3	124.5	130.5	135.0	144.0	147.5	147.0	143.5	139.5	136.0
13	4.3	131.0	136.0	140.0	144.5	147.5	141.0	139.0	135.5	129.5
13	6.5	124.0	130.5	136.5	140.0	147.5	142.0	140.0	134.5	129.5
13	3.2	136.5	139.5	141.5	145.0	146.5	141.5	139.5	135.0	130.0
13	10.8	116.0	124.0	130.5	131.5	142.0	139.5	138.0	134.0	128.0
17.3	4.3	133.0	137.0	142.0	141.5	145.0	139.0	136.5	133.5	128.0
17.3	6.5	126.5	134.0	141.5	140.0	147.0	138.5	135.5	132.0	126.0
17.3	10.8	119.0	128.5	136.5	136.5	143.0	139.0	137.0	133.0	127.5
26	6.5	126.5	135.0	140.5	140.5	136.0	133.5	132.5	125.0	119.0
26	10.8	123.5	134.0	142.0	140.0	133.5	134.0	133.5	126.5	121.0

[a] Sound pressure levels in db re 0.0002 microbar.

[b] Three-inch nozzle diameter, plenum reference No. 1 (see Table V).

TABLE VIII

ONE-EIGHTH SCALE MODEL AR-1 ROCKET SOUND LEVELS[a]

Plenum Reference Number[b]	Distance of Test Point From Nozzle Exit, N.D.[c]		Octave Pass Bands - cps								
	Axial	Radial	150-300	300-600	600-1200	1200-2400	2400-4800	4800-10K	10K-20K	20K-40K	40K-80K
13	0	6	122.0	129.0	137.0	136.5	139.0	144.5	146.5	146.0	143.0
13	0	12	126.5	132.5	132.5	135.5	138.0	142.0	—	—	—
13	0	18	121.5	130.0	133.0	137.0	137.0	143.0	148.5	141.5	137.0
13	6	18	122.0	131.5	132.0	138.5	142.5	144.0	146.0	145.5	142.0
13	12	18	125.0	133.0	134.0	141.0	145.5	149.0	154.0	147.0	141.0
13	18	18	123.5	134.0	133.5	143.0	147.5	152.5	148.0	145.5	140.0
13	24	18	125.5	136.5	136.5	144.0	147.5	147.0	146.5	141.5	137.5
13	30	18	125.0	136.0	136.5	144.0	144.0	146.0	141.0	137.0	133.5
12	0	6	120.0	122.0	132.0	134.5	138.0	142.0	143.0	144.0	141.0
12	0	12	123.0	125.5	126.0	132.5	135.5	141.0	—	—	—
12	0	18	122.0	125.5	130.5	140.5	136.0	142.5	148.5	140.5	136.5
12	6	18	123.5	126.0	129.5	138.0	141.0	144.0	145.5	145.0	140.5
12	12	18	127.0	130.0	130.5	140.5	145.0	148.5	156.0	147.5	141.0
12	18	18	126.5	131.5	131.0	141.0	148.0	149.5	150.0	148.0	143.0
12	24	18	128.5	134.0	134.5	145.0	149.0	149.0	148.5	143.0	139.0
12	30	18	128.5	134.0	136.0	145.0	145.0	145.0	143.5	139.5	134.5

[a] Sound pressure levels in db re 0.0002 microbar.

[b] See Table V.

[c] Nozzle diameter = 1.489 inches.

TABLE IX

ONE-THIRTY-SIXTH SCALE MODEL JUPITER ROCKET SOUND LEVELS[a]

Test Point Location 1/4" From Missile Skin N.D. Above Nozzle Exit[b]	Octave Pass Bands - cps								
	150-300	300-600	600-1200	1200-2400	2400-4800	4800-10K	10K-20K	20K-40K	40K-80K
1.3	119.5	127.0	134.5	142.0	144.5	150.5	150.5	149.5	148.5
4	116.5	123.5	131.5	138.5	141.0	146.0	146.0	145.0	140.5
6.5	117.5	123.5	130.5	138.5	139.5	145.0	145.5	143.0	139.0
8	118.5	123.0	129.5	136.5	139.0	148.0	142.5	140.5	136.0
10.5	115.5	121.5	128.5	136.5	138.0	148.5	145.5	139.0	135.0
13	116.0	121.0	128.5	135.0	137.0	142.5	142.0	139.0	135.0
6.5[c]	119.5	125.0	131.0	138.5	141.0	149.0	149.5	146.5	142.5

[a] Sound pressure levels in db re 0.0002 microbar.

[b] Nozzle diameter = 1.275 in., plenum reference No. 14 (see Table V).

[c] On opposite side of missile.

TABLE X

SOUND LEVELS[a] MEASURED NEAR SMALL NOZZLES OF VARIOUS DIAMETERS

Distance of Test Point From Nozzle Exit, N.D.[b]		Octave Pass Bands - cps									Octave Pass Bands - cps								
Axial	Radial	150-300	300-600	600-1200	1200-2400	2400-4800	4800-10K	10K-20K	20K-40K	40K-80K	150-300	300-600	600-1200	1200-2400	2400-4800	4800-10K	10K-20K	20K-40K	40K-80K
		3" Nozzle Diameter									1.5" Nozzle Diameter								
0	16.5	100.5	105.5	110.0	114.5	119.5	121.5	122.5	119.0	114.5	96.0	98.5	103.0	108.0	113.5	117.5	124.5	121.0	117.0
8	16.5	101.5	107.5	113.0	118.5	123.5	124.0	124.5	122.5	119.0	97.0	100.0	105.5	111.0	120.0	118.5	123.0	123.5	120.5
16	16.5	104.5	111.5	119.5	124.5	130.0	127.5	127.0	121.5	117.5	101.0	102.0	109.5	116.5	123.5	125.5	128.0	125.5	120.0
0	9	103.5	108.0	112.5	117.5	122.5	127.0	125.5	124.0	120.0	97.0	99.5	105.0	111.5	117.5	122.5	129.0	125.0	121.0
8	9	109.0	115.5	121.0	126.5	132.0	134.0	133.0	131.5	126.5	101.5	106.5	112.5	118.5	128.0	127.5	132.5	132.0	129.0
16	9	116.0	124.0	133.5	138.0	141.5	136.0	133.0	128.5	122.0	109.5	114.0	122.0	131.0	139.5	141.0	140.0	134.0	127.5
0	5.7	105.5	109.0	114.0	119.5	124.5	129.5	129.0	126.0	120.5	98.5	101.0	106.5	113.5	120.0	127.0	130.5	127.5	124.0
8	5.7	119.0	125.0	130.5	136.5	143.0	142.5	139.5	134.5	129.5	112.0	115.5	121.0	128.5	138.5	138.5	142.5	140.0	135.0
16	5.7	127.5	132.0	138.5	136.5	135.5	131.0	128.5	122.0	115.5	121.5	124.0	130.0	137.5	143.5	140.0	138.0	129.5	123.0
0	4	106.5	109.5	115.0	120.0	126.0	131.5	130.5	127.0	123.0	99.5	101.5	107.0	113.5	121.5	129.0	131.5	127.5	123.0
8	4	126.5	131.0	137.5	144.0	148.5	146.5	140.0	135.0	130.0	116.0	120.0	126.5	133.5	143.5	144.0	145.5	139.0	132.0
4	4	113.5	119.0	123.5	128.5	132.0	135.0	—	—	c	104.5	108.5	115.0	120.5	125.0	128.5	—	—	c
4	5.7	109.0	114.0	119.0	123.5	127.0	130.0	—	—	c	100.5	105.5	111.5	117.0	121.5	125.0	—	—	c
4	9	104.0	109.5	114.5	119.0	121.5	124.0	—	—	c	99.0	99.5	105.5	110.5	116.0	119.0	—	—	c
4	16.5	99.5	104.5	109.5	113.0	116.0	118.0	—	—	c	99.5	98.0	100.5	105.5	109.5	112.0	—	—	c
		.75" Nozzle Diameter									.375" Nozzle Diameter								
0	4	—	100.0	100.0	105.5	112.0	120.0	127.0	128.0	124.5	—	100.0	99.0	102.0	107.0	114.0	123.0	128.0	128.5
0	5.7	—	98.0	99.0	104.5	111.5	119.0	125.0	127.5	124.5	—	98.5	98.0	101.0	105.0	113.5	122.5	124.0	127.0
0	9	—	100.0	100.0	104.0	110.0	116.0	122.0	123.5	120.0	—	97.5	97.0	100.5	104.5	112.5	121.0	122.0	122.0
0	16.5	—	97.0	97.5	102.0	108.0	113.0	120.5	120.5	119.0	—	96.5	96.5	100.0	104.5	112.5	119.5	119.5	118.0
4	4	100.5	101.0	107.0	113.0	118.5	123.0	—	—	c	96.0	96.0	100.5	106.0	111.0	118.5	—	—	c
4	5.7	96.0	98.5	104.0	110.0	115.0	120.0	—	—	c	90.0	93.0	98.5	103.5	108.5	116.0	—	—	c
4	9	89.0	94.0	100.5	106.0	111.5	116.5	—	—	c	—	90.0	96.0	102.0	108.0	112.5	—	—	c
4	16.5	85.0	89.0	96.0	102.0	108.0	112.5	—	—	c	84.5	85.0	92.0	98.0	103.0	109.0	—	—	c
8	4	—	109.0	114.5	120.5	128.0	134.0	137.0	137.0	136.0	—	111.5	117.0	124.5	130.0	137.5	144.5	148.5	147.5
8	5.7	—	107.0	112.0	118.0	124.0	131.5	135.0	134.0	133.0	—	103.0	108.5	114.0	119.5	127.0	134.5	137.5	139.5
8	9	—	100.0	103.0	110.0	115.5	121.0	126.0	128.0	127.5	—	98.0	100.5	106.0	110.5	119.0	127.0	128.5	129.0
8	16.5	—	97.0	99.0	104.0	111.5	115.5	123.0	122.5	122.0	—	96.5	96.5	100.0	106.0	115.0	121.0	122.5	123.0
16	5.7	—	119.5	124.5	129.0	135.5	139.5	138.0	129.5	123.0	—	115.5	120.5	124.0	129.0	137.5	142.0	140.5	131.5
16	9	—	106.0	111.5	119.0	127.0	134.0	135.0	131.0	123.0	—	104.5	107.0	113.0	120.0	130.0	137.0	138.5	135.0
16	16.5	—	98.5	101.0	108.0	116.0	122.0	126.0	124.0	121.0	—	97.5	97.5	102.0	108.0	116.5	123.0	123.5	121.5

[a]Sound pressure levels in db re 0.0002 microbar. [b]Plenum reference No. 1 (see Table V). [c]Measured with Altec microphones.

TABLE XI

SOUND LEVELS[a] MEASURED NEAR SMALL HELIUM JET

Distance of Test Point From Nozzle Exit, N.D.[b]		Octave Pass Bands - cps							
Axial	Radial	300-600	600-1200	1200-2400	2400-4800	4800-10K	10K-20K	20K-40K	40K-80K
0	5.7	115.5	116.5	119.5	123.5	135.5	146.0	141.0	139.5
0	9	—	111.0	117.5	122.0	133.0	142.0	141.5	139.5
4	4	128.0	127.0	129.0	132.5	141.0	151.0	155.5	157.0
4	5.7	115.5	120.5	126.0	130.5	142.0	148.0	150.0	148.0
4	9	111.5	116.0	122.5	126.5	137.5	146.5	145.5	144.5
8	4	128.0	132.5	136.5	142.0	150.0	157.0	155.0	151.5
8	5.7	124.5	128.5	133.5	139.5	149.0	155.0	152.0	148.0
8	9	116.5	120.5	127.0	132.5	145.5	152.5	151.0	147.5
8	16.5	110.5	114.0	120.5	125.0	136.5	144.5	143.0	141.5
16	4	141.0	144.0	145.0	148.0	150.0	153.0	148.5	142.0
16	9	123.5	128.0	135.5	142.5	147.5	148.0	146.0	142.0

[a]Sound pressure levels in db re 0.0002 microbar.

[b]Nozzle diameter = 0.75 in., plenum reference No. 8 (see Table V).

TABLE XII

SOUND LEVELS[a] MEASURED NEAR SMALL AFTERBURNING JET

Plenum Reference Number[b]	Distance of Test Point From Nozzle Exit, N.D.[c]		Octave Pass Bands - cps							
	Axial	Radial	150-300	300-600	600-1200	1200-2400	2400-4800	4800-10K	10K-20K	20K-40K	40K-80K
6	0	4	111.5	113.5	117.5	126.5	131.5	137.0	143.0	141.0	140.0
6	0	5.7	109.5	112.5	117.5	126.0	131.5	137.5	141.0	139.5	137.5
6	0	10.7	109.5	112.0	116.5	125.0	131.0	136.0	140.5	139.5	138.5
6	0	16.5	104.0	109.0	114.0	121.0	127.5	132.5	135.5	134.5	131.0
6	4	4	120.0	122.5	128.0	134.5	141.5	149.0	155.5	154.0	149.5
6	4	5.7	114.0	118.0	124.0	131.5	139.0	146.0	150.5	150.5	147.5
6	4	10.7	111.0	115.0	119.5	127.0	133.0	139.0	144.0	143.0	140.0
6	8	4	123.5	129.0	135.5	143.5	151.0	154.0	155.5	154.0	147.0
6	8	5.7	122.0	125.5	131.5	140.0	149.0	153.0	157.5	153.5	149.0
6	8	10.7	116.0	118.5	123.0	131.5	139.5	146.5	150.5	147.5	143.5
6	8	16.5	106.0	111.5	116.0	123.0	133.5	136.0	143.0	138.5	134.0
6	16	4	134.5	139.0	142.0	147.0	149.5	147.5	147.5	142.0	137.0
6	16	10.7	121.0	124.5	131.5	140.0	148.5	149.0	149.0	143.5	139.0
7	0	4	109.5	110.5	115.0	124.0	130.0	135.0	140.0	138.5	137.5
7	0	5.7	107.0	110.0	115.0	123.5	129.5	136.0	139.5	137.0	135.0
7	0	10.7	109.0	110.0	114.0	123.0	129.0	134.5	139.5	138.5	137.0
7	0	16.5	102.5	107.5	112.0	119.5	126.0	132.0	135.0	132.5	133.0
7	4	4	—	122.0	124.0	131.0	136.0	144.5	150.5	153.0	147.5
7	4	5.7	111.0	115.5	120.5	128.5	136.0	143.0	147.0	149.5	146.5
7	4	10.7	110.0	112.5	116.5	125.5	131.0	137.5	141.5	141.5	138.0
7	8	4	122.5	126.5	134.0	140.5	149.0	153.0	154.5	154.0	146.5
7	8	5.7	120.0	122.5	129.0	136.5	146.0	151.5	156.5	153.0	148.0
7	8	10.7	112.5	115.5	120.0	128.0	136.5	142.5	148.0	146.0	142.0
7	8	16.5	105.0	109.5	115.0	121.0	131.0	134.0	142.0	138.5	132.5
7	16	4	133.5	137.5	141.0	146.5	150.0	148.5	148.5	142.5	137.5
7	16	10.7	120.5	123.0	129.0	139.0	147.5	148.5	149.0	143.5	139.5

[a]Sound pressure levels in db re 0.0002 microbar.

[b]See Table V.

[c]Nozzle diameter = 1.5 inches.

TABLE XIII

SOUND LEVELS[a] MEASURED NEAR SUPERHEATED STEAM JET

Distance of Test Point From Nozzle Exit, N.D.[b]		Octave Pass Bands - cps							
Axial	Radial	300-600	600-1200	1200-2400	2400-4800	4800-10K	10K-20K	20K-40K	40K-80K
		3" Nozzle Diameter							
[c]0	4	—	—	—	124.5	130.5	129.5	128.5	127.0
[c]0	9	—	—	—	123.5	128.0	127.0	126.0	122.5
16	5.7	130.0	136.5	140.5	138.0	131.5	125.0	120.5	116.0
[c]16	9	125.0	134.0	140.0	141.5	137.0	130.0	127.0	122.0
16	16.5	114.5	124.0	135.0	136.0	132.0	128.5	126.5	121.0
		1.5" Nozzle Diameter							
[c]0	4	—	—	—	122.0	130.0	131.0	130.0	127.0
[c]0	5.7	—	—	—	120.5	125.5	129.5	128.5	125.0
[c]0	9	—	—	—	118.0	122.5	126.5	125.5	122.0
[c]0	16.5	—	—	—	115.0	120.5	122.0	122.0	118.0
[c]16	4	—	—	—	138.0	138.5	137.5	125.0	119.0
[c]16	5.7	—	—	—	140.5	141.5	137.5	128.5	122.5
16	9	117.0	125.0	136.0	139.5	147.5	139.5	133.0	126.0
16	16.5				130.0	134.5	131.5	126.5	121.0
		.75" Nozzle Diameter							
0	4	—	—	—	115.0	125.0	131.0	133.5	128.5
0	9	—	—	—	114.5	121.0	125.5	128.0	121.5
4	4	105.0	116.0	120.0	124.5	131.5	—	—	d
[c]16	4	130.0	133.0	135.0	138.5	139.5	137.5	129.0	121.5
[c]16	5.7	119.0	124.0	130.0	136.0	142.0	140.0	131.5	124.0
16	9	109.5	121.0	125.0	138.0	140.5	143.5	137.5	129.0
16	16.5	—	—	117.0	124.0	133.0	131.0	[illegible]	123.5

[a]Sound pressure levels in db re 0.0002 microbar.

[b]Plenum reference No. 9 (see Table V).

[c]Eleven points used in Figure 43 (lower).

[d]These data measured with Altec microphone.

☆U.S. GOVERNMENT PRINTING OFFICE:1961 O—609173